

Application of Advanced Reservoir Characterization, Simulation, and Production
Optimization Strategies to Maximize Recovery in Slope and Basin Clastic
Reservoirs, West Texas (Delaware Basin)

Annual Report

By

Shirley P. Dutton
Mark D. Barton
Mohammad A. Malik
George B. Asquith
Jose I. Guzman
Sigrid J. Clift
Andrew G. Cole

April 1998

Work Performed Under Contract No. DE-FC22-95BC14936

Prepared for
U.S. Department of Energy
Assistant Secretary for Fossil Energy

Jerry Casteel, Project Manager
National Petroleum Technology Office
P.O. Box 3628
Tulsa, OK 74101

Prepared by:
Bureau of Economic Geology
The University of Texas at Austin
Austin, TX 78713-8924

CONTENTS

ABSTRACT	1
EXECUTIVE SUMMARY	2
INTRODUCTION	5
Summary of Project Objectives	5
Project Description	6
Project Structure	6
Summary of Progress	7
DELAWARE MOUNTAIN GROUP OIL PLAY	7
OUTCROP CHARACTERIZATION OF BELL CANYON SANDSTONE	
RESERVOIR ANALOGS	11
Introduction	11
Regional Setting and Stratigraphic Framework	12
Models of Basinal Sandstone Deposition	13
Study Area	16
Sedimentology	18
Facies	18
Depositional Elements	22
Willow Mountain High-Order Cycle	25
Conclusions	29
RESERVOIR CHARACTERIZATION OF FORD GERALDINE UNIT	29
Porosity Distribution	34
Saturation Distribution	38
Permeability Distribution	43
Structure	48
Net Pay	50

Vertical Porosity and Permeability Profiles	53
FIELD DEVELOPMENT HISTORY	53
Primary Recovery	53
Secondary Recovery	59
Tertiary Recovery	59
Evaluation of Reservoir Heterogeneity	62
Production Constraints	66
SIMULATIONS OF TERTIARY RECOVERY	70
Simulation Results	73
Sensitivity Study	78
Economic Analysis	81
CONCLUSIONS	81
ACKNOWLEDGMENTS	83
REFERENCES	84

Figures

1. Map showing location of Delaware Basin and paleogeographic setting during the late Permian	8
2. Stratigraphic nomenclature of the Delaware Mountain Group in the Delaware Basin subsurface and outcrop areas and time-equivalent formations on the surrounding shelves	10
3. Sand-body architecture for turbidity-current model and saline-density-current model	15
4. Map showing location of study area and outcrop exposure of Bell Canyon Formation	17
5. Cross section based on outcrop measured sections from Willow Mountain	26
6. Diagram illustrating depositional facies model for high-order cycle examined at Willow Mountain	28
7. Status of wells in the Ford Geraldine unit and distribution of core control	30
8. Typical log from the Ford Geraldine unit well No. 108	32
9. Distribution of geophysical log suites available in Ford Geraldine unit	33

10.	Distribution of porosity in Ramsey sandstone from 4900 core analyses	35
11.	Map of average porosity for the Ramsey sandstone	36
12.	Map of porosity \times thickness for the Ramsey sandstone	37
13.	Distribution of water saturation in Ramsey sandstone from 4900 core analyses	39
14.	Map of bulk volume water for the Ramsey 2 sandstone	40
15.	Map of water saturation for the Ramsey sandstone	41
16.	Map of mobile oil saturation for the Ramsey sandstone	42
17.	Distribution of permeability in Ramsey sandstone from 4900 core analyses	44
18.	Map of geometric mean permeability for the Ramsey sandstone interval	45
19.	Isopach map of the Ramsey 1 sandstone	46
20.	Map of permeability \times thickness for the Ramsey sandstone	47
21.	Map of percentage of the Ramsey sandstone that is cemented by calcite	49
22.	Map of volume of clay in Ramsey sandstone	51
23.	Map of net pay for the Ramsey sandstone	52
24.	Map of hydrocarbon-pore-feet for the Ramsey sandstone	54
25.	Vertical permeability profiles from core-analysis data for 5 wells in the Ford Geraldine unit	55
26.	Vertical porosity profiles from core-analysis data for 5 wells in the Ford Geraldine unit	56
27.	Plots of primary, secondary, and tertiary production in the Ford Geraldine unit, and volumes of water and CO ₂ injected	57
28.	Map of primary recovery for the Ramsey sandstone	58
29.	Map of secondary production resulting from the waterflood conducted from 1969 to 1980	60
30.	Map of tertiary production through 1995 resulting from the CO ₂ flood that started in 1981	61
31.	Dip cross section A-A' down the length of Geraldine Ford field	63
32.	Cross section B-B' through the northern end of Geraldine Ford field	64
33.	Representative cores of the Ramsey sandstone and bounding Trap and Ford laminated siltstones	65

34.	Capillary pressure curves and calculated radii of pore throats for Ramsey sandstones	67
35.	Structure contours on the top of the Lamar limestone dip to the east and northeast	68
36.	Map of total production from the Ford Geraldine unit through 1995	69
37.	Map of the percentage of water produced during initial potential tests	71
38.	Map of water cut at the end of primary production in 1969	72
39.	Oil recovery as a fraction of remaining oil in place for stochastic and layered permeability cases	75
40.	Surface oil rate in stock tanks barrels/day for stochastic and layered permeability cases	77
41.	Surface water-oil ratio for stochastic and layered permeability cases	77
42.	Surface gas-oil ratio for stochastic and layered permeability cases	77
43.	Gross and net gas utilization for stochastic and layered permeability cases	79
44.	Effect of water saturation on oil recovery for stochastic and layered permeability cases	79
45.	Comparison of oil recovery for WAG and continuous CO ₂ injection for stochastic permeability case	80
46.	Effect of reduction of vertical permeability on oil recovery for layered permeability case	80
47.	Oil recovery in base with stochastic permeability as affected by (1) reduction in injection pressure from 2,000 to 1,500 psia and (2) pressurizing the reservoir with injection of CO ₂ instead of water	82

Tables

1.	Facies characteristics of Bell Canyon sandstones and siltstones	19
2.	Characteristics of depositional elements	23
3.	Areal and vertical description of reservoir	31
4.	Fluid characteristics of reservoir	74

ABSTRACT

The objective of this Class III project is to demonstrate that detailed reservoir characterization of clastic reservoirs in basinal sandstones of the Delaware Mountain Group in the Delaware Basin of West Texas and New Mexico is a cost-effective way to recover more of the original oil in place by strategic infill-well placement and geologically based enhanced oil recovery. The study focused on the Ford Geraldine unit, which produces from the upper Bell Canyon Formation (Ramsey sandstone). Reservoirs in this and other Delaware Mountain Group fields have low producibility (average recovery <14 percent of the original oil in place) because of a high degree of vertical and lateral heterogeneity caused by depositional processes and post-depositional diagenetic modification.

Outcrop analogs were studied to better interpret the depositional processes that formed the reservoirs at the Ford Geraldine unit and to determine the dimensions of reservoir sandstone bodies. Facies relationships and bedding architecture within a single genetic unit exposed in outcrop in Culberson County, Texas, suggest that the sandstones were deposited in a system of channels and levees with attached lobes that initially prograded basinward, aggraded, and then turned around and stepped back toward the shelf. Channel sandstones are 10 to 60 ft thick and 300 to 3,000 ft wide. The flanking levees have a wedge-shaped geometry and are composed of interbedded sandstone and siltstone; thickness varies from 3 to 20 ft and length from several hundred to several thousands of feet. The lobe sandstones are broad lens-shaped bodies; thicknesses range up to 30 ft with aspect ratios (width/thickness) of 100 to 10,000. Lobe sandstones may be interstratified with laminated siltstones.

The 0- to 60-ft-thick Ramsey sandstone interval in the Ford Geraldine unit is interpreted as a channel-levee and lobe system similar to the one described in outcrop. Siltstones interbedded with levee and lobe sandstones and zones of extensively calcite-cemented sandstone are the most important causes of reservoir complexity and reduced sweep efficiency in Delaware Mountain Group reservoirs. Mapping of reservoir properties in this old field with sparse porosity logs was

improved by supplementing geophysical log data with porosity, permeability, and water saturation data from core analyses. The expanded water-saturation data base was used to improve the maps of mobile oil saturation, net pay, and hydrocarbon pore feet.

An area of approximately 1 mi² in the northern part of the Ford Geraldine unit was chosen for reservoir simulation to estimate the tertiary recovery potential of a CO₂ flood. A quarter of a five-spot injection pattern in the area was selected for flow simulations, and two cases of permeability distribution were considered, one using stochastic permeability distribution generated by conditional simulation and the second using layered permeabilities. Flow simulations were performed using UTCOMP, an isothermal, three-dimensional, compositional simulator for miscible gas flooding. Results indicate that 10 to 30 percent (1 to 3 MMbbl) of remaining oil in place in the demonstration area can be produced by CO₂ injection.

EXECUTIVE SUMMARY

Slope and basin clastic reservoirs in sandstones of the Delaware Mountain Group in the Delaware Basin of West Texas and New Mexico contained more than 1.8 billion barrels (Bbbl) of oil at discovery. Recovery efficiencies of these reservoirs have averaged only 14% since production began in the 1920's, and thus a substantial amount of the original oil in place remains unproduced. Many of these mature fields are nearing the end of primary production and are in danger of abandonment unless effective, economic methods of enhanced oil recovery can be implemented. The goal of this project is to demonstrate that reservoir characterization, using 3-D seismic data, outcrop characterization, subsurface field studies, and other techniques, and integrated with reservoir simulation, can optimize infill drilling and enhanced oil recovery (EOR) projects in Delaware Mountain Group reservoirs.

The target of this study was the Ford Geraldine unit, which produces from the most prolific horizon in the Delaware Mountain Group in Texas, the Ramsey sandstone of the upper Bell Canyon Formation. Work performed during the third year of the contract focused on completing

reservoir characterization of the Ford Geraldine unit, simulating a CO₂ flood in the northern end of the unit, and transferring technology. Through workshops, a field trip, and presentations at professional meetings, the knowledge gained in the study of the Ford Geraldine unit was transferred to operators of other Delaware Mountain Group reservoirs. The information and approaches developed during this project can be applied to increase production from the more than 100 other Delaware Mountain Group reservoirs, which together contain more than 686 MMbbl of remaining mobile oil and 872 MMbbl of residual oil.

Reservoir characterization focused on three main topics this year: (1) refining the depositional model for Delaware Mountain Group sandstones developed from outcrop, (2) improving the maps of reservoir properties in the Ford Geraldine unit by incorporating core-analysis data, and (3) estimating tertiary recovery potential of the northern part of the Ford Geraldine unit by simulating a CO₂ flood.

Bell Canyon sandstones exposed in outcrop 24 mi west of the Ford Geraldine unit are analogs of slope and basin clastic reservoirs in the Delaware Basin. The sandstones were deposited in a system of channels and levees with attached lobes, and the depositional elements within the system are organized in a systematic fashion to form cyclic successions referred to as high-order cycles. The cycles are bounded by organic-rich siltstones that display gradational contacts with overlying and underlying laminated siltstones. Laminated siltstones at the base of the cycle coarsen upward and are interstratified with broad, lens-shaped sandstone bodies. The succession is locally incised and replaced by amalgamated channels that pass upward into winged channel-form bodies interstratified with irregularly shaped sandstone bodies. The winged channels display cross-cutting relationships, and they stack vertically and laterally to form multistoried complexes. Channel orientation within a complex varies by as much as 90 degrees. An upward-fining succession of laminated siltstones interstratified with broad, lens-shaped sandstone bodies abruptly overlies the deposits and caps the cycle.

The high-frequency cycle is interpreted to record deposition from a channel-levee system with distal lobes. The multistoried channel complex records repeated episodes of channel

aggradation and avulsion. The systematic change in cycle architecture indicates the system prograded into the basin, aggraded, and then retrograded. Bounding, organic-rich siltstones record periods when sediment was prevented from entering the basin.

The depositional model developed from characterization of Bell Canyon outcrops guided correlations of the Ramsey reservoir at the Ford Geraldine unit. An important focus of reservoir characterization this year was to improve the mapping of reservoir properties. The use of porosity, permeability, and water-saturation data from core analyses significantly increased the available well control and provided more detailed maps of reservoir properties compared with the previous maps that were made using only porosity-log data.

Many of the reservoir properties are not continuous but instead show areas of better reservoir quality separated by poorer areas, particularly on the margins of the field. These marginal zones of higher porosity and permeability are interpreted as being levee deposits that formed when low-density turbidity currents overtopped the channel margins and deposited sand in the generally lower-reservoir-quality interchannel areas. Some of the discontinuity between areas of better reservoir quality may be enhanced by diagenetic effects. Localized precipitation of calcite cement increases heterogeneity within the sandstones. Although the cemented zones are not interpreted as being laterally continuous between wells, their presence causes “spiky” vertical permeability trends in the reservoir. Fluid flow is likely to occur preferentially along the high permeability streaks, leaving poorly swept zones of lower permeability.

Compositional simulations of a CO₂ flood indicate that at least 10 percent of the remaining oil in place at the northern end of the Ford Geraldine unit can be recovered at breakthrough. Simulation results show that continuing the CO₂ injection beyond breakthrough can result in significant incremental oil recovery. A sensitivity study shows that oil recovery in a CO₂ flood is adversely affected by an increase in postwaterflood water saturation, reduction in injection pressure, and pressurizing the reservoir with CO₂ injection. The recovery is slightly improved by the WAG process, but the flood takes considerably longer.

The results of the simulations were used by Conoco, Inc. to perform an economic analysis of a CO₂ flood in the northern part of the Ford Geraldine unit. The economics of the project were found to be positive but did not meet Conoco's profitability criteria (K. R. Pittaway, written communication, 1997). Conoco has therefore elected not to continue into Phase 2 of the project.

INTRODUCTION

Summary of Project Objectives

The objective of this project is to demonstrate that detailed reservoir characterization of slope and basin clastic reservoirs in sandstones of the Delaware Mountain Group in the Delaware Basin of West Texas and New Mexico is a cost effective way to recover a higher percentage of the original oil in place through strategic placement of infill wells and geologically based field development. One of the most important lessons learned from 75 years of reservoir development experience in the Permian Basin is that comprehensive geologic and engineering investigations of reservoir character (that is, description of the geologic controls on engineering attributes and the effects of internal heterogeneity on the distribution of hydrocarbons) are essential prerequisites for designing efficient production strategies (Ruppel and others, 1995). Primary production, infill drilling, waterflooding, and enhanced oil recovery operations undertaken without thorough reservoir characterization will not realize maximum potential production. The goal of this project is to demonstrate that reservoir characterization incorporating 3-D seismic and reservoir simulation can optimize infill drilling and enhanced oil recovery (such as CO₂ flood) projects and thus increase production and prevent premature abandonment of slope and basin clastic reservoirs in mature fields.

Project Description

This project involves reservoir characterization of two Late Permian slope and basin clastic reservoirs in the Delaware Basin, West Texas. The fields investigated were Geraldine Ford and Ford West (4100) fields in Reeves and Culberson Counties, Texas (Dutton and others, 1997a). Work performed this year focused on Geraldine Ford field because it has more complete data available than Ford West field, thus allowing a more detailed reservoir model to be developed. In addition, Geraldine Ford field has a larger volume of oil in place than Ford West field, making it the better target for enhanced recovery.

Geraldine Ford field, which is operated as the Ford Geraldine unit by Conoco, Inc., produces at 2,600 ft from a stratigraphic trap in the upper part of the Bell Canyon Formation of the Delaware Mountain Group. The 99 million bbl of original oil in place (Pittaway and Rosato, 1991) makes it the largest Delaware Mountain Group field in the basin. Thirteen years of primary production and 28 years of secondary (waterflood) and tertiary (CO₂ flood) development in the Ford Geraldine unit have resulted in a recovery efficiency of only 28%. This recovery efficiency is higher than that of most reservoirs in this play because the Ford Geraldine unit is one of the first to undergo tertiary development. Thus, secondary and tertiary recovery programs at Ford Geraldine unit resulted in incremental recovery, but overall recovery efficiency remains poor because reservoir heterogeneity causes serious producibility problems. Because of the low recovery efficiencies, much of the oil will remain in the ground in this and other Delaware Mountain Group fields unless new recovery methods are developed.

Project Structure

Project objectives are divided into two major phases. The objective of the reservoir characterization phase is to provide a detailed understanding of the architecture and heterogeneity of the Ford Geraldine unit and Ford West field using 3-D seismic data, high-resolution sequence stratigraphy, subsurface field studies, outcrop characterization, and other

techniques. On the basis of the reservoir characterization, an area of approximately 1 mi² at the northern end of the Ford Geraldine unit was chosen for reservoir simulation of a CO₂ flood.

The objectives of the implementation phase of the project are to (1) apply the knowledge gained from reservoir characterization and simulation studies to increase recovery, (2) demonstrate that economically significant unrecovered oil can be recovered by a CO₂ flood, and (3) test the accuracy of reservoir characterization and flow simulation as predictive tools in resource preservation of mature fields. Through technology transfer workshops and other presentations, the knowledge gained from this project can then be applied to increase production from the more than 100 other Delaware Mountain Group reservoirs.

Summary of Progress

This annual report documents technical work during the third year of the contract, from April 1997 through March 1998. Work performed this year focused on completing reservoir characterization of the Ford Geraldine unit and performing a simulation of a CO₂ flood in the northern part of the unit. Major tasks accomplished this year were (1) completing the study of a Bell Canyon reservoir analog exposed in outcrop, (2) improving the subsurface mapping of reservoir properties in the Ford Geraldine unit, (3) performing a compositional simulation of a CO₂ flood in the northern part of the unit, and (4) studying sensitivity of a CO₂ flood to various geologic and engineering factors.

DELAWARE MOUNTAIN GROUP OIL PLAY

The Permian Basin is the most prolific, and one of the oldest, oil-producing basins in the continental United States, and it still contains an estimated 35 billion barrels (Bbbl) of remaining mobile oil (Holtz and Major, 1994). The Delaware Basin, the western subbasin of the Permian Basin, is located in west Texas and southeastern New Mexico (fig. 1) and extends from Pecos County, Texas northward to Eddy County, New Mexico. Upper Permian (Guadalupian) Delaware

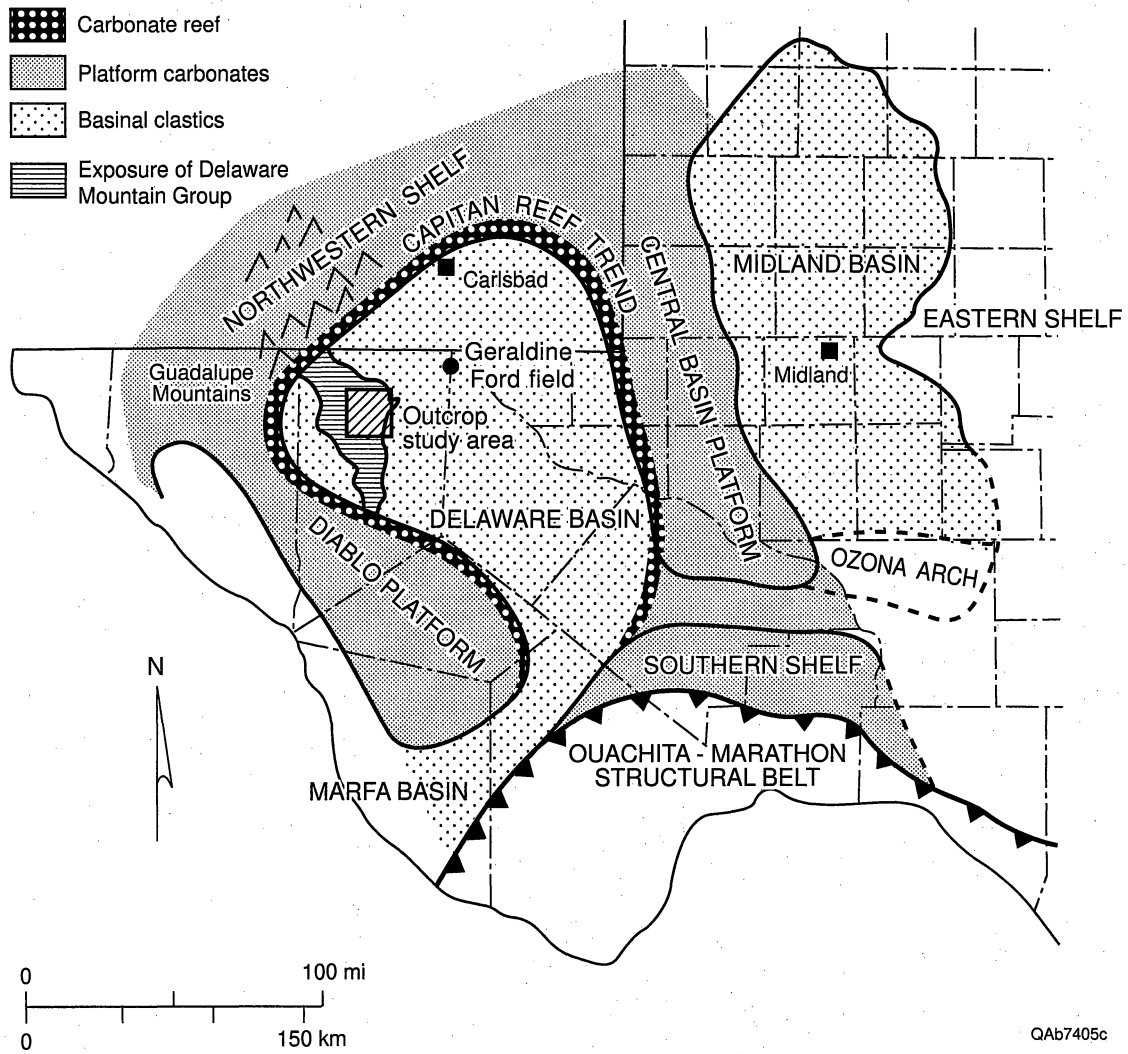


Figure 1. Map showing location of Delaware Basin and paleogeographic setting during the late Permian. Present-day exposures of the Delaware Mountain Group are superimposed onto the paleogeographic map. Geraldine Ford field is on the boundary of Reeves and Culberson Counties, Texas.

Mountain Group strata (fig. 2) comprise a 3,500-ft-thick succession of slope and basin reservoirs in the Delaware Basin that are important contributors to Permian Basin production (Gardner, 1997b). Fields in the Delaware play produce oil and gas from slope and basin sandstone deposits that form long, linear trends. Structural contours on limestone beds capping the reservoir sandstones indicate monoclinial dip to the east and northeast. Most hydrocarbons are trapped by stratigraphic traps formed by an updip lateral facies change from higher permeability reservoir sandstones to low permeability siltstones. Fields show minor structural closure because linear trends of thick sandstones formed compactional anticlines by differential compaction during burial (Ruggiero, 1985, 1993).

Individual fields in the Delaware play produce from lenticular sandstone bodies interbedded vertically with organic-rich siltstone, pelagic carbonate mudstone, and laminated siltstone. Reservoir sandstones are depositionally and diagenetically complex, with heterogeneity demonstrated by an average 14% recovery efficiency from fields in the play.

The Delaware play is now mature and has a drilling history of progressive deeper pool discoveries in the Bell Canyon, Cherry Canyon, and Brushy Canyon Formations (fig. 2). In the 1920's, reservoirs were discovered in the Ramsey sandstone, the upper part of the Bell Canyon Formation. Geraldine Ford field, located about 2 mi south of the Texas–New Mexico state line in Reeves and Culberson Counties, Texas (fig. 1), was discovered in 1956 from shallow (2,600 ft) Ramsey sandstone reservoirs. The field was unitized in 1958 and is operated by Conoco as Ford Geraldine unit. As of March, 1997, cumulative production was 28 MMbbl of the 99 MMbbl of original oil in place. By the late 1970s, more than 100 fields produced from the Bell Canyon Formation (Williamson, 1977, 1978).

In the 1950's, deeper reservoirs were discovered in the Cherry Canyon Formation (fig. 2). By 1985, 39 Cherry Canyon fields had been developed (Linn, 1985). Ford West (4100) field, which was discovered in 1976 as an updip extension of Geraldine Ford field, produces from the upper part of the Cherry Canyon Formation and the lower Bell Canyon Formation. More recently, deeper pool discoveries have been made in the Brushy Canyon Formation (DeMis and

Cole, 1996). Deeper pool potential exists in many Delaware Mountain Group fields. Early exploration typically drilled only into the upper part of the Bell Canyon Formation, leaving untapped many deeper horizons in densely drilled fields (Gardner, 1992 and 1997a).

The Delaware Basin is an ideal location for a reservoir-characterization study of slope and basin clastic reservoirs. Seventy years of exploration and development in the Delaware play provides a wealth of subsurface data. Furthermore, nearby outcrops showing the internal structure of reservoir strata are present within 24 miles of Geraldine Ford field (fig. 1). The present Delaware Basin configuration approximates the upper Permian depositional basin. Geraldine Ford field is located near the paleogeographic center of the upper Permian Delaware Basin, about 65 miles from the paleo-shelf margin. The outcrops selected for this study are also from a basin-floor setting, many miles from the shelf edge.

OUTCROP CHARACTERIZATION OF BELL CANYON SANDSTONE RESERVOIR ANALOGS

Introduction

Additional outcrop characterization during the past year has refined the depositional model for upper Bell Canyon sandstones and siltstones (Barton, 1997). The outcrops were examined to provide unambiguous and high-resolution information on sandstone and seal architecture that could then be used to interpret the reservoir at Ford Geraldine unit and other Delaware Mountain Group fields. The field work was concentrated on exposures of the Bell Canyon Formation that were deposited in the deep-water Delaware Basin during the late Permian. The origin of Bell Canyon Formation sandstones has been a source of controversy, with depositional interpretations ranging from contourites, turbidity-current deposits, and saline-density-current deposits. The outcrop study focuses on a stratigraphic unit in the Bell Canyon Formation that is analogous to the highly productive Ramsey Sandstone. This unit shows complex stacking patterns and facies

changes that are related to the progradation and retrogradation of a system of channel levees and attached lobes (Barton, 1997).

Regional Setting and Stratigraphic Framework

The Bell Canyon Formation is a deep-water siliciclastic unit that accumulated in the Delaware Basin during the Late Permian. The Delaware Basin, located in West Texas and southeast New Mexico, is a circular basin about 120 mi in diameter (fig. 1). The basin was semirestricted, with its southern end partly open to the seaway and its northern end surrounded by an extensive carbonate shelf and reef complex. Shelf-to-basin-floor correlations of time-equivalent strata indicate water depths were between 1,000 and 2,000 ft during deposition of the Bell Canyon Formation (Kerans and others, 1992).

The Bell Canyon is the youngest formation in the Delaware Mountain Group, which also includes, in ascending stratigraphic order, the Brushy Canyon and Cherry Canyon Formations (fig. 2). The Bell Canyon Formation is composed of sandstones, siltstones, and minor amounts of carbonate. Detrital clay-sized material is almost completely absent. Maximum thickness of the Bell Canyon Formation is about 1,200 ft near the center of the basin. Near the margins of the basin it interfingers with and onlaps adjacent carbonate slope deposits of the Capitan Formation. Time-equivalent shelf strata include, in ascending stratigraphic order, the Seven Rivers, Yates, and Tansill Formations (Kerans and Fitchen, 1995). The Bell Canyon Formation is overlain by gypsum deposits of the Castile Formation.

Basinal limestones and organic-rich siltstones divide the Delaware Mountain Group at several scales into cyclic successions of sandstone and siltstone (Jacka and others, 1968; Meissner, 1972, Jacka, 1979; Gardner, 1992, 1997a and b). At least three scales, classified as low, intermediate, and high, have been recognized. At the largest scale (low order), thick limestones or organic-rich siltstones that are basinwide in extent, divide the Delaware Mountain Group into three clastic wedges. These clastic wedges are 1,000 to 1,500 ft thick and roughly

approximated by the Brushy Canyon, Cherry Canyon, and Bell Canyon Formations. At the intermediate scale, limestones and multiple, thin, organic-rich siltstones subdivide each clastic wedge into sandstone bodies that are 100 to 300 ft in thickness. The Bell Canyon Formation contains five limestone tongues that, from oldest to youngest, include the Manzanita, Pinery, Rader, McCombs, and Lamar (fig. 2). These limestone tongues extend basinward from the shelf margin and divide Bell Canyon into five sandstone bodies or intermediate cycles. The sandstone bodies are further subdivided by thin organic-rich siltstones into units referred to as high-order cycles (Gardner, 1992, 1997a and b). The high-order cycles are 20 to 100 ft thick and tend to show a trend of upward-increasing followed by upward-decreasing sandstone content.

The cyclic interbedding of sandstones and siltstones with organic-rich siltstones and limestones has been interpreted to record frequent changes in relative sea level (Meissner, 1972). During highstands in relative sea level, sands were trapped behind a broad, flooded shelf and prevented from entering the basin. Thin, widespread, organic-rich siltstones accumulated on the basin floor through the slow settling of marine algal material and airborne silt. Basinal limestones were deposited by sediment gravity flows that originated from the slumping of carbonate debris along the flanks of a steep, rapidly aggrading carbonate platform. During subsequent lowstands in relative sea level the carbonate shelf was exposed and sandstones bypassed to the basin floor. Textural characteristics of the sands, such as the absence of clay-sized material, and the lack of channels on the shelf suggest wind was an important agent in transporting the sands to the shelf margin (Fischer and Sarnthein, 1988; Gardner 1992, 1997a). Paleocurrent indicators suggest the sands entered the basin from the Northwest Shelf and Central Basin Platform.

Models of Basinal Sandstone Deposition

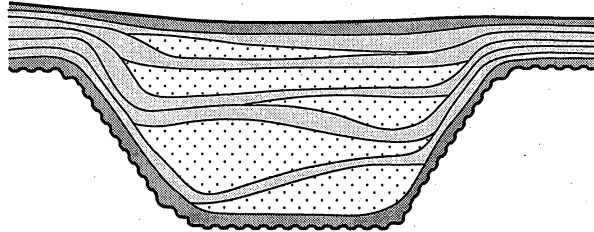
Production from many Bell Canyon reservoirs comes from the distal end of long, linear sandstones bodies that extend basinward from the shelf margin (Williamson, 1978). Although

this feature has been recognized for some time, the processes that deposited the sandstone bodies have been the source of considerable controversy. Most investigators agree that the sands were carried into the basin by density currents. However, disagreement exists over whether the currents derived their higher densities from a high suspended sediment load (sediment gravity flow) or high salinities (saline density current). The significance of the disagreement has importance with regard to predicting sandstone distribution and reservoir architecture.

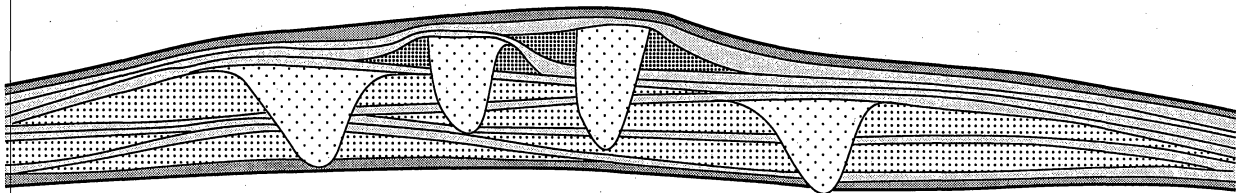
In the sediment gravity flow model, dense sediment-rich mixtures were generated on the shelf edge by the slumping of sand masses that had accumulated by eolian processes during lowstands in relative sea level (Fischer and Sarnthein, 1988; Gardner, 1992 and 1997a). Density differences between the sediment-rich mixtures and ambient waters caused them to move downslope as turbulent sediment gravity flows (Payne, 1976; Berg, 1979; Jacka, 1979; Zelt and Rossen, 1995; Bouma, 1996). The flows passed through channels and emerged on the basin floor where they spread as unconfined flows. Flows that spilled over the channels deposited sediment to form levees adjacent to the channels. The model predicts that clean channel sands are flanked by wedge-shaped levee deposits composed of interbedded sandstone and siltstone. Basinward, the channels bifurcate and terminate in broad, fan-shaped lobes of sand that are interstratified with siltstone deposited from the fallout of airborne silt or derived from density interflows. The model predicts that systematic changes in facies should be developed as the system progrades and the lobes are overlain and incised by channels and levees (Figure 3). Sandstones displaying traction-produced stratification should be rare, while structureless, graded sandstones displaying partial Bouma sequences should be relatively common.

In the saline density current model, dense saline fluids were generated behind a carbonate reef by evaporation (Harms, 1968, Harms, 1974; Williamson, 1977; Williamson, 1978; Williamson, 1979; Bozanich, 1979; Ruggiero, 1985; Harms and Williamson, 1988; Harms and Brady, 1996). The dense fluid moved down the slope and into the basin carrying with it entrained sediment. Along the way, currents scoured out channels and deposited sands in those channels during subsequent flows. Less dense flows moved into the basin as density interflows, depositing

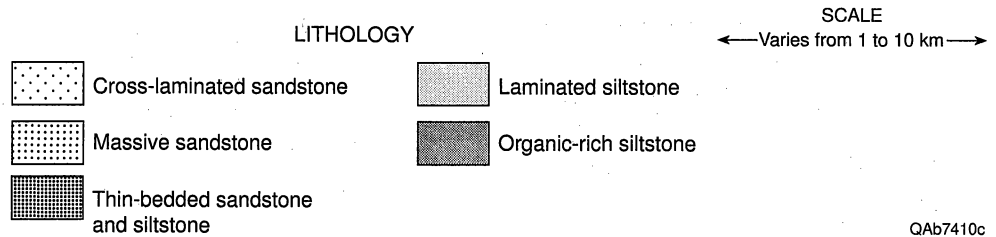
Salinity density current model – scour infilled with mantling siltstones and amalgamated channels



Sediment gravity flow composed of lobes interstratified with mantling siltstones, overlain and incised by channels with levees



Sandstones represent lobes, channels, and levees



QAb7410c

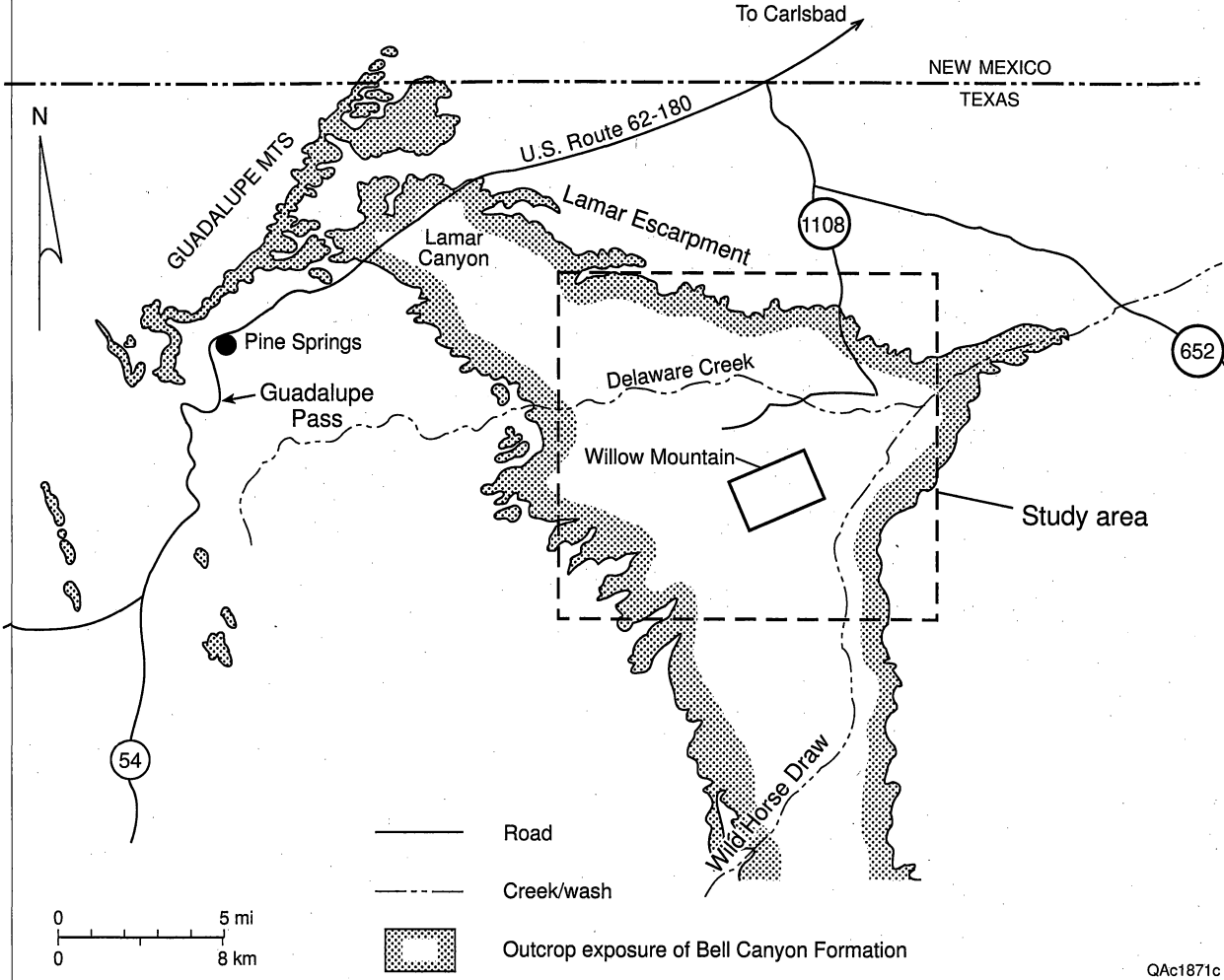
Figure 3. Sand-body architecture for turbidity-current model and saline-density-current model (from Barton, 1997).

topography-mantling siltstones from suspension. The model predicts that sandstones should be restricted to infilled scours or channels that lack adjacent levees or distal lobes. The sandstones are interstratified with topography-mantling siltstones that extend into interchannel areas (see figure 3). Sandstones should consist largely of traction-produced stratification, and systematic change in facies should be poorly developed.

Study Area

The Bell Canyon Formation is exposed in the Delaware Mountains of West Texas (fig. 4). The Delaware Mountains extend southeast from the southern end of the Guadalupe Mountains for a distance of about 50 mi. The trend of the Delaware Mountains roughly parallels the direction of sediment transport to the south and southeast in this part of the Delaware Basin (Williamson, 1979). The Guadalupe Mountains define the northwest margin of the basin and expose deposits of an ancient carbonate platform. Bedding surfaces within the carbonate reef and slope deposits dip steeply into the basin, dropping as much as a 1,000 ft over the distance of less than a mile.

The outcrops examined in the study are located on Cowden Ranch, Culberson County, Texas, about 20 mi southeast of the Guadalupe Mountains (Barton, 1997). Most of the outcrop work focused on stratigraphic relationships within the uppermost high-order cycle in the interval between the McCombs and Rader Limestones (fig. 2). The top of this high-order cycle is represented by the McCombs Limestone, and the base by the first regionally correlative organic-rich siltstone. The scale and position of this stratigraphic unit are directly analogous to the highly productive Ramsey interval that correlates with the uppermost high-order cycle below the Lamar Limestone (fig. 2).



QAc1871c

Figure 4. Map showing location of study area and outcrop exposure of Bell Canyon Formation, (after Barton, 1997).

Sedimentology

The outcrops were characterized by mapping facies and bounding surfaces (Barton, 1997). The data consist of measured logs and photomosaics that provide complete coverage of the outcrops. Facies is a widely used term for grouping rock types on the basis of origin or any number of similar characteristics. Here, facies are used to define groups with similar sedimentary features at the laminae to bed scale. Bounding surfaces represent breaks in sedimentation that may be erosional or conformable. They record a hierarchy of events that range in scale from individual laminae to basinwide unconformities or flooding surfaces. Bounding surfaces can be classified according to order and type. The mapping of facies together with bedding surfaces has proved to be a useful approach for dividing ancient rocks into sediment bodies that are depositionally related and are characterized by their geometry, lithology, bedding architecture, and scale (Allen, 1982, Friend, 1983, Miall, 1985).

Facies

Six facies are described and categorized by number: facies 1 is an organic-rich, laminated siltstone; facies 2 is a massive organic-rich siltstone; facies 3 is a laminated siltstone; facies 4 is composed of thin-bedded sandstones and siltstones that are graded or display partial Bouma sequences (Bouma, 1962); facies 5 is a structureless sandstone; and facies 6 is a large-scale, cross-laminated sandstone (Barton, 1997). The six facies are summarized in Table 1. Although most of the sandstones are not graded and do not display classic turbidite-bedding characteristics in the sense of the Bouma sequence, they are interpreted to have been deposited from turbulent sediment gravity flows. This interpretation is based on a variety of features that include bedding architecture, the lack of lamination, and indications of rapid deposition from highly turbulent flows. The absence of lamination or grading may reflect the uniform grain size of the sediment-rich fluids and the rapid fallout of grains from suspension during deposition (Lowe, 1982; Kneller, 1996). The lack of complete Bouma sequences may be due to the fact that the lithologic

Table 1. Facies characteristics of Bell Canyon sandstones and siltstones.

Facies	Description	Bed Aspect	Transport Mechanisms	Depositional Setting
Facies 1 Massive, organic-rich siltstone	Dark-gray to black. Lacks extremely fine, parallel lamination of facies 1.	Thickness: 0.03 ft to 1.0 ft Length: 30 ft to 3000 ft	Suspension deposition from turbidity current. Similar to E division of Bouma sequence.	May occur as discontinuous drapes along the base of channels or along the top of sandstone beds.
Facies 2 Finely laminated, organic-rich siltstone	Dark-gray to black. Often interbedded with centimeters-thick volcanic ash beds.	Thickness: 0.03 ft to 3.3 ft Length: 10's miles	Suspension fallout of pelagic matter and airborne silt.	Deposition during prolonged periods of sediment starvation.
Facies 3 Laminated siltstone	Light-tan to brown. Extremely even parallel lamination that is a fraction of a millimeter to a few millimeters thick.	Thickness: 0.03 ft to 10 ft Length: Miles in length	Regular fluctuations in the settling of marine algal material and airborne silt, or silt derived from low-density interflows.	Occur as laterally extensive sheets that mantle underlying deposits.
Facies 4 Thin-bedded sandstones and siltstones	Current lamination, consisting of ripple drift and to a lesser extent horizontal, are the dominated sedimentary structures.	Thickness: 0.2 ft to 3.3 ft Length: 30 to 300 ft	Deposition from waning turbidity currents. Similar to BCD division of Bouma sequence.	Deposited along flanks of channel by flows that spill over channel margin.
Facies 5 Structureless sandstone	Sandstones lack lamination and have a massive appearance. Floating siltstone clasts, water escape features, and load structures are other common features.	Thickness: 0.3 ft to 7 ft Length: 100's to 1000's ft	Rapid deposition from sediment gravity flow. Equivalent to A division of Bouma sequence.	Deposited at mouths of channels and in overbank areas by unconfined flows. May also occur within upper channel fill.
Facies 6 Cross-laminated sandstone	Dune-scale cross-lamination that varies from infilled scours to climbing dunes.	Thickness: 0.7 ft to 66 ft Length: 10's to 100's ft	Deposition from confined, turbulent, sediment gravity flows.	Largely confined to channels.

assemblages that make up a Bouma sequence are areally distributed according to Walther's Law, so that finding true, complete Bouma sequences is difficult (Kneller, 1996).

Facies 1 is a massive, organic-rich siltstone that lacks the extremely fine, parallel lamination of facies 2. It varies in thickness from one inch to 1 ft and often occurs as a relatively thin, discontinuous drape at the base of a channel or top of a sandstone bed. Contacts with other facies vary from abrupt to gradational with gradational contacts occurring at the top of graded and ripple-laminated sandstone beds. Burrowing is common near the top of the bed. The organic-rich siltstones are interpreted to record the fallout from suspension of silt and organic matter from a turbulent sediment gravity flow. The facies is similar to the E division of the Bouma sequence.

Facies 2 is a dark-gray to black, finely-laminated, organic-rich siltstone. The fine laminations are the result of tan to light-gray siltstone laminae that are a fraction of a millimeter thick. Organic content varies systematically depending on regular increases or decreases in the thickness of the organic-poor siltstone laminae. Analysis of the organic matter has shown that the majority is derived from marine algal matter (Williamson, 1978; Bozanic, 1979). Fossilized bones or teeth, nodular concretions of chert, siderite, and phosphate, and thin, centimeter-thick beds of volcanic ash are common constituents. Facies 2 displays gradational contacts with facies 3 and occurs at the top of upward-fining, or at the base of the upward-coarsening, successions of laminated siltstone. Facies 2 is interpreted to have been deposited by the settling of marine algal material and airborne silt. The presence of fossils and volcanic ash beds suggests it was deposited during a prolonged period when coarser particles were prevented from entering the basin (Gardner, 1992).

Facies 3 is a laminated siltstone that is similar to facies 2 but contains considerably less organic matter. The dominant sedimentary structure is extremely even, parallel lamination produced by the regular alteration of dark, organic-rich siltstone laminae that are < 0.1 inch thick, with tan to light-gray siltstone laminae that are from < 0.1 to 0.1 inch thick. Individual laminae are graded with the transition from light to dark laminae recording a decrease in grain size and an increase in organic matter. Rarely, the siltstone laminae are truncated by shallow

scours displaying 0.1 inch of relief. The scoured surfaces are usually draped by overlying laminae but may occasionally be overlain by isolated current ripples that are widely spaced, have rounded profiles, and are less than 0.4 inch thick. Burrowing is not common and is usually restricted to horizontal bedding planes. Laminae are often organized into sets that are 1 inch to 1 ft in thickness and show a progressive increase or decrease in laminae thickness or organic content. In turn, the sets may combine to form upward-fining or upward-coarsening successions that are as much as several meters in thickness. The laminated siltstones occur as laterally extensive sheets that mantle underlying deposits. Facies 3 is interpreted to record regular fluctuations in the settling of marine algal material and airborne silt or silt derived from low-density interflows. The presence of truncated laminae and current ripples suggests that weak bottom currents occasionally reworked the sediments.

Facies 4 consists of thin-bedded sandstones and siltstones that display an abundance of current lamination (table 1). Sandstone beds are 1 inch to 1 ft thick and often display erosional bases. Individual beds usually grade upward from sandstone at the base to siltstone at the top. The most common sequence of stratification types is similar to the BC or BCD division of the Bouma sequence with beds beginning with a horizontally laminated sandstone or ripple-drift, cross-laminated sandstone, and passing upward into a wavy-laminated siltstone. Graded sandstones at the base of the bed are rarely observed. The sequence of stratification types and abundance of ripple-drift cross-lamination indicates facies 4 was deposited from waning, turbulent sediment gravity flows.

Facies 5 consists of sandstones that are structureless or massive in appearance. Sandstone beds are 1 to 10 ft thick and display abrupt, nonerosional bases. Flame structures and convoluted bedding that are contemporaneous with deposition are common at the base of many sandstone beds. Dewatering features that include dish and pillar structures are common in the upper portions of the beds. Other common features include siltstone clasts that float in a matrix of fine sand and are concentrated near the top of the bed. The lack of lamination, presence of floating

clasts, and abundance of water escape and load structures suggest the sandstones were rapidly deposited from high-density sediment gravity flows (Lowe, 1982).

Facies 6 consists of sandstones displaying dune-scale cross-lamination that varies from infilled scours to climbing dunes. The infilled scours are scoop-shaped with sides inclined up to 75 degrees in dip. In plan view the scours have an elliptical shape that is about 4 ft long and 2 ft across. Laminae may onlap the sides of the scour or overlap the margins. The climbing, dune-scale cross-lamination, often referred to as a megaripple drift, is similar to a ripple-drift cross-lamination, only larger in scale. The most common form showed full preservation of laminae on the stoss side of the dune. Laminae on the lee side of the bed form display tangential bases suggesting the presence of turbulent eddies. The cross-laminated sandstones are restricted to channel fills. The scale, form, and occurrence of the cross-lamination suggests the sands were deposited from confined, highly turbulent sediment gravity flows.

Depositional Elements

Depositional elements are sediment bodies defined by their bounding surfaces, geometry, bedding architecture, and facies. They represent a particular process or suite of processes occurring within a depositional system (Miall, 1985). Depositional elements recognized within the Bell Canyon include: (1) channels; (2) winged channels; (3) lobes; (4) interchannel lobes; (5) sheets of laminated siltstones; and (6) sheets of organic-rich siltstone (Barton, 1997). The geometry, dimensions, and lithology of the six depositional element are summarized in table 2.

The channels have a convex-downward geometry. They are bounded at the base by an erosion surface and composed largely of cross-laminated sandstone. The bodies are 10 ft to 60 ft thick and 30 ft to 3,000 ft wide. Individual channels are often highly truncated and may amalgamate to form a composite body with a larger aspect ratio (50 to 100) than an individual channel-form body. The bodies are interpreted as incised channel fills.

The winged-channel elements have a body with a biconvex geometry that is flanked on both sides by beds which gradually thin and taper away from the body. The bodies have an erosive

Table 2. Characteristics of depositional elements.

Depositional element	Geometry	Dimensions: T-Thickness W-Width AR-Aspect Ratio	Lithology	Depositional Setting/Process
Condensed section	Sheet	T: 0.2 to 2 ft W: Miles	Facies 2 Gradational contacts with facies 3.	Deposition of pelagic material during prolonged period of sediment starvation. Bound stratigraphic cycles at multiple scales.
Siltstone sheet	Sheet	T: 1-10 ft W: Miles	Facies 3 May form upward-coarsening or -fining successions.	Topography mantling siltstones deposited by density interflows or airborne silt.
Lobe	Broad lens	T: 3-30 ft W: 0.5--6 miles AR: 100-10,000	Facies 5 Facies 6 near the top of body. Abrupt, nonerosive basal contact.	Sandy lobe deposited by unconfined sediment gravity flows at mouth of channel.
Channel	Convex downward	T: 10--60 ft W: 300-3,000 ft AR: 10-100	Facies 6 Facies 5 in upper portion of fill. Facies 1 may drape base of channel.	Incised channel or amalgamated channels.
Winged channel	Biconvex body with wings	Channel: T: 10-60 ft W: 60-700 ft AR: 10-20 Wings: T: 3-20 ft W: 700-7,000 ft AR: 100-1,000	Channel fill composed of facies 6. Wings composed of facies 4. Facies 1 may drape base of channel.	Aggradational channel levee.
Inter-channel lobe	Irregular	T: 3-30 ft W: 3,000 ft AR: 100-10,000	Facies 5 Facies 6 near top of body. Abrupt, nonerosive basal contact.	Overbank sandstones deposited in topographic lows by unconfined sediment gravity flows.

base and are composed largely of cross-laminated sandstones. They vary in size from 10 ft to 60 ft thick and 30 ft to 700 ft wide. The flanking wings have a wedge-shaped geometry with an aspect ratio of around 100. Thickness varies from 3 to 20 ft and width from 700 to 7,000 ft. The wings consist largely of thin-bedded sandstones and siltstones that tend to become finer grained farther from the channel. Paleocurrents within the wings deviate by about 15 degrees away from the axis of the channel. Bedding features indicate that the biconvex bodies are aggradational channel fills and the wings are adjacent levees that maintained the channel margins (Mutti and Normark, 1987). The beds are interpreted to have been deposited by turbidity currents that spilled over the margin of the channel.

The broad lens-shaped bodies generally lack an erosive base and are composed chiefly of medium- to thick-bedded massive sandstones. Thicknesses range up to 30 ft with aspect ratios on the order of 100 to 10,000. The geometry and abundance of structureless sandstone suggest the lens-shaped bodies were deposited as sandy lobes at the mouth of channels by unconfined, highly depletive sediment gravity flows.

The irregularly shaped sandstone bodies displayed features that are similar to the lens-shaped bodies. They lack an erosive base and consist chiefly of massive sandstones with lesser amounts of cross-laminated sandstones. Width-to-thickness ratios, however, are poorly correlated, and geometry appears to be closely associated with underlying topography. Stratigraphic relationships indicate that they are contemporaneous with, or succeed, associated channel-levee deposits. Features of the sandstone and bedding relationships indicate the irregularly shaped bodies were deposited as interchannel lobes within topographic lows that existed between adjacent channel levees.

The laminated siltstones occur as sheets that mantle underlying deposits. The sheets are less than 1 ft to more than 10 ft thick. Over a distance of 3 miles they displayed little variation in thickness except where they had been incised by overlying channels. The sheets of laminated siltstone were not observed to drape a channel base/margin or occur as part of a channel fill. The uniform thickness and lateral extent suggest the sheets were deposited by airborne silt or laterally extensive, low-density interflows.

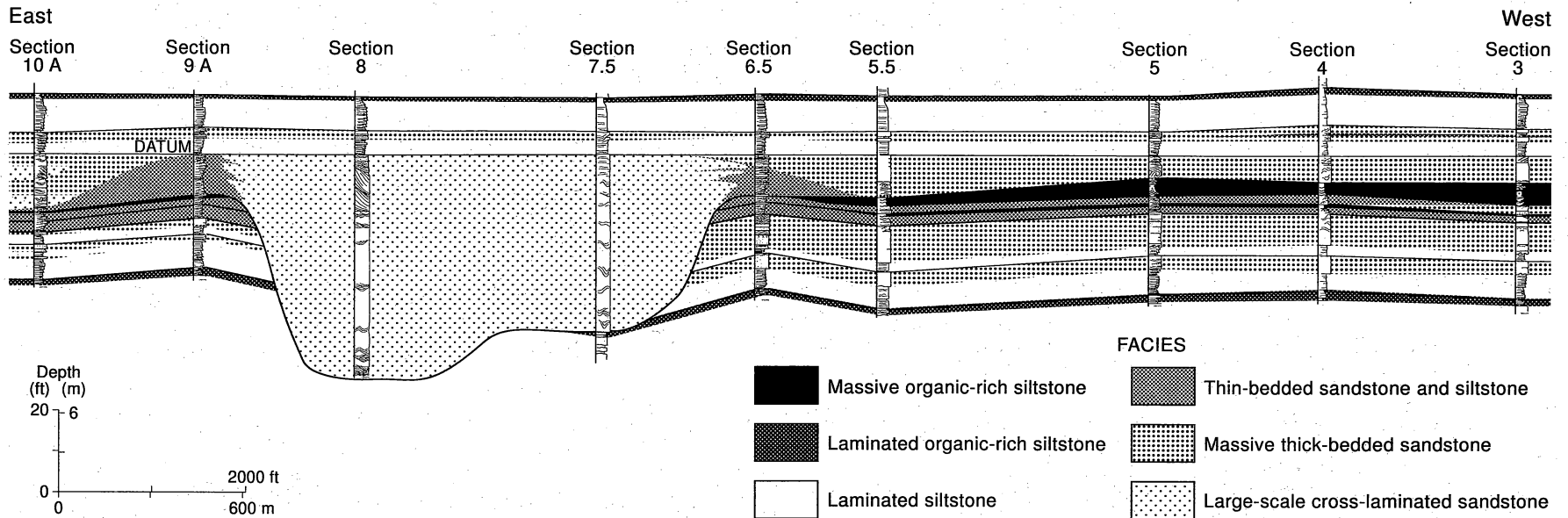
The sheets of organic-rich siltstones are similar to the sheets of laminated siltstone but are thinner and less common. They occur at the tops of upward-fining successions or at the bases of upward-coarsening successions of laminated siltstone. The organic-rich siltstone sheets are interpreted as condensed sections deposited by the slow settling of marine algal matter during a prolonged period when the basin was starved of sediment. Their distinctive lithology and lateral extent make them excellent correlation markers.

The depositional elements are organized in a systematic fashion to form cyclic successions referred to as high-order cycles. The cycles are bounded by organic-rich siltstones that display gradational contacts with overlying and underlying laminated siltstones. Laminated siltstones at the base of the cycle coarsen upward and are interstratified with broad, lens-shaped sandstone bodies. The succession is locally incised and replaced by amalgamated channels that pass upward into winged channel-form bodies interstratified with irregularly shaped sandstone bodies. The winged channels display cross-cutting relationships, and they stack vertically and laterally to form multistoried complexes. Channel orientation within a complex varies by as much as 90 degrees. An upward-fining succession of laminated siltstones interstratified with broad, lens-shaped sandstone bodies abruptly overlies the deposits and caps the cycle.

The high-frequency cycle is interpreted to record deposition from a system of channel levees with distal lobes (Barton, 1997). The multistoried channel complex records repeated episodes of channel aggradation and avulsion. The systematic change in cycle architecture indicates the system prograded into the basin, aggraded, and then retrograded. Bounding, organic-rich siltstones record periods when sediment was prevented from entering the basin.

Willow Mountain High-Order Cycle

The stacking pattern of channels and lobes in one high-order cycle was documented at Willow Mountain over an area of several square miles (fig. 4) (Barton, 1997). The high-order cycle is 45 to 75 ft thick and is bounded by thin, 1- to 2-ft-thick, organic-rich siltstones (fig. 5).



QAb9692(a)c

Figure 5. Cross section based on outcrop measured sections from Willow Mountain showing distribution of facies and traces of key surfaces within a single high-order cycle, Bell Canyon Formation (from Barton, 1997).

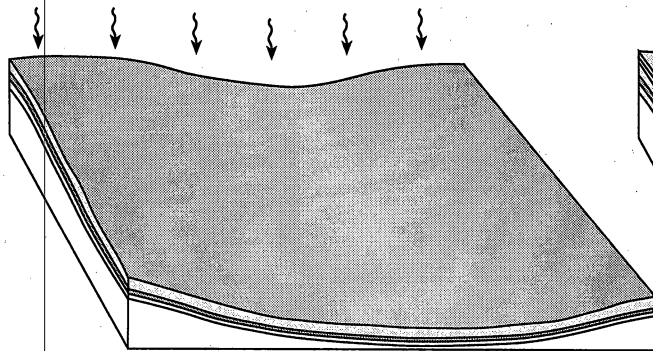
The bounding, organic-rich siltstones display transitional contacts with laminated siltstone and are traceable across the entire study area except where the basal siltstone has been eroded. The cycle thickness correlated with the sandstone content, which varied from 15 to 75 percent. The cycle is composed of two to five distinct sandstones that varied in thickness from 1 to 60 ft.

Within the cycle, sandstone thickness varied systematically showing either a trend of upward bed thickening followed by bed thinning or an upward bed-thinning trend that begins with a relatively thick sandstone.

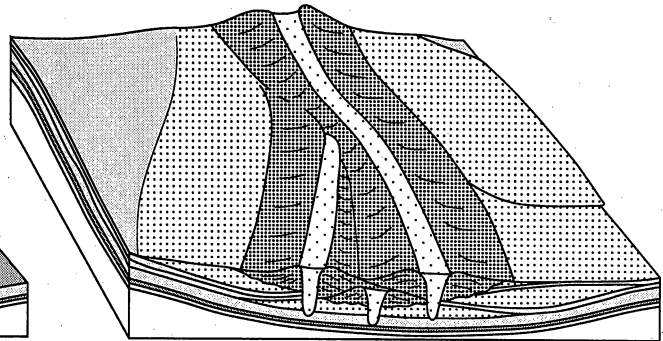
Sandstones in the upper and lower half of the cycle display a broad tabular geometry up to 10 ft thick and thin to the east. The sandstones are interstratified with sheets of laminated siltstone that are between 3 and 8 ft thick and show little variation laterally in composition or thickness. Contacts between the tabular sandstones and siltstone sheets are abrupt but nonerosional. The middle of the cycle consists of a heterogeneous mix of lenticular, channel-form bodies interstratified with wedges of thin-bedded sandstone and siltstone and broad, lenticular sandstone bodies. The channel-form bodies are up to 65 ft thick and 2,000 ft wide (fig. 5) and can be traced to the south and southeast for two miles. Within the complex, channel-stacking patterns change in a systematic fashion. In the lower part, the channel-form bodies are highly amalgamated and truncated. In the middle part, they are vertically stacked in an offset pattern and are flanked by wedges of thin-bedded sandstone and siltstone. In the upper part, the channel-form bodies bifurcate and are flanked by broadly lenticular sandstone bodies.

Facies relationships and bedding architecture suggest that the high-order cycle was deposited by a system of channel levees with attached lobes that initially prograded basinward, aggraded, then turned around and stepped back toward the shelf (fig. 6). The upward-bed-thickening succession of sandstones and siltstones was deposited during the progradational phase (step II). The vertical stack of channel-levees was deposited during the aggradational phase (step III). The system of bifurcating channels flanked by interchannel lobes was deposited during the retrogradational phase of the cycle (step IV). During the retrogradational phase a system of back-stepping lobes may also have been deposited (not shown).

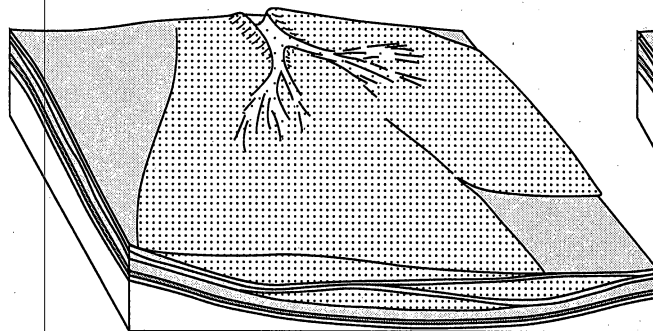
I. Deposition of silt and organic matter from suspension



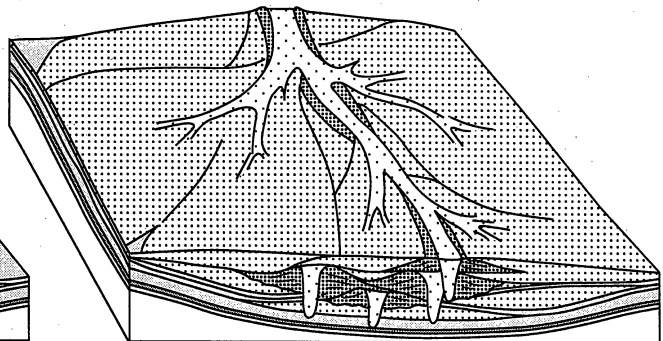
III. Deposition of channel and levee deposits/may be preceded by erosion



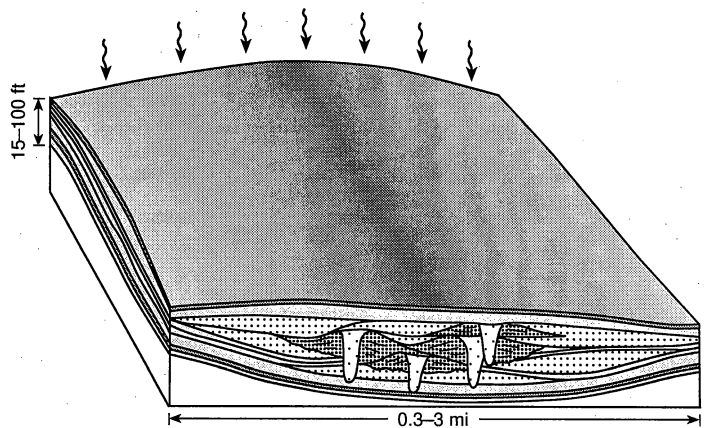
II. Deposition of lobes and laminated siltstones







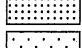
IV. Deposition of lobes in interchannel areas



V. Deposition of silt and organic matter from suspension



FACIES

-  Organic-rich laminated siltstone
-  Laminated siltstone
-  Thin-bedded, rippled, and horizontally laminated sandstone and siltstone
-  Massive sandstone
-  Cross-stratified sandstone

QAc1872c

Figure 6. Diagram illustrating depositional facies model for high-order cycle examined at Willow Mountain (from Barton, 1997).

Conclusions

The Bell Canyon Formation represents a sand-rich, deep-water system that accumulated in the Delaware Basin. Outcrop investigations of the upper Bell Canyon Formation indicate that sandstones were deposited on the basin floor by turbidity currents. Based on composition, geometry, and bounding surfaces, the fundamental depositional elements are submarine channels with levees and attached lobes. Within a high-order cycle, additional stratigraphic complexity results from abrupt lateral shifts in the stacking pattern of the submarine channel and lobe elements.

RESERVOIR CHARACTERIZATION OF FORD GERALDINE UNIT

Ford Geraldine unit includes 8,540 acres (fig. 7, table 3). The main reservoir is the Ramsey sandstone, but there is also some production from the underlying Olds sandstone (fig. 8). Ramsey sandstone is a 0- to 60-ft-thick sandstone that is bounded by the Ford and Trap laminated siltstones. In the northern part of the Ford Geraldine unit, the Ramsey is divided into two sandstones (Ramsey 1 and Ramsey 2) separated by a 1- to 3-ft-thick siltstone (SH1) (Ruggiero, 1985). In the southern part of the Ford Geraldine unit, only the Ramsey 1 sandstone is present. The Ford-Ramsey-Trap interval is interpreted as a high-order cycle that was deposited in a channel-levee and lobe system (Dutton and others, 1997a, b, and c) similar to the one that was described in outcrop at Willow Mountain.

An excellent subsurface data base for reservoir characterization was available from Ford Geraldine unit. Logs were available from 305 of the 340 wells in the field, most commonly gamma ray or gamma ray and neutron logs (fig. 9). Porosity logs were available from 182 wells, but only 38 wells have both porosity and resistivity logs (fig. 9). A total of 3,615 ft of core of the Ramsey sandstone and adjacent siltstones from 70 wells was available to the project, and these data were supplemented by descriptions of 681 ft of core from 13 additional wells by Ruggiero (1985). Core analyses (permeability, porosity, water saturation, and oil saturation) from 4,900

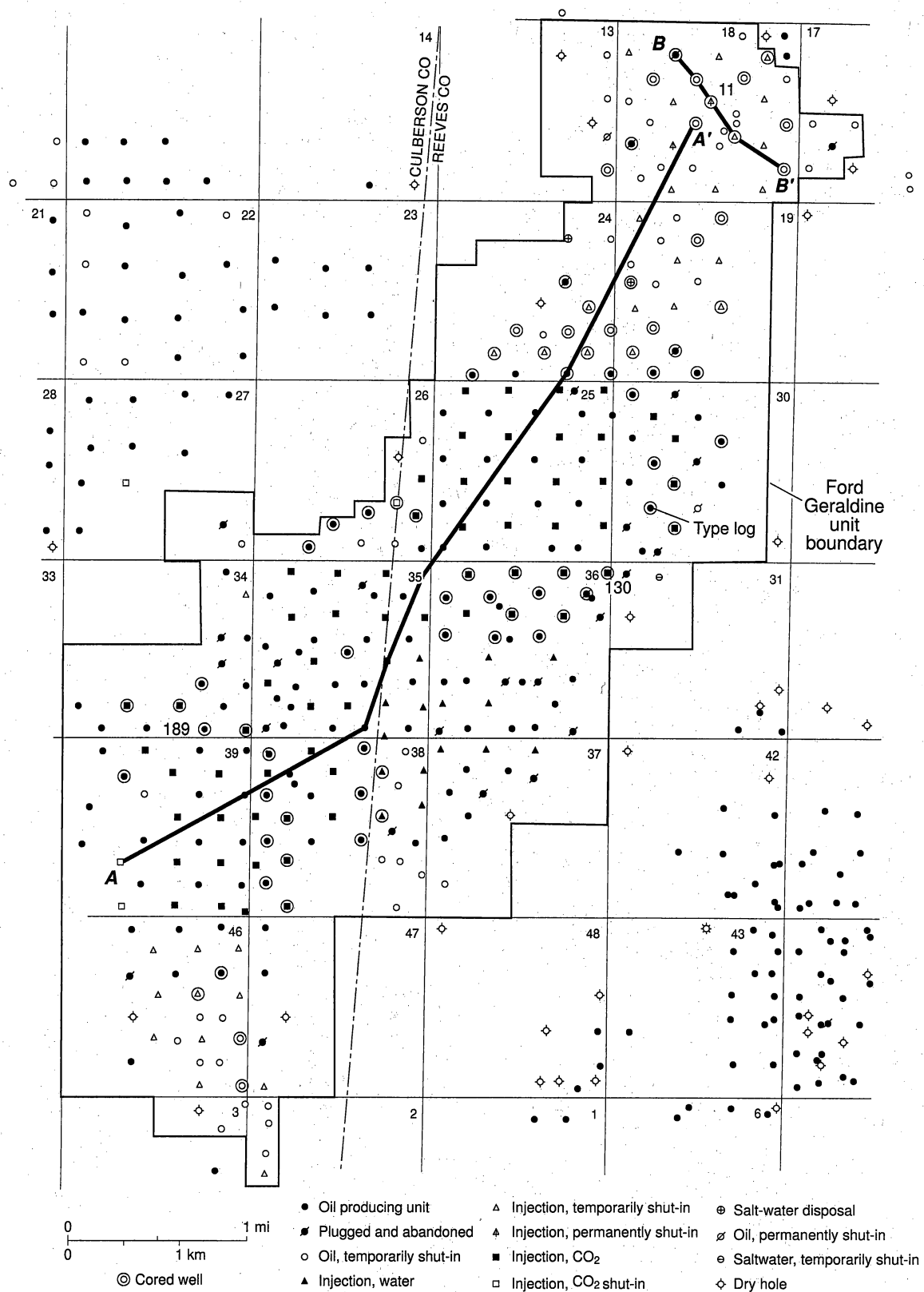
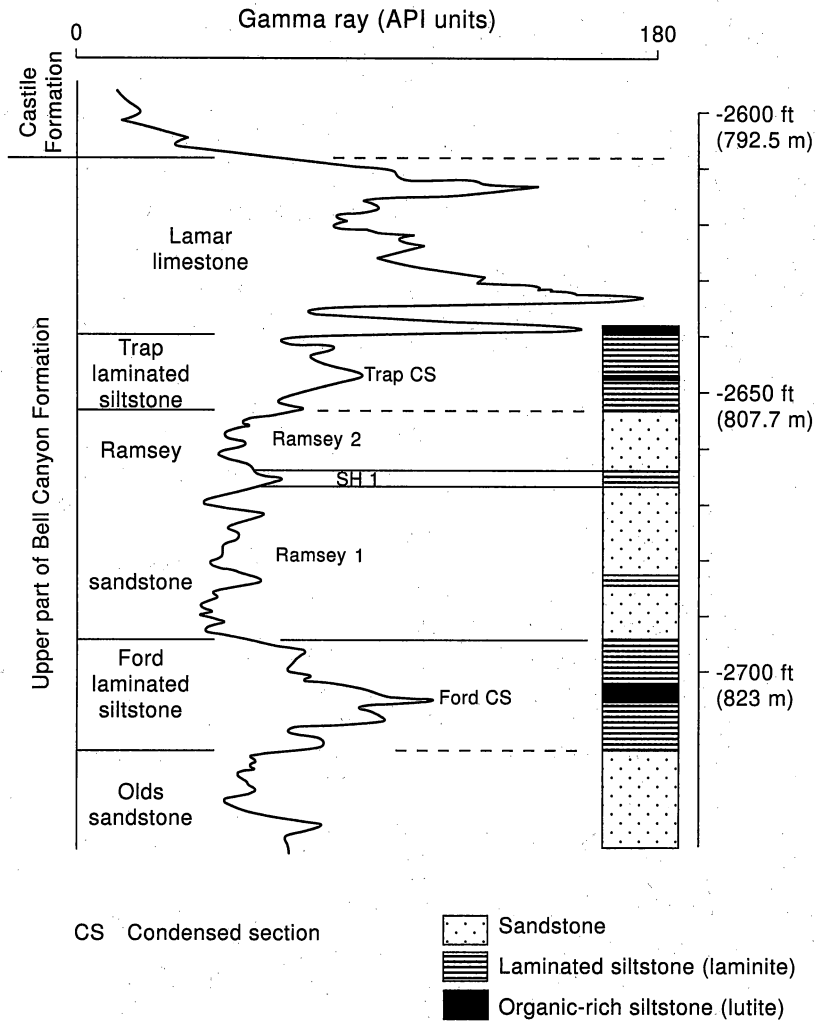


Figure 7. Status of wells in the Ford Geraldine unit and distribution of core control. Type log is shown in figure 8, cross section A-A' in figure 31, and cross section B-B' in figure 32. Core descriptions of the three wells identified by number (FGU-11, FGU-130, and FGU-189) are shown in figure 33.

Table 3. Areal and vertical description of reservoir.

Areal extent	Ford Geraldine Unit is 8540 acres
Porosity mean	22.0%
Original saturation mean at discovery	Oil 52.3% Water 47.7%
Current saturation mean	Average fieldwide oil saturation after waterflood = 38%. Average fieldwide water saturation after waterflood = 62%
Permeability mean	38.4 md (arithmetic average) 16.2 md (geometric mean)
Directional permeability (Kv/Kh)	0.01
Reservoir dip	0.7° to the northeast
Average net pay thickness	25 ft
Average gross pay thickness	31 ft
Number of reservoir layers	Two; Ramsey 1 and Ramsey 2

Ford Geraldine Unit No. 108



QAb8124c

Figure 8. Typical log from the Ford Geraldine unit well No. 108 (modified from Ruggiero, 1985). Well location is shown in figure 7.

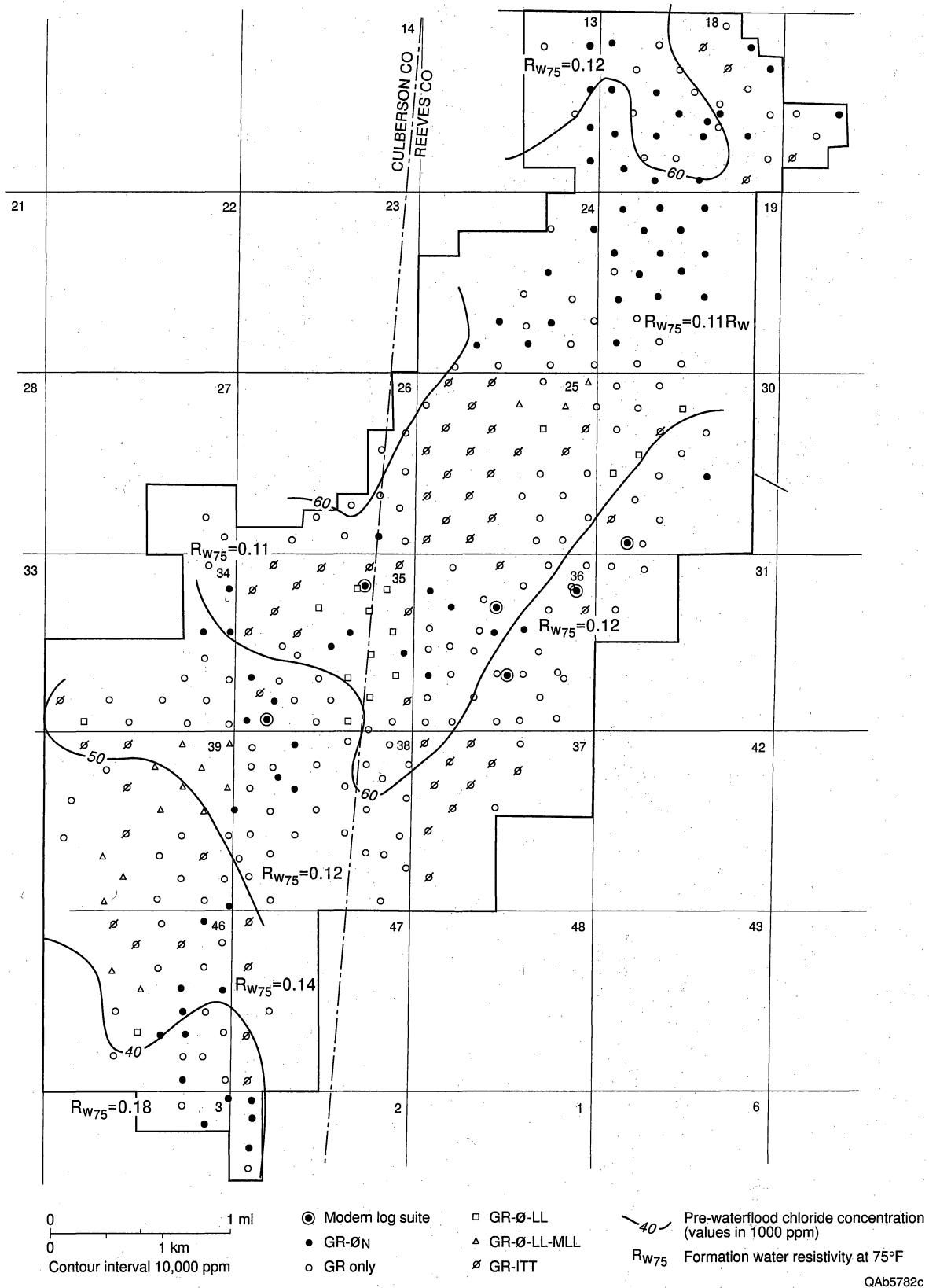


Figure 9. Distribution of geophysical log suites available in Ford Geraldine unit. Map also shows prewaterflood water-salinity distribution and formation-water resistivities (R_w) at 75°F for the Ford Geraldine unit. Water-salinity distribution from Ruggiero, 1985.

samples from 152 wells throughout the Ford Geraldine unit were entered into a spreadsheet. Areal mapping of reservoir properties across the field was accomplished using geophysical logs and core-porosity to log-data transforms and core-porosity to core-permeability transforms. An important focus of reservoir characterization this year was to improve the mapping of reservoir properties.

Porosity Distribution

Average porosity in the Ramsey interval (Ramsey 1 and Ramsey 2 sandstone and the SH1 siltstone) is 22.0 percent (fig. 10, table 3), as determined by 4,900 core analyses. Standard deviation is 4.1 percent. Areal distribution of porosity was mapped from geophysical log data using core-log porosity transforms (Asquith and others, 1997b; Dutton and others, 1997a) and from porosities measured from cores. In wells with both porosity logs and core-analysis data, the log-porosity values were used. The use of core-analysis data significantly increases the available well control and provides a more detailed map of porosity distribution compared with the previous map that was made using only porosity-log data (Dutton and others, 1997a, 1997c). The map of average porosity (fig. 11) for the Ramsey sandstone in the Ford Geraldine unit exhibits a general northeast-southwest trend of high porosity, but the areas of highest porosity values are broken up.

The same log and core-analysis data were used in the map of porosity-feet (fig. 12). The map shows a strong linear northeast-southwest trend of high porosity-feet (8 to 10 ft), with the greatest thickness (> 10 ft) in the northeast part of the unit (shelfward). The decrease in average porosity and porosity-feet to the northwest and southeast is the result of a loss of reservoir rock along the edges of the Ramsey channel complex. The separation of high average porosity into different areas is caused in part by calcite cement (see section on Permeability).

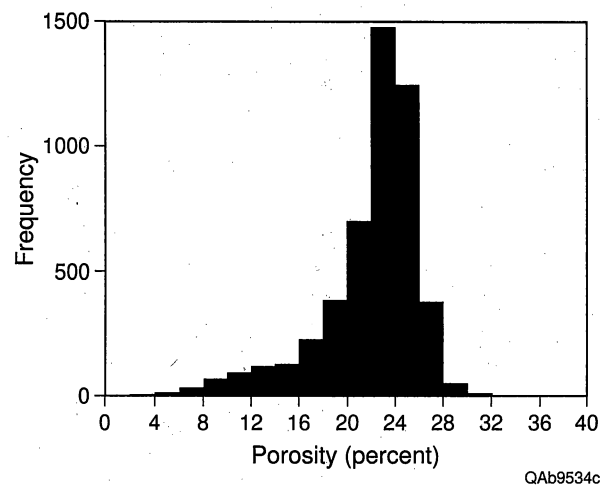
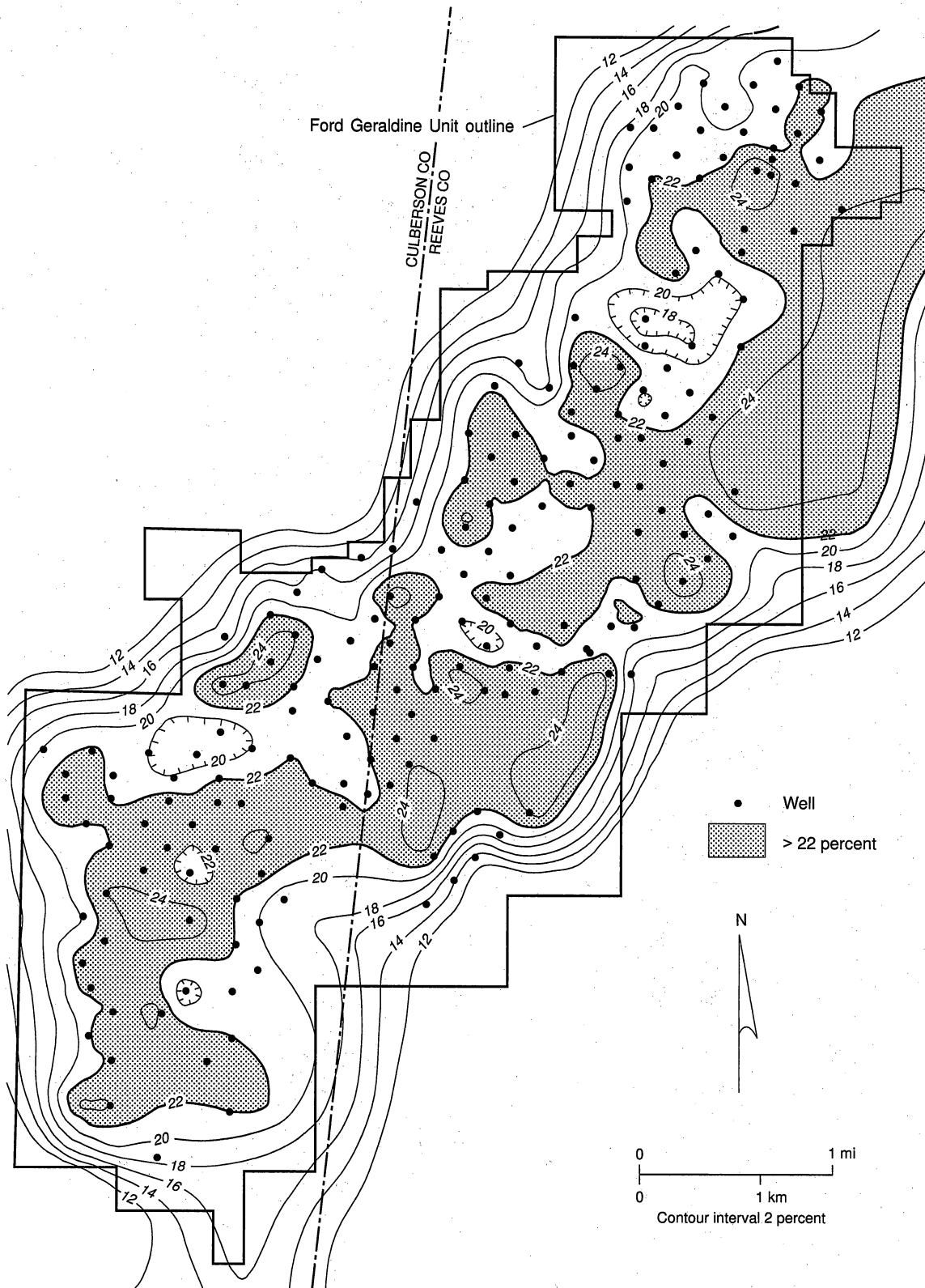
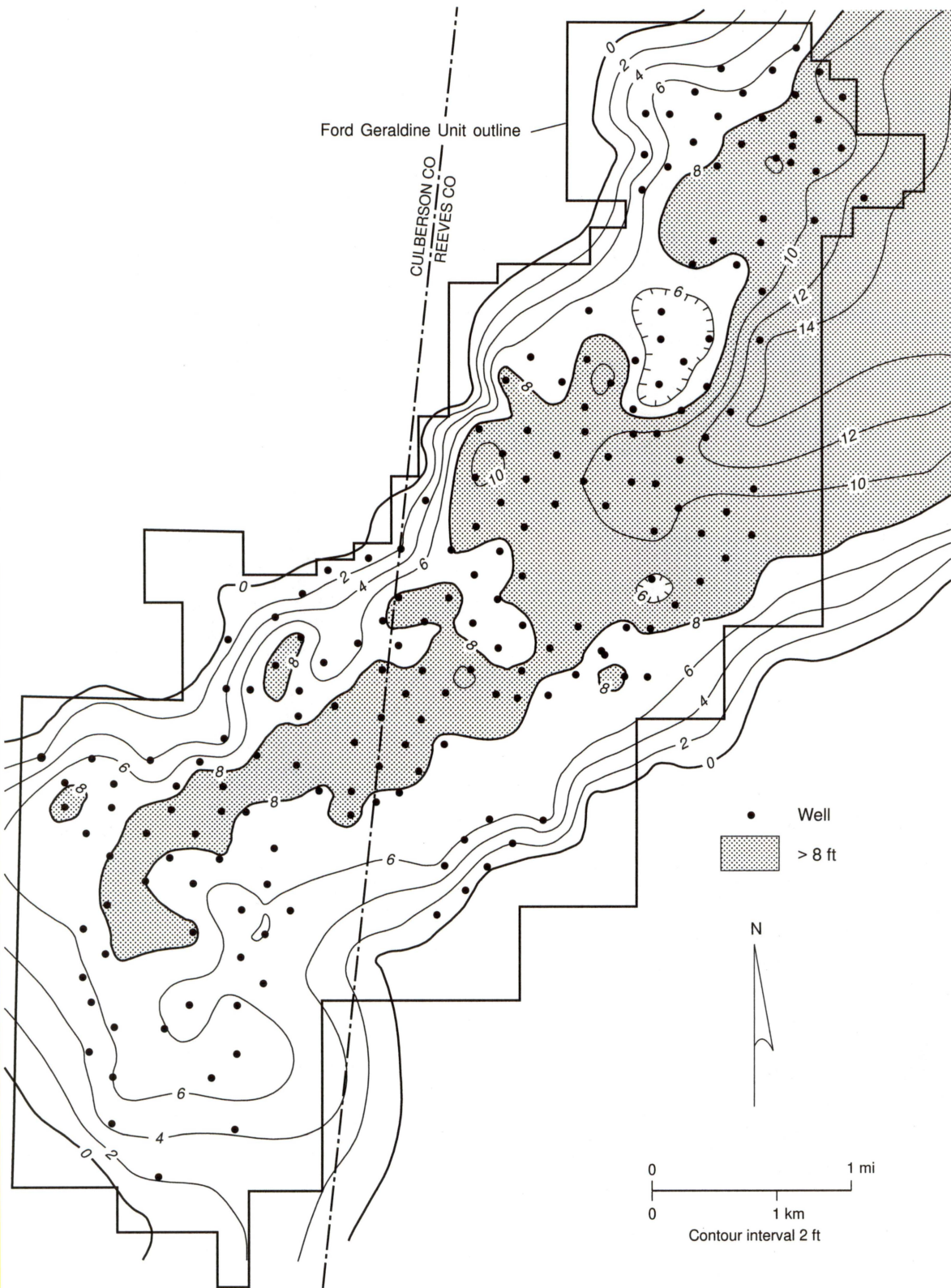


Figure 10. Distribution of porosity in Ramsey sandstone from 4900 core analyses.



QAAct1104c

Figure 11. Map of average porosity for the Ramsey sandstone in the Ford Geraldine unit. The porosities were determined by core-log porosity transforms (Asquith and others, 1997b; Dutton and others, 1997a) and from core-analysis data.



QAc1098c

Figure 12. Map of porosity \times thickness for the Ramsey sandstone in the Ford Geraldine unit. The narrow, linear northeast-southwest trend of high porosity-feet down the central axis of the unit corresponds to the area of thick total Ramsey sandstone.

Saturation Distribution

Water saturation (S_w) at field discovery averaged 47.7 percent, well above the irreducible water saturation of 35 percent (Pittaway and Rosato, 1991). Most wells produced some water at discovery. Average S_w measured in 4,900 core analyses of the Ramsey interval was 46.4 percent (fig. 13); standard deviation was 10.1 percent. Average S_w calculated from log data is 52 percent and standard deviation is 10 percent.

An new map of areal distribution of S_w was made using geophysical log data supplemented by water-saturation data from cores. First, a map of average bulk volume water (BVW) in the Ramsey 1 sandstone was constructed (Dutton and others, 1997a) in order to determine S_w northeast of sections 25 and 30, where no resistivity logs were run (fig. 9). To obtain S_w , average BVW values were extrapolated to the northeast, and BVW values assigned to wells with porosity logs. Water saturations were calculated in these wells by the formula $S_w = BVW_{ave}/\phi$ (Asquith and others, 1997a and b). Second, a BVW map was constructed for the Ramsey 2 interval using water saturations and porosity measured in cores (fig. 14), and BVW values were assigned to wells with porosity logs in the Ramsey 2 interval on the basis of this map. Finally, a map of S_w in the total Ramsey interval was made using S_w data from porosity logs where available and supplemented with core S_w data in wells without porosity logs (fig. 15).

The S_w map shows an increase to the northeast, which is to be expected because that direction is down structural dip. No gas cap was originally present in the field, so oil saturation at field discovery was $1.0 - S_w$. For an average S_w of 47.7 percent, average oil saturation was 52.3 percent. Mobil oil saturations (MOS) were calculated from log data by the formula $MOS = (1.0 - S_w) - ROS$. The values for residual oil saturation (ROS) were calculated using the following porosity-ROS transform: $ROS = -0.74 (\text{porosity}) + 41.41$ (Dutton and others, 1997a). Average MOS calculated from log data is 22 percent and standard deviation is 10 percent. Average ROS calculated from log data is 25 percent and standard deviation is 1 percent. A new MOS map was made that includes S_w data from wells with core analyses (fig. 16). High MOS

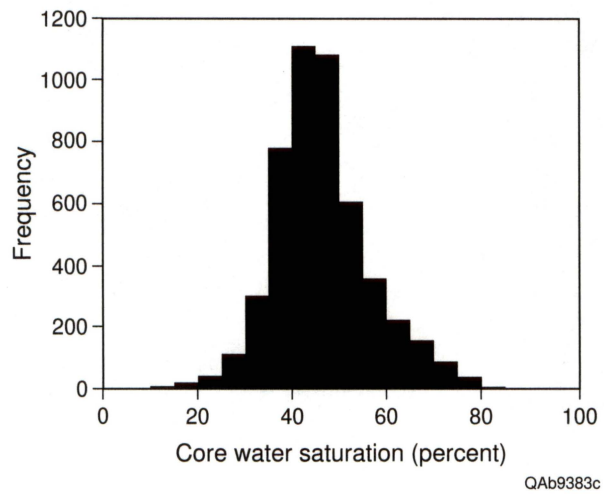
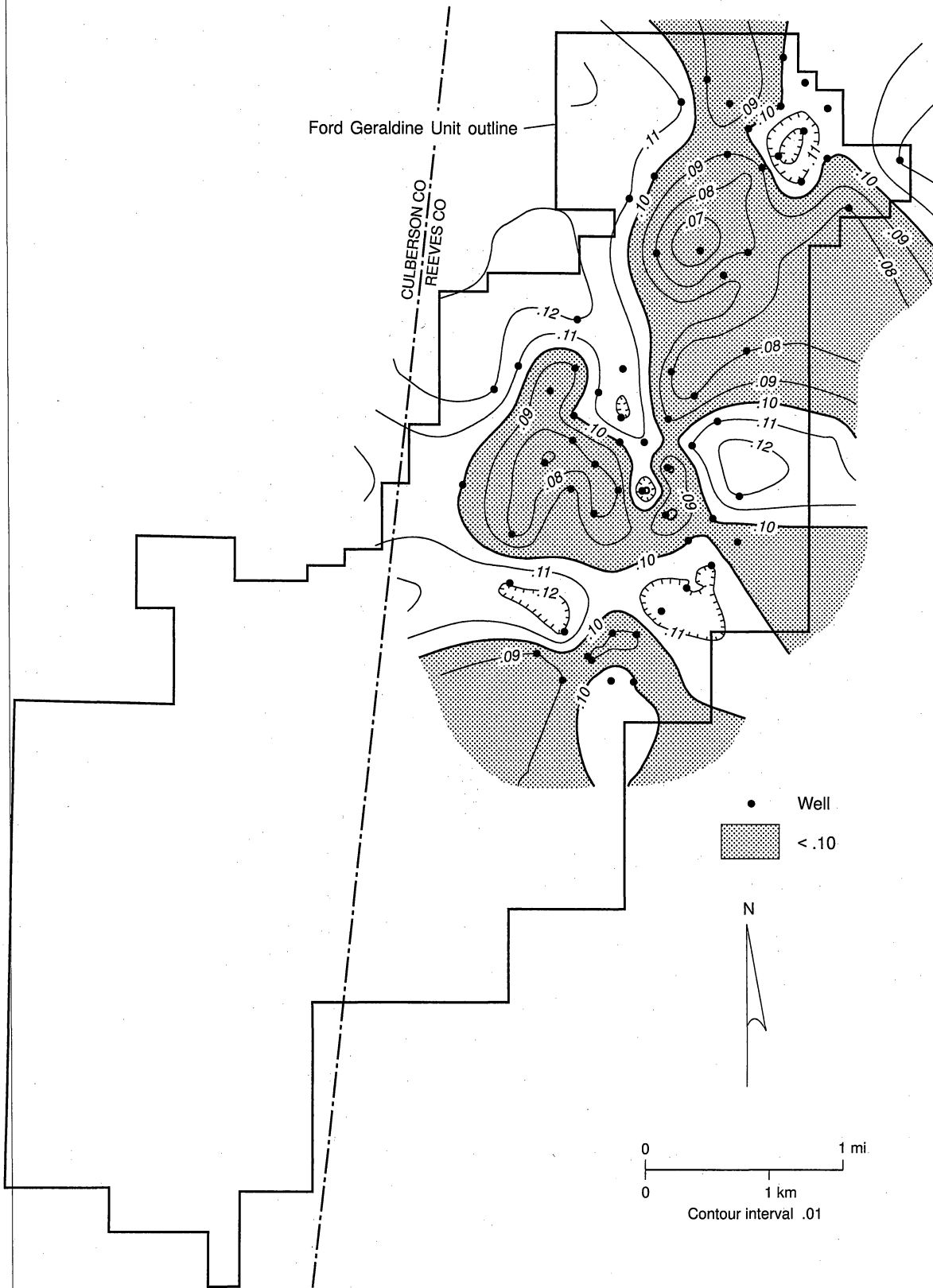


Figure 13. Distribution of water saturation in Ramsey sandstone from 4900 core analyses.



QAac1096c

Figure 14. Map of bulk volume water (BVW) for the Ramsey 2 sandstone in the Ford Geraldine unit. The BVW values are derived from water-saturation data from cores.

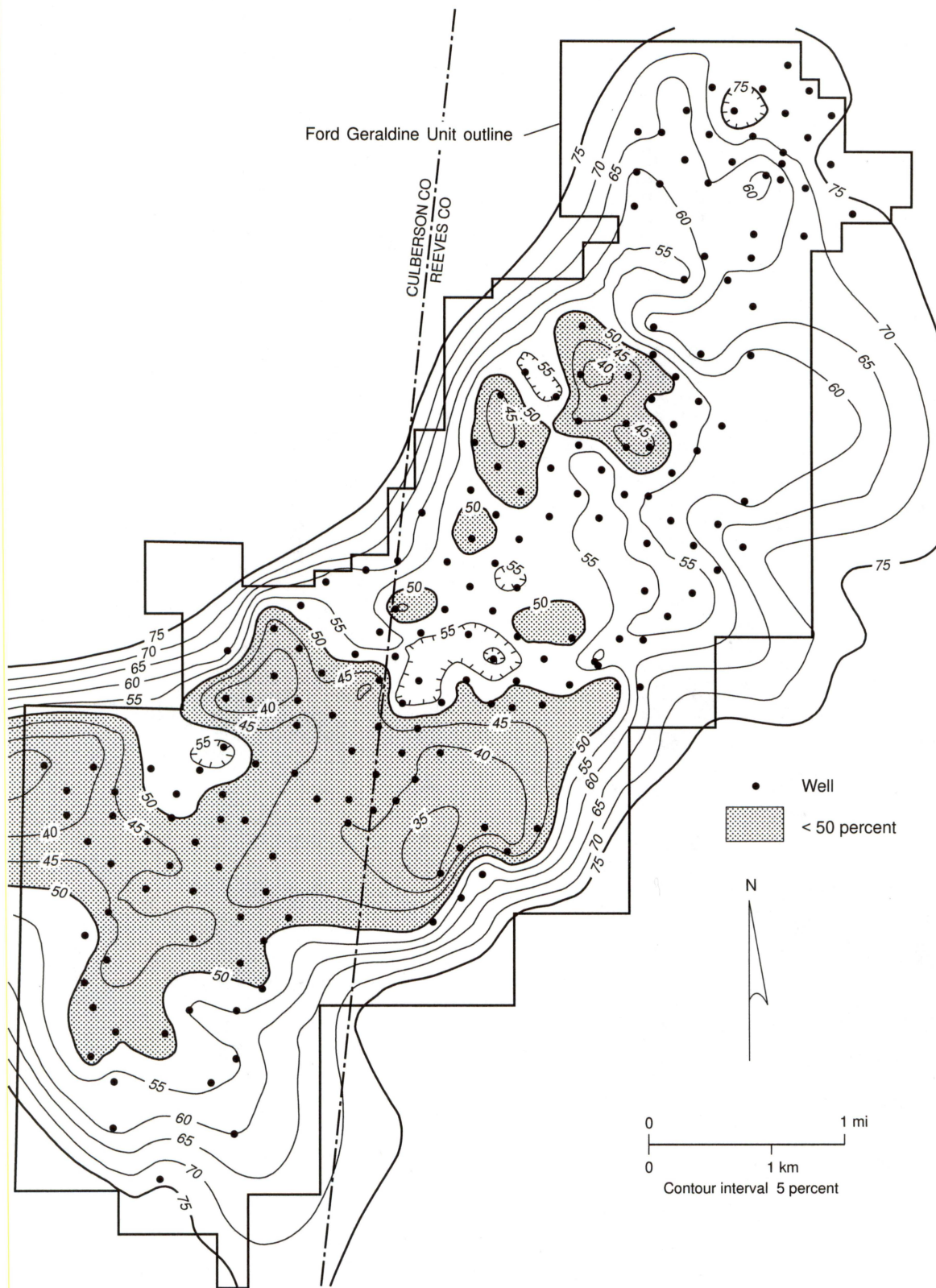
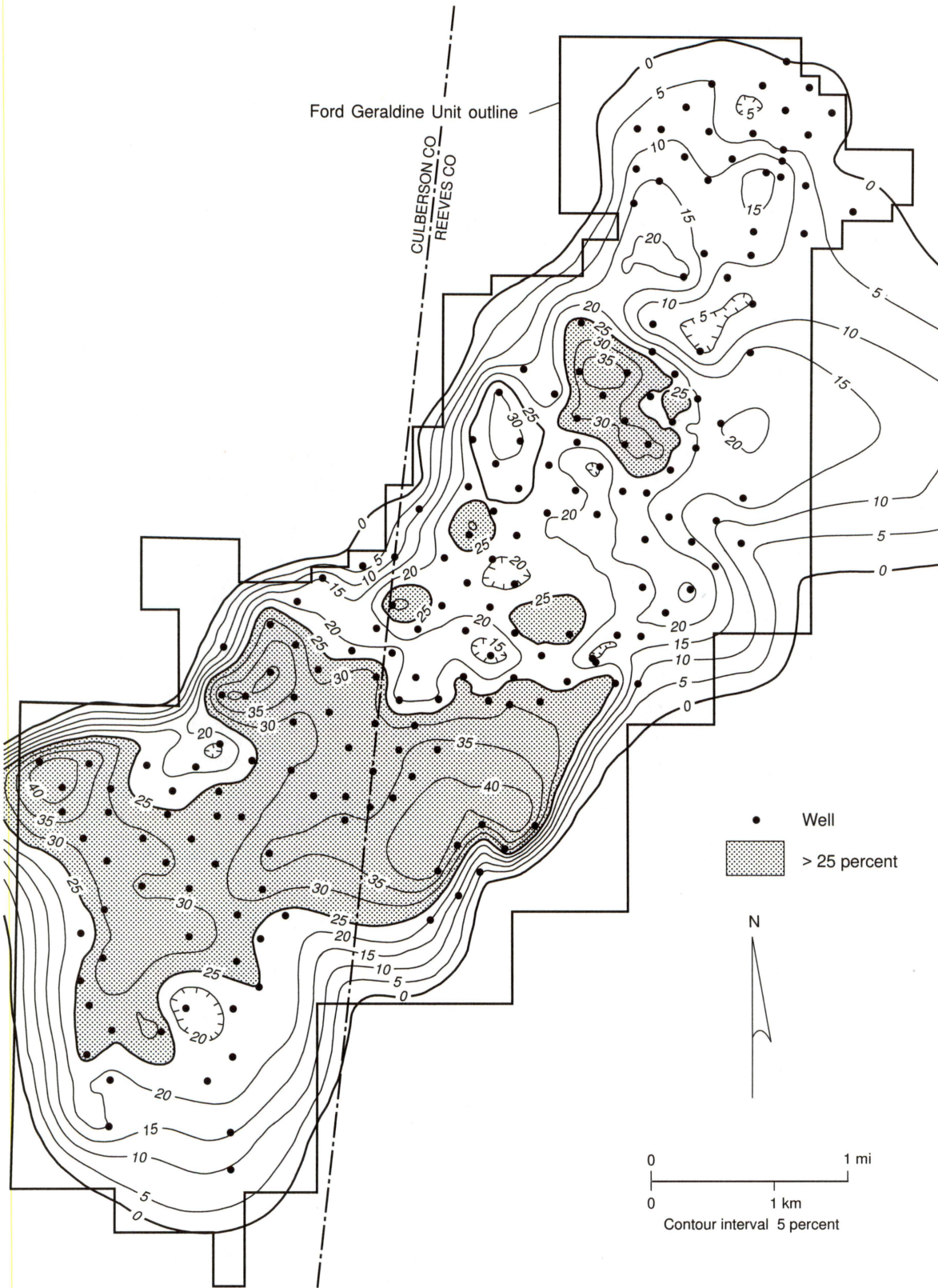


Figure 15. Map of water saturation (S_w) for the Ramsey sandstone in the Ford Geraldine unit. The water saturations in the Ramsey 1 sandstone in the northeast part of the unit were calculated from the average bulk volume water (BVW) values by the formula $S_w = BVW_{avg}/\phi$. Water saturations in the Ramsey 2 sandstone were taken from core-analysis data.



QAc1107c

Figure 16. Map of mobile oil saturation (MOS) for the Ramsey sandstone in the Ford Geraldine unit. Higher values of MOS occur in the southwest part of the unit, which is structurally high.

values are concentrated to the southwest (up-dip) and in the central portions of the Ford Geraldine unit (fig. 16). Average fieldwide oil saturation after waterflood was 38 percent, and average fieldwide water saturation was 62 percent (Conoco, 1979).

Permeability Distribution

Arithmetic average permeability in the Ramsey interval (Ramsey 1 and Ramsey 2 sandstone and the SH1 siltstone) is 38.4 md (table 3), as determined by 4,900 core analyses. Standard deviation is 43.5 md. Geometric mean permeability of the Ramsey interval is 16.2 md, with a standard deviation of 6.3 md (fig. 17). The ratio of vertical to horizontal permeability (K_v/K_h) is 0.01. A new map of areal distribution of permeability was made from geophysical log data using a core-porosity-to-permeability transform together with core-porosity-to-log-porosity transforms (Asquith and others, 1997b; Dutton and others, 1997a and 1997c). The geophysical log data were supplemented by core-analysis permeability data in wells that lacked porosity logs. The map of geometric mean permeability determined from combined log and core data (fig. 18) for the Ramsey sandstone in the Ford Geraldine unit shows that most areas of high permeability occur along the trend of the Ramsey 1 channel (fig. 19), but some of the highest average permeability occurs along the northwest margin of the field, in what is interpreted to be a levee facies (Dutton and others, 1997c).

The log- and core-permeability data were also used to construct a new map of permeability-feet (fig. 20). The map of average permeability-feet exhibits a strong linear trend of high (>750) permeability-feet to the northeast that reflects the total Ramsey sandstone thickness. Most areas of high permeability-feet are within the Ramsey 1 channel, but some levee deposits on the northwest margin of the field also have high values of permeability-feet (fig. 19).

Some areas of low average permeability and permeability-feet correspond to areas having high percentages of calcite-cemented sandstone in the Ramsey interval. There is a statistically significant relationship between permeability and volume of calcite cement. In samples with

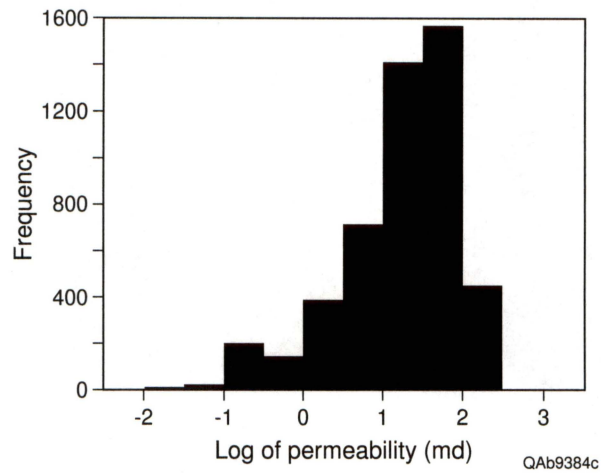
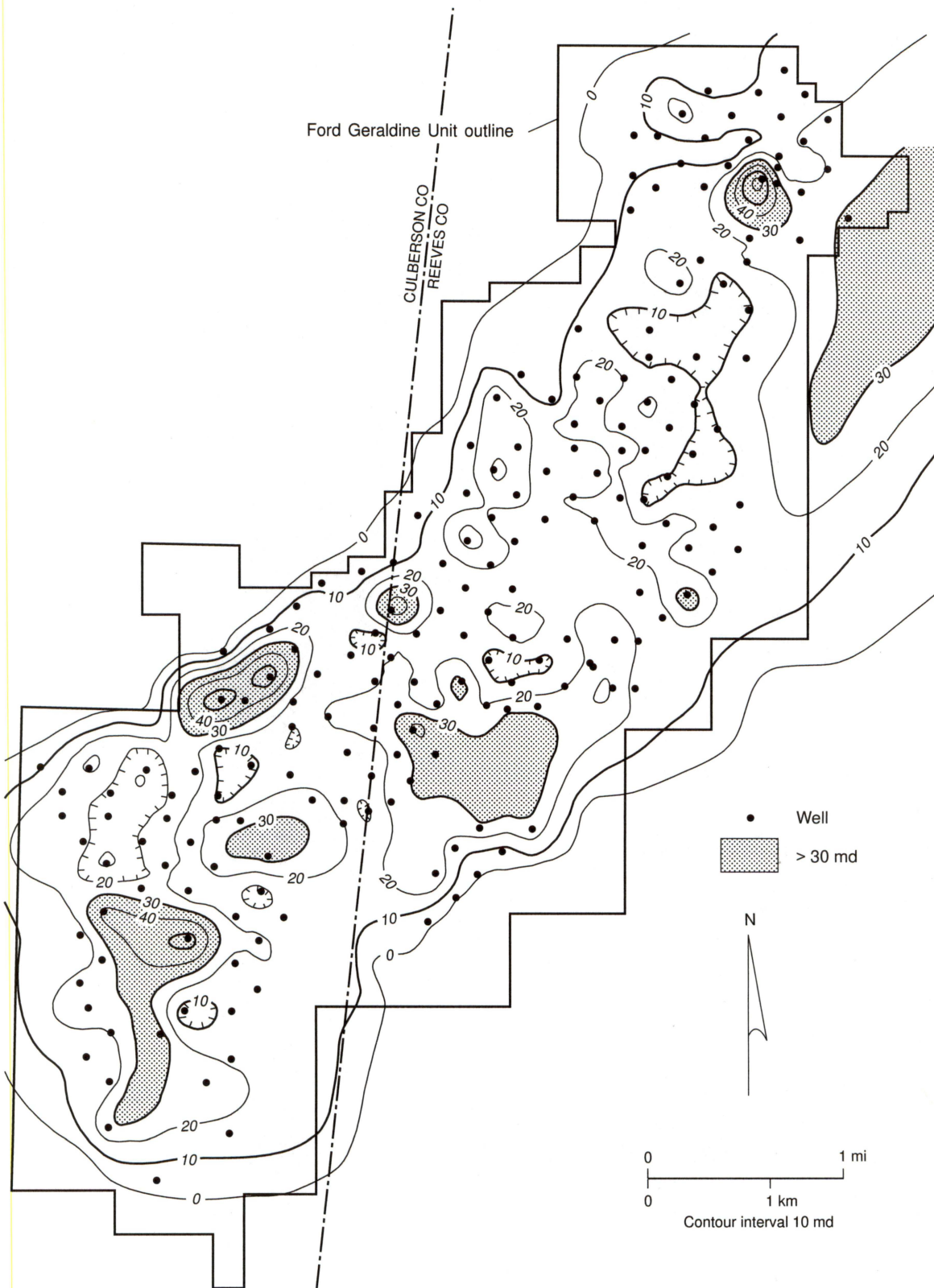
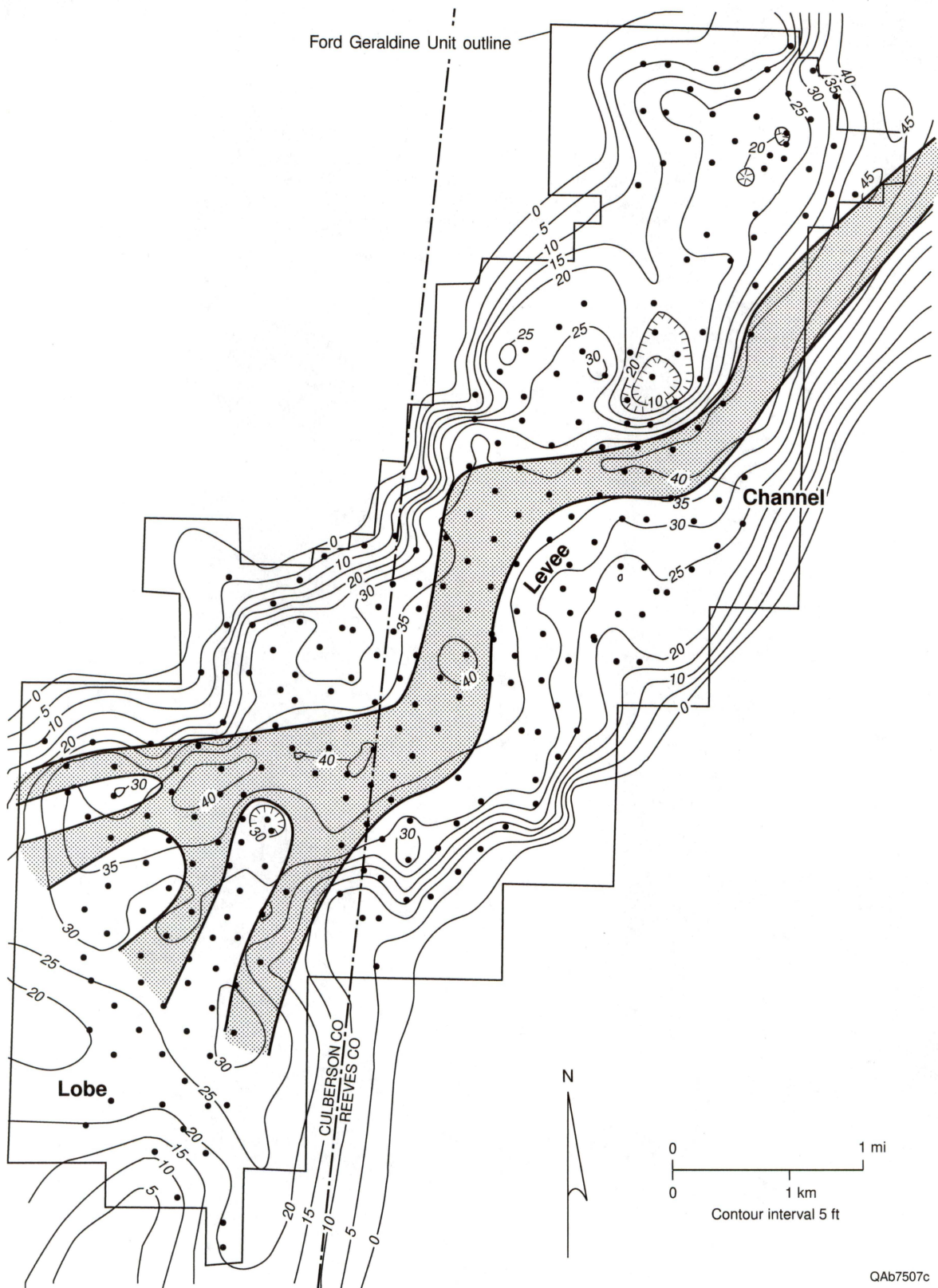


Figure 17. Distribution of permeability in Ramsey sandstone from 4900 core analyses. The mean of the log-permeability values is 1.21, thus the geometric mean permeability of the Ramsey sandstone is 16.2 md ($10^{1.21} = 16.2$).



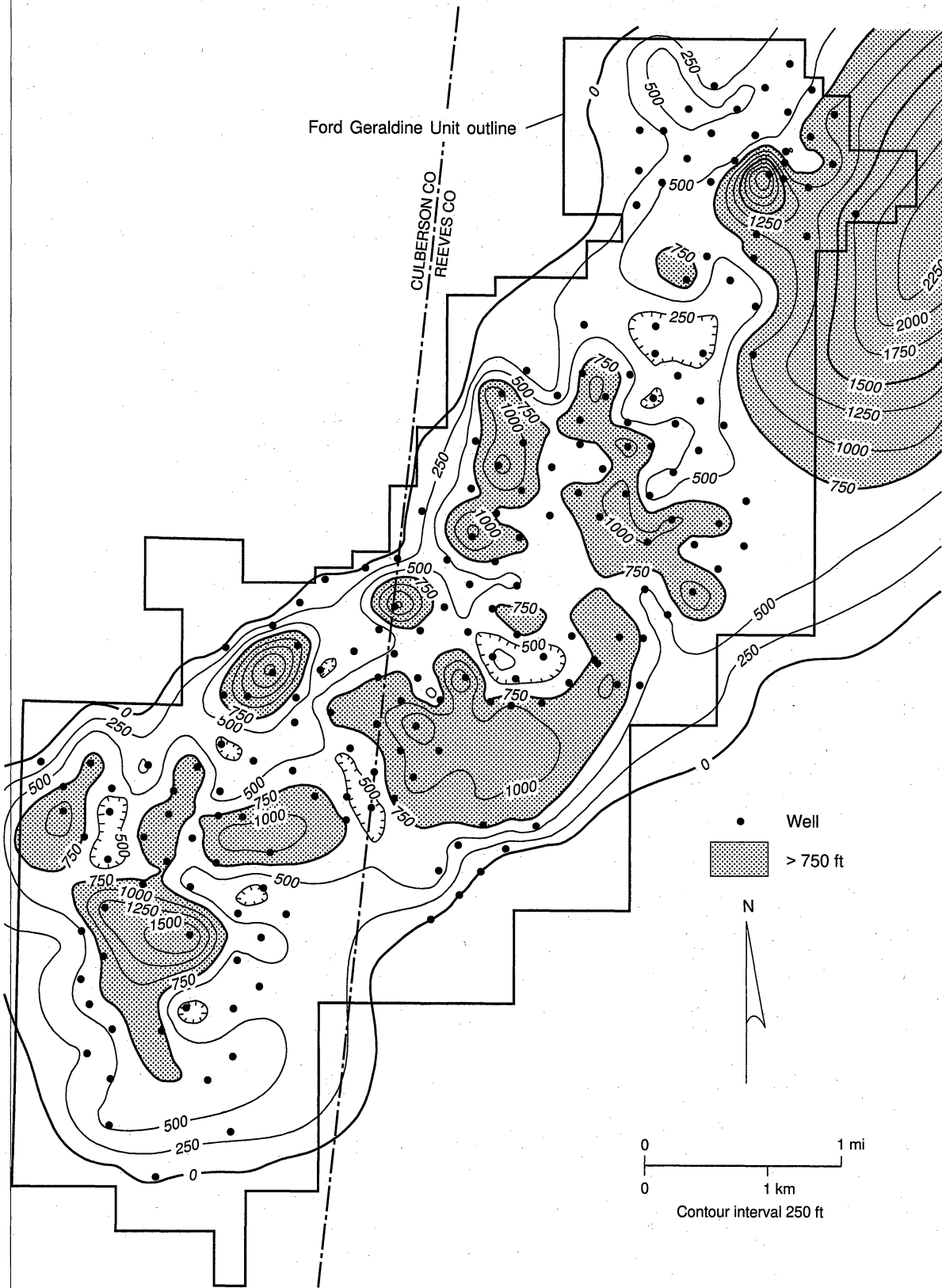
QAc1099c

Figure 18. Map of geometric mean permeability for the Ramsey sandstone interval, calculated from porosity data from geophysical logs and the core-porosity versus core-permeability transform, supplemented by core-analyses of permeability in wells without porosity logs.



QAb7507c

Figure 19. Isopach map of the Ramsey 1 sandstone, the main reservoir interval at Geraldine Ford field. It is interpreted as a channel-levee system that progrades over an elongate lobe. At the southwestern end of the field, the channel apparently breaks up into many smaller branches with attached lobes.



QAc1097c

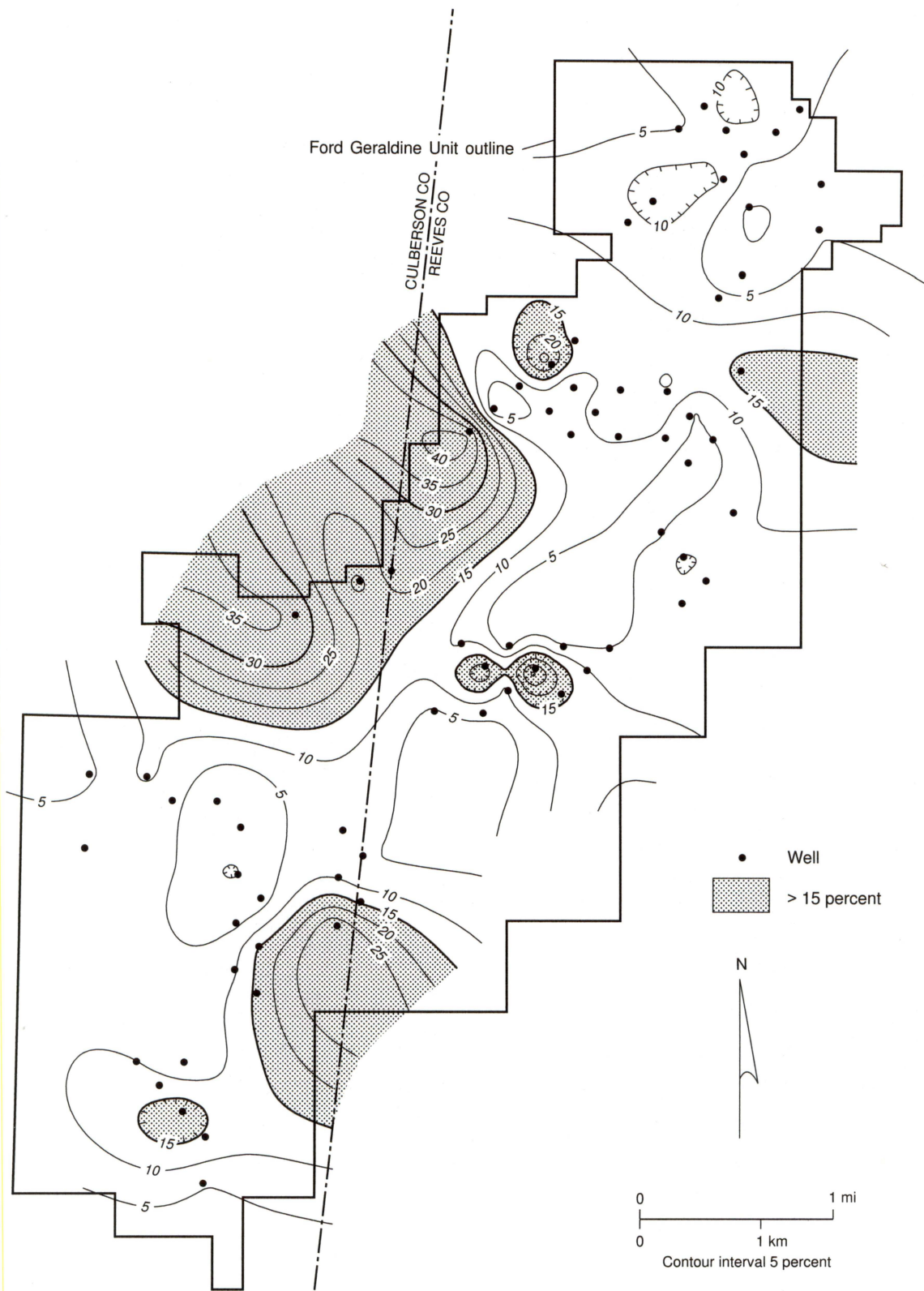
Figure 20. Map of permeability \times thickness for the Ramsey sandstone in the Ford Geraldine unit. The northeast-oriented trend of high permeability-feet (>750) is broken up into many isolated pods.

more than 10 percent calcite cement, geometric mean permeability is reduced to 1.3 md and average porosity to 14.4 percent. Sandstones having less than 10 percent calcite cement have geometric mean permeability of 46 md and average porosity of 23.1 percent. Thus, calcite-cement distribution is an important control on porosity and permeability in the Ramsey sandstone.

The distribution of calcite cement in the Ford Geraldine unit can be determined from the cores because highly calcite-cemented zones have a distinct white color. Calcite-cemented intervals were noted and described along with other sedimentary features in the cores, and these data were used to map the percentage of the Ramsey sandstone that is cemented by calcite (fig. 21). Most of the areas having a high percentage of calcite-cemented sandstone (>15 percent) occur along the margins of the field, where the sandstone pinches out into siltstone. Highly calcite-cemented sandstones occur in all three sandstone facies—channel, levee, and lobe. Most cemented zones in the core are approximately 0.5 to 1 ft thick; their dimensions are unknown, but they probably are not laterally extensive or continuous. Although they can occur anywhere within the vertical Ramsey sandstone section, they are more common near the top and base of sandstones. The source of some of the calcite may be from the adjacent siltstones, which would explain the greater abundance of calcite near the sandstone-siltstone contacts and at the margins of the field.

Structure

The Ramsey sandstone at Ford Geraldine unit dips 0.7° to the northeast, almost directly opposite original depositional dip, because Late Cretaceous movement associated with the Laramide Orogeny tilted the Delaware Basin eastward (Hills, 1984). No faults are interpreted to cut the Ramsey sandstone at the Ford Geraldine unit. Production from Geraldine Ford field and other upper Bell Canyon fields in the Delaware Basin occurs from the distal (southwest) ends of east-dipping, northeast-oriented linear trends of thick Ramsey sandstone deposits. Most



QA1102c

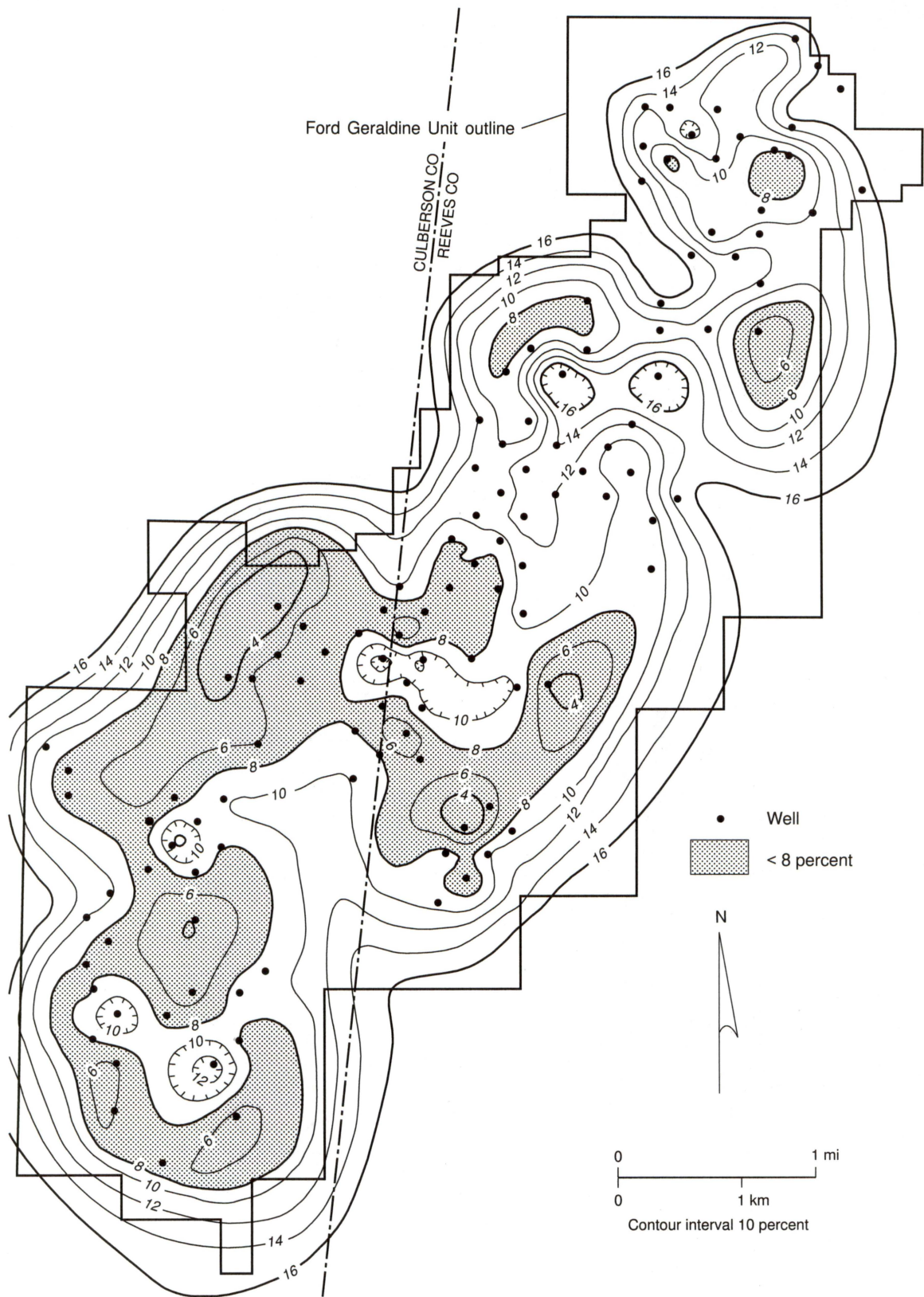
Figure 21. Map of percentage of the Ramsey sandstone that is cemented by calcite. Calcite-cemented zones were measured in wells with core.

hydrocarbons in these fields are trapped by stratigraphic traps formed by an updip lateral facies change from higher permeability reservoir sandstones to low permeability siltstones. Several of the fields, including Geraldine Ford, show minor structural closure because linear trends of thick sandstones formed compactional anticlines by differential compaction during burial (Ruggiero, 1985).

Net Pay

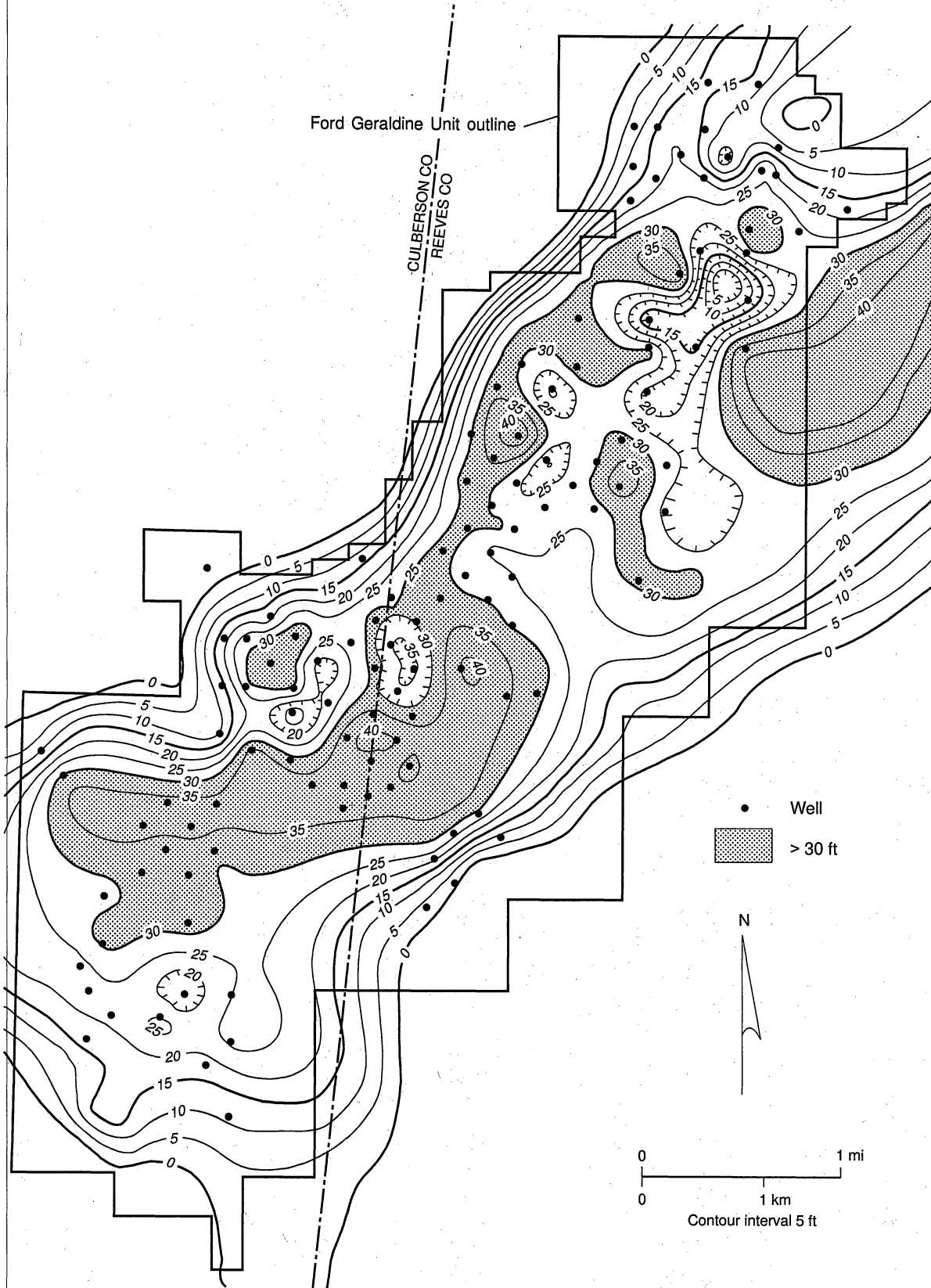
Net pay in the Ramsey reservoir was calculated from geophysical logs, using cut-offs for volume of clay (V_{cl}), porosity (\emptyset), and water saturation (S_w). The selection of a V_{cl} cut-off was based on the work of Dewan (1984), which suggests a V_{cl} cut-off of 15 percent for reservoirs with dispersed authigenic clay. The dispersed authigenic clay cut-off was used because of the lack of detrital clay but the common occurrence of authigenic clay in the Delaware sandstones (Williamson, 1978; Thomerson, 1992; Walling, 1992; Asquith and others, 1995; and Green and others, 1996). Volume of clay was calculated from gamma-ray and interval-transit-time logs (Asquith and others, 1997b; Dutton and others, 1997a). A map of V_{cl} distribution (fig. 22) shows that some of the lowest values (<8 percent) occur in lobe facies at the south end of the unit and in levee facies at the northwest and southeast margins of the field (compare figures 19 and 22).

Using published information and log and core data, net pay cutoffs of porosity ≥ 15 percent and water saturation < 60 percent were determined for the Ramsey sandstone (Asquith and others, 1997b; Dutton and others, 1997a). The average net pay of the Ramsey sandstone calculated from geophysical logs using these cutoffs is 23.1 ft, with a standard deviation of 11.4 ft. This value is similar to the average net pay cited by Pittaway and Rosato (1991) of 25 ft. A new map of net pay of the Ramsey sandstone was made by calculating net pay separately for the Ramsey 1 and Ramsey 2 sandstones, then adding the values together (fig. 23). Net pay is greatest to the southwest (up structural dip) and along the northwest margin of the unit. A new map of hydrocarbon pore-feet ($S_o \times \emptyset \times h$), which was made using the revised calculations of



QA1100c

Figure 22. Map of volume of clay in Ramsey sandstone in the Ford Geraldine unit. Volume of clay was calculated from gamma-ray and interval-transit-time logs.



QAcl106c

Figure 23. Map of net pay for the Ramsey sandstone in the Ford Geraldine unit. The cut-offs for net pay were $V_{cl} \leq 15$ percent, $\phi \geq 15$ percent, and $S_w < 60$ percent.

water saturation (see section on Saturation Distribution), shows a strong northeast-southwest trend of high $S_o \times \emptyset \times h$ values (> 4 ft) down the central part of the unit that correlates best with the porosity-feet map (fig. 12). The slight loss of $S_o \times \emptyset \times h$ to the northeast (fig. 24) is to be expected due to the more downdip position.

Vertical Porosity and Permeability Profiles

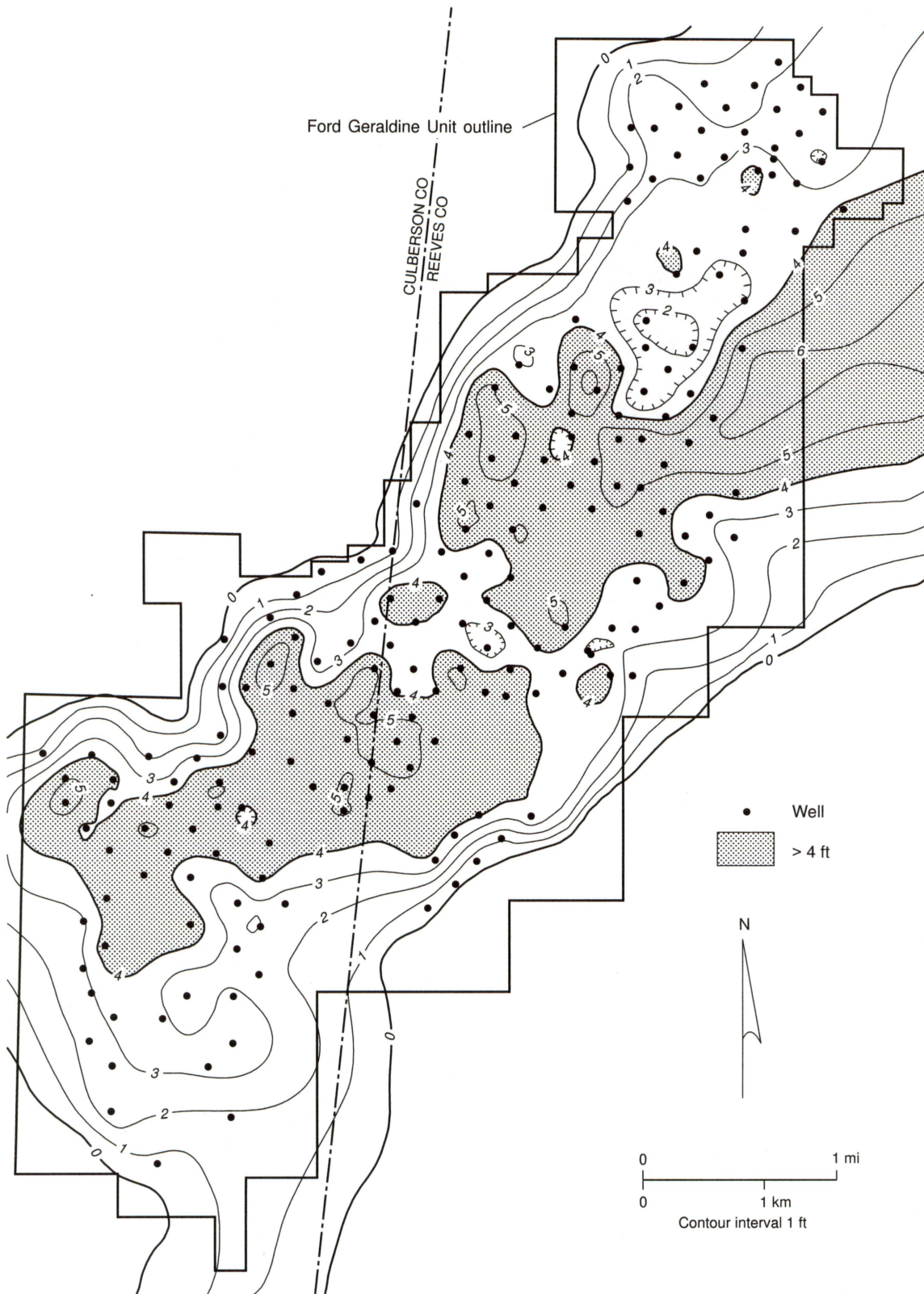
Vertical permeability profiles through the Ramsey sandstone are quite variable (fig. 25). In the northern part of the unit, where the Ramsey is divided by the SH1 siltstone, the higher permeabilities of the Ramsey 1 and 2 sandstones are separated by the low permeability SH1 siltstone (see wells FGU-17 and FGU-70 on figure 25). Even within the Ramsey 1 and 2 sandstones permeability is highly variable, with numerous spikes of high and low permeability. In many, but not all wells, the highest permeability streaks occur at the top of the Ramsey sandstone, in either the Ramsey 1 or 2 sandstone, whichever is at the top of the interval at that location (see wells FGU-70, FGU-193, and FGU-241 on figure 25). Low permeability commonly occurs immediately below these high permeability streaks at the top of the Ramsey. The low-permeability zones correspond to calcite-cemented zones, and the high permeability streaks may result from leaching of carbonate cement (Dutton and others, 1996).

Vertical porosity profiles show a similar irregular distribution of porosity (fig. 26), with numerous low-porosity streaks throughout Ramsey 1 and 2 sandstones. Low-porosity zones are interpreted as corresponding to the low-permeability, calcite-cemented nodules.

FIELD DEVELOPMENT HISTORY

Primary Recovery

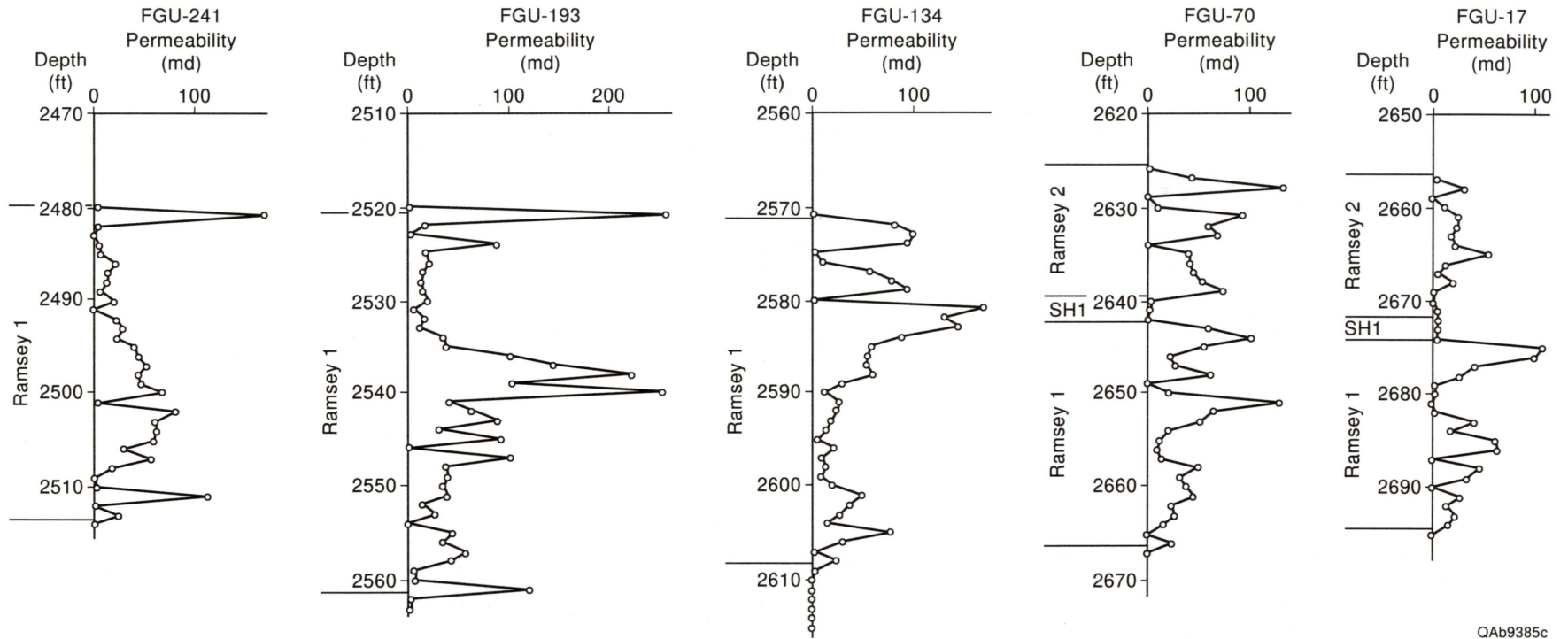
Primary recovery in the Geraldine Ford field began 1956 and continued until June 1969. A total of 301 wells were drilled for primary production. Primary cumulative production was 13.2 MMbbl (figs. 27, 28), or 13.3 percent of the 99 MMbbl of original oil in place.



QAc1105c

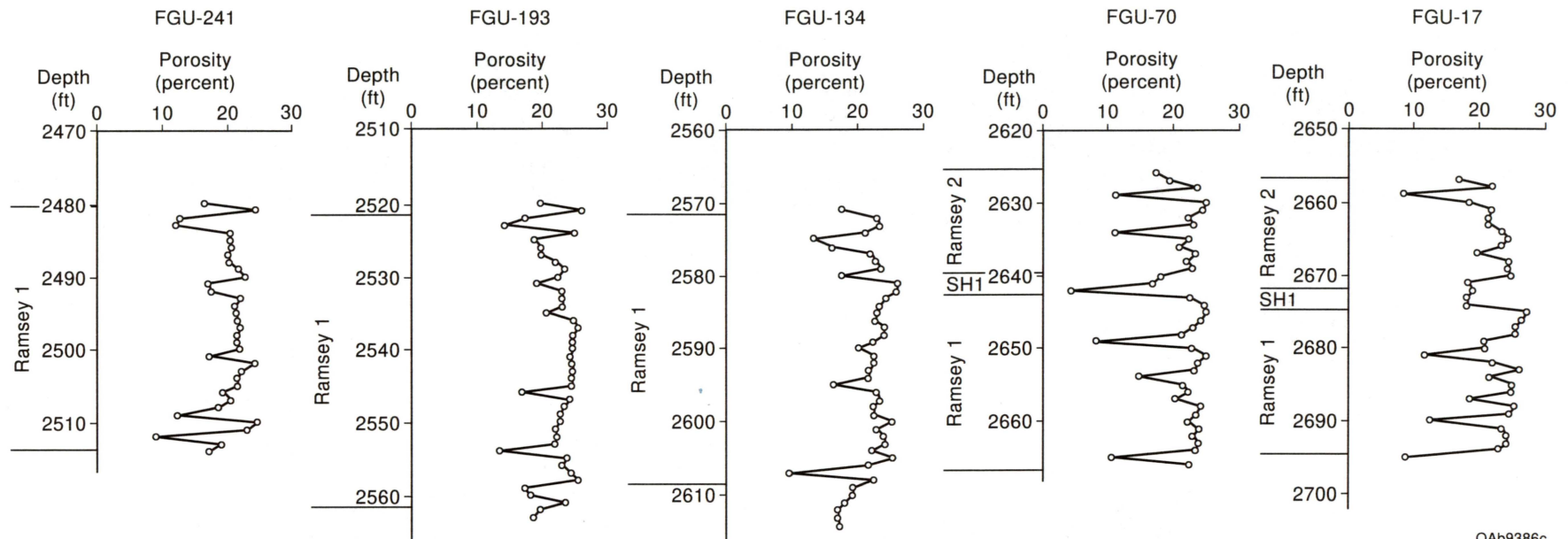
Figure 24. Map of hydrocarbon-pore-feet ($S_0 \times \emptyset \times h$) for the Ramsey sandstone in the Ford Geraldine unit. Higher $S_0 \times \emptyset \times h$ values occur in the southwestern, structurally high part of the unit.

SS



QAb9385c

Figure 25. Vertical permeability profiles from core-analysis data for 5 wells in the Ford Geraldine unit.



QAb9386c

Figure 26. Vertical porosity profiles from core-analysis data for 5 wells in the Ford Geraldine unit.

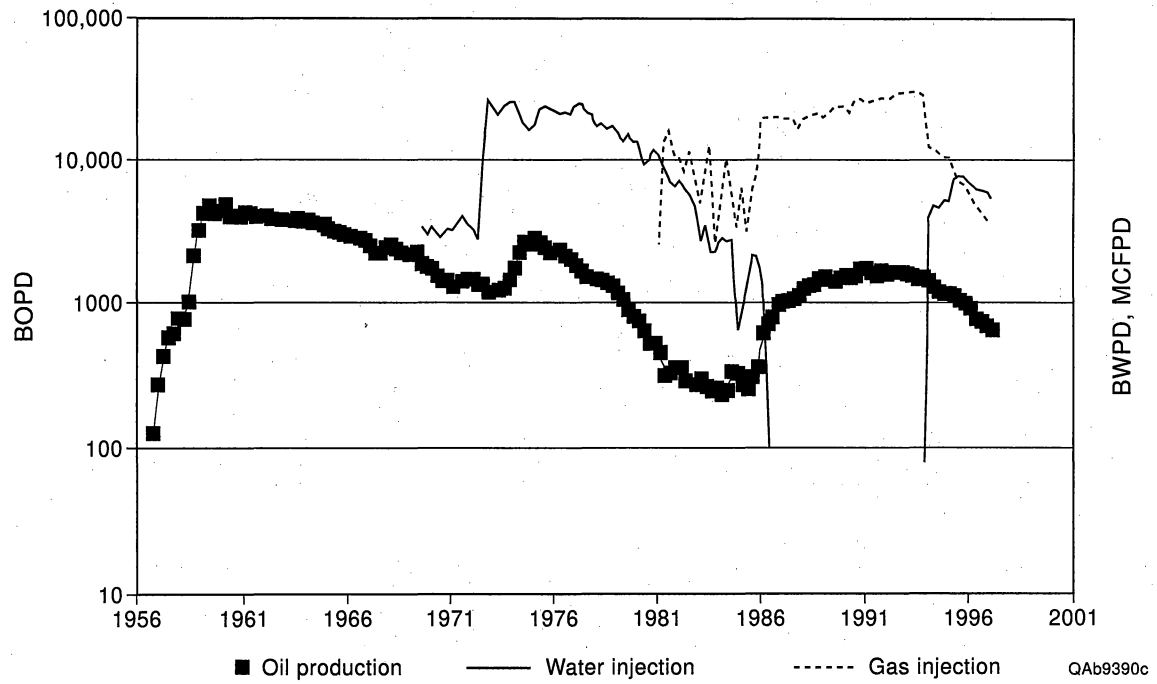
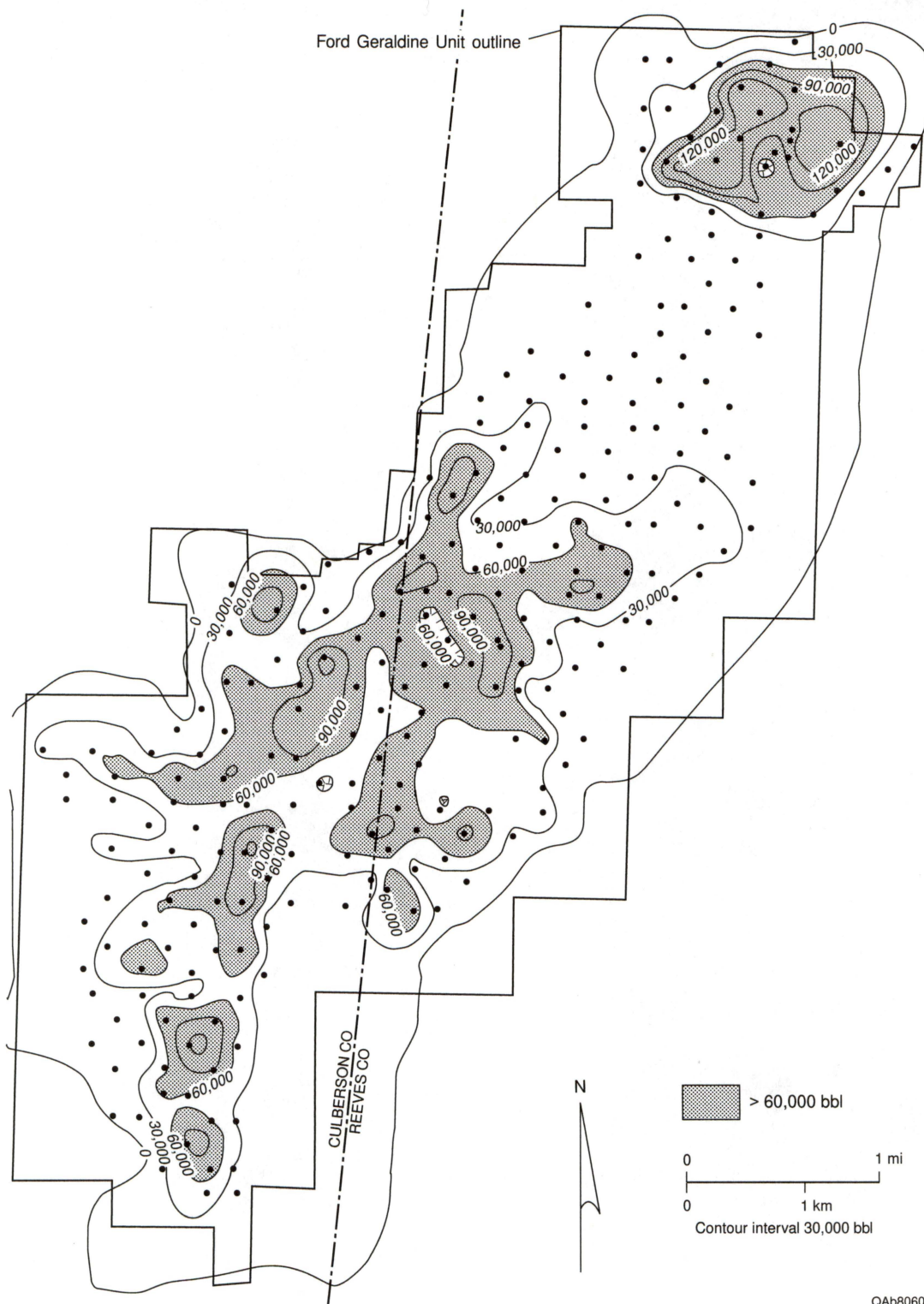


Figure 27. Plots of primary, secondary, and tertiary production in the Ford Geraldine unit, and volumes of water and CO₂ injected.



QAb8060c

Figure 28. Map of primary recovery for the Ramsey sandstone in the Ford Geraldine unit, Reeves and Culberson Counties, Texas. The highest primary recovery was in the southwest part of the unit. To the northeast (down structural dip) there is an isolated area of high oil recovery. The high recoveries to the southwest are from the Ramsey 1 sandstone, and the high recoveries to the northeast are from the Ramsey 1 sandstone and the overlying Ramsey 2 sandstone. The Ramsey 2 sandstone is not developed to the southwest, therefore the Ramsey 2 sandstone represents a separate trap.

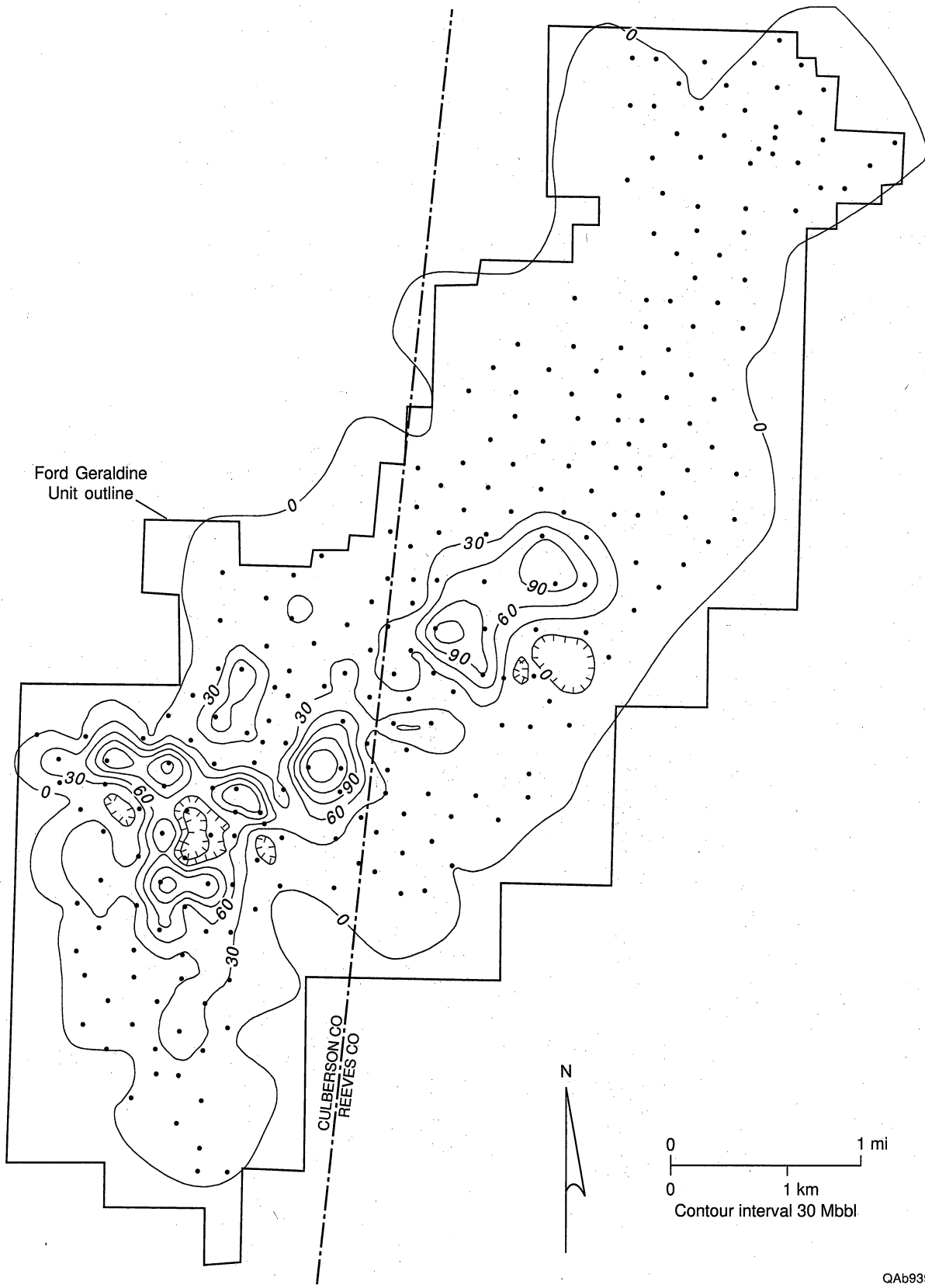
Secondary Recovery

The Ford Geraldine unit was formed in November, 1968, and a pilot waterflood project started in June, 1969 (Pittaway and Rosato, 1991). The waterflood was expanded throughout the southern part of the unit in stages between 1972 and 1980, but the northern area of the unit received only a short, low-volume waterflood. Eighteen new producing wells and 6 new water-injection wells were drilled for the waterflood, and 67 old wells were converted for water injection.

The best response was from the same area with high primary production (fig. 29). An additional 6.8 MMbbl of oil was produced after unitization, but only 4.5 MMbbl was attributed to the waterflood (fig. 27), significantly less than predicted from reservoir simulation. By the end of secondary development, recovery efficiency had increased to only 22.5 percent. Of that, 18% is attributed to primary recovery and 4.5% to secondary recovery (Pittaway and Rosato, 1991).

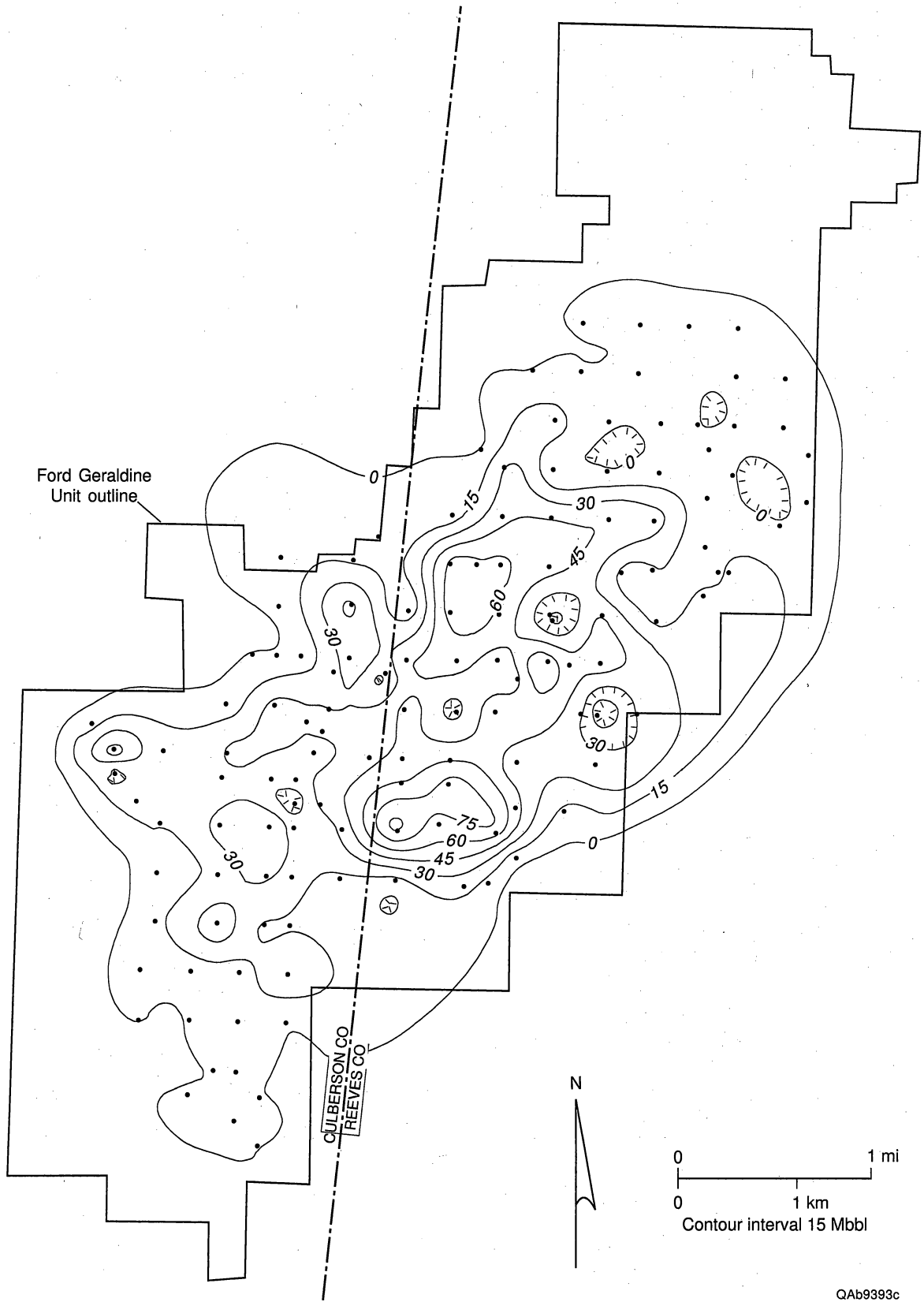
Tertiary Recovery

Tertiary recovery by CO₂ injection began in March, 1981, in the entire unit except for the northern end, but CO₂ supply was erratic until December, 1985. Production response occurred in 1986 after higher and constant CO₂ injection began in December, 1985 (fig. 27) (Pittaway and Rosato, 1991). Six new producing wells and 4 new CO₂-injection wells were drilled for the flood, and 97 old wells were converted for CO₂-injection, including some water-injection wells. Cumulative tertiary production to date has been 5.7 million barrels (fig. 30), and tertiary recovery efficiency is 5.8 percent (K. R. Pittaway, written communication, 1997). Estimated ultimate tertiary recovery is 9.0 percent (K. R. Pittaway, written communication, 1997).



QA9394c

Figure 29. Map of secondary production resulting from the waterflood conducted from 1969 to 1980. Only minor water injection was done in the north end of the unit.



QAb9393c

Figure 30. Map of tertiary production through 1995 resulting from the CO₂ flood that started in 1981. The north end of the unit was not CO₂ flooded.

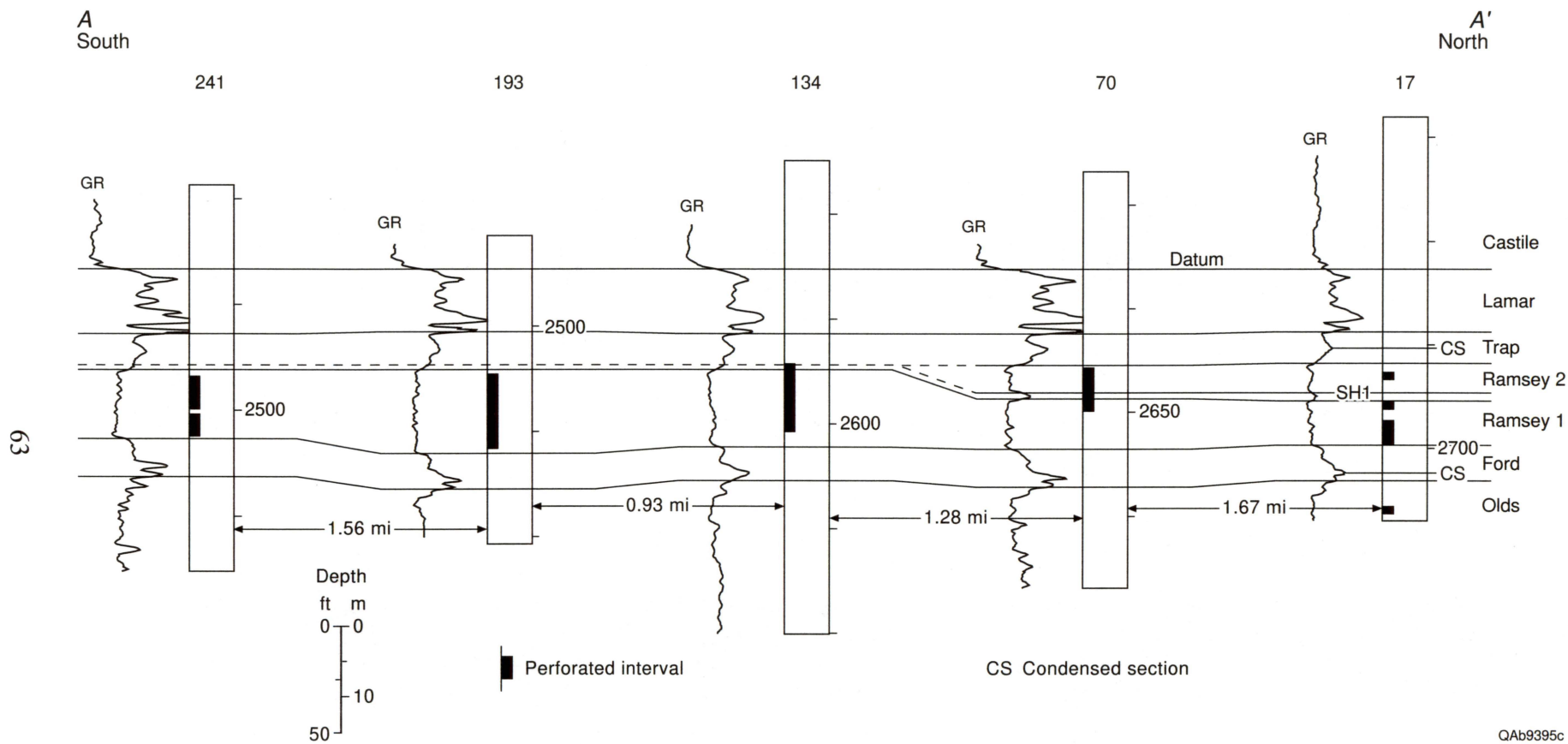
Evaluation of Reservoir Heterogeneity

The low recovery efficiency of the Ramsey sandstone reservoir suggests that greater heterogeneity of reservoir sandstones exists at Ford Geraldine unit than previously thought (Ruggiero, 1985). Megascopic (field-scale) heterogeneity is provided by the subdivision of the reservoir into the Ramsey 1 and 2 sandstones. In the northern part of Ford Geraldine unit, the Ramsey 1 and Ramsey 2 sandstones are separated by a 1- to 3-ft-thick laminated siltstone (SH1) (Ruggiero, 1985 and 1993), but in the southern part of Ford Geraldine unit, only the Ramsey 1 sandstone is present (figs. 31–33).

In the proposed channel-levee and lobe model for Ramsey sandstone deposition, progradation, aggradation, and retrogradation of the system resulted in lateral and vertical offset of channel, levee, and lobe facies (figs. 6, 32). Laminated siltstones provide the greatest amount of depositional heterogeneity because of the grain size and permeability contrast between sandstones and siltstone facies (fig. 25). The sandstones facies all have similar grain sizes, and thus there may not be much permeability contrast and inhibition of flow at sandstone-on-sandstone contacts, for example, where channels incise into lobe facies.

Many of the reservoir properties of the field are not continuous but instead show areas of better reservoir quality separated by poorer areas (figs. 11, 18), particularly on the margins of the field. These marginal zones of higher porosity and permeability are interpreted as being levee deposits that formed when low-density turbidity currents overtopped the channel margins and deposited sand in the generally lower-reservoir-quality interchannel areas.

Some of the discontinuity between areas of better reservoir quality may be enhanced by diagenetic effects. Localized precipitation of calcite cement increases heterogeneity within the sandstones. Although the cemented zones are not interpreted as being laterally continuous between wells, their presence causes “spiky” vertical permeability trends in the reservoir (fig. 25). Fluid flow is likely to occur preferentially along the high permeability streaks, leaving poorly swept zones of lower permeability.

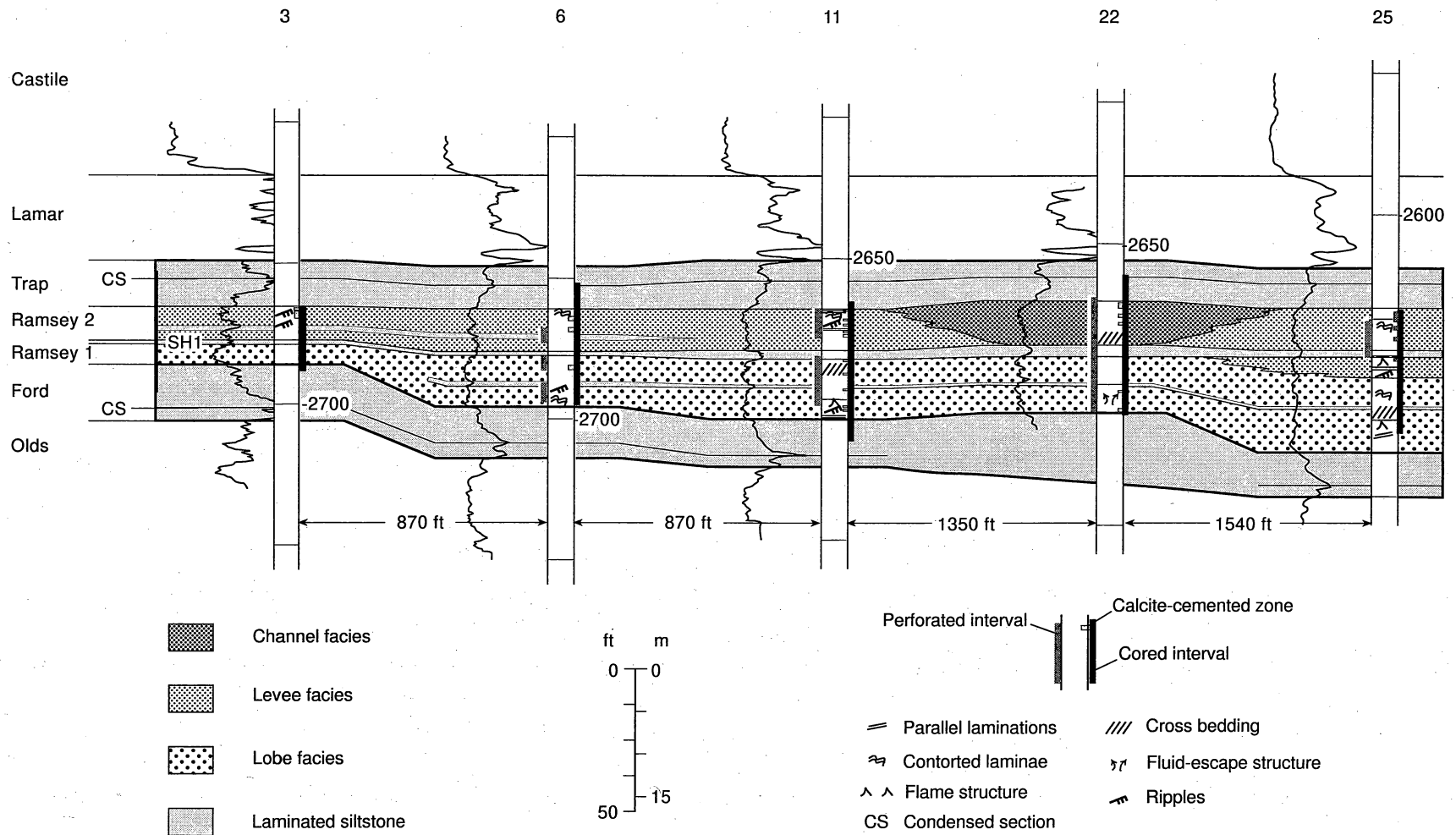


QAb9395c

Figure 31. Dip cross section A-A' down the length of Geraldine Ford field. In the northern part of the field the SH1 laminated siltstone separates the reservoir into Ramsey 1 and Ramsey 2 sandstones. Only Ramsey 1 sandstone is present in the southern part of the field. Location of cross section is shown in figure 7.

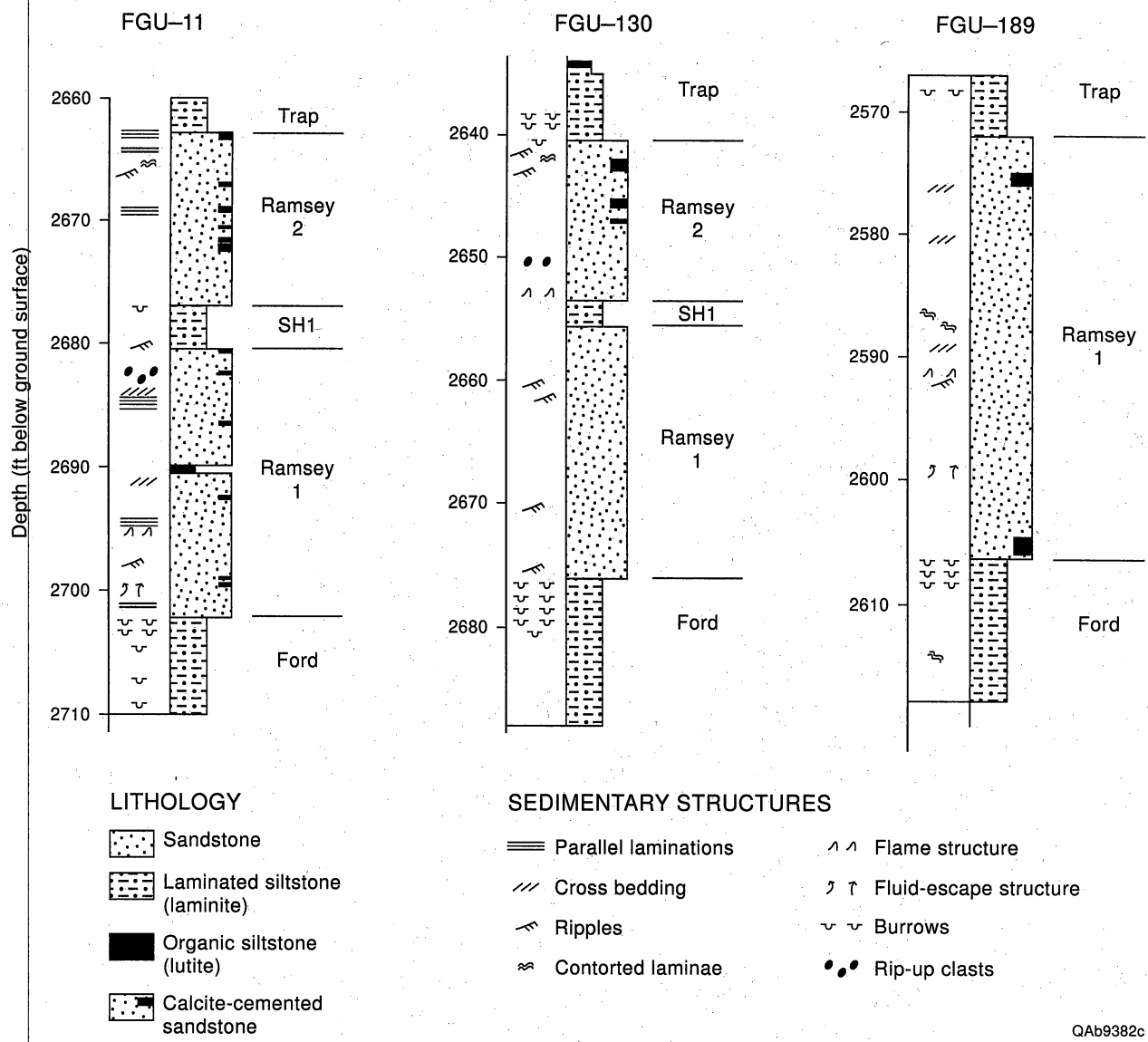
B
Northwest

B'
Southeast



QAb9376c

Figure 32. Cross section B-B' through the northern end of Geraldine Ford field, where the SH1 laminated siltstone separates the reservoir into Ramsey 1 and Ramsey 2 sandstones. Deposition of Ramsey sandstones is interpreted to have occurred by sandy high- and low-density turbidity currents that carried a narrow range of sediment size, mostly very fine sand to coarse silt. On the basis of core descriptions and study of the outcrop analog, Ramsey sandstones are interpreted as having been deposited on the basin floor in a sand-rich, channel-levee system with attached lobes. Location of cross section is shown in figure 7.



QAb9382c

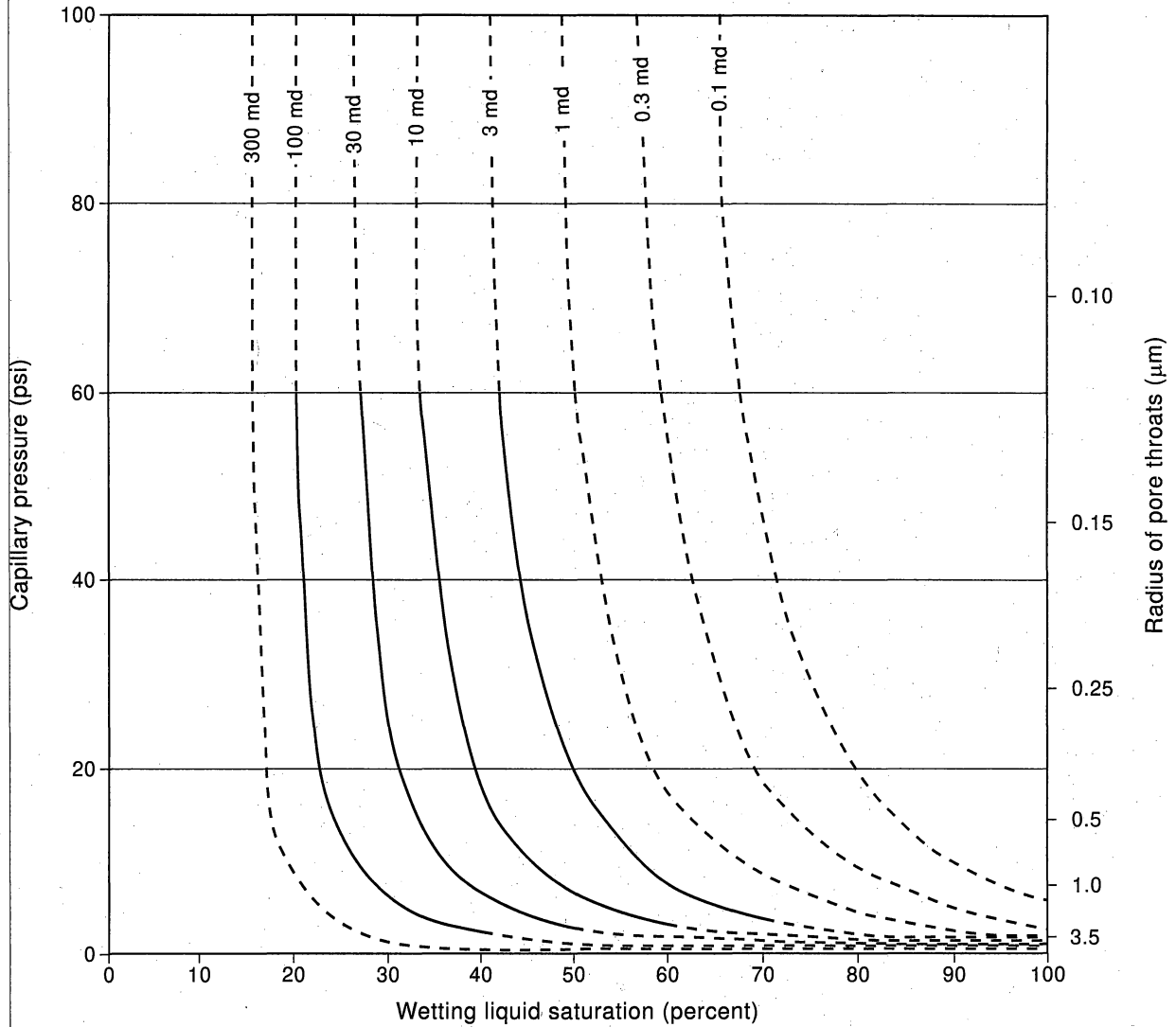
Figure 33. Representative cores of the Ramsey sandstone and bounding Trap and Ford laminated siltstones. Location of wells FGU-11, FGU-130, and FGU-189 is shown in figure 7.

Microscopic heterogeneity of Ramsey sandstones is controlled primarily by diagenesis. Precipitation of calcite and chlorite have the greatest effect on pore-throat-size distribution. Capillary pressure curves show that uncemented sandstones, which have permeabilities in the 30 to 300 md range, have 60 to 80 percent of their pore-throat radii greater than 1.0 μm (fig. 34). Cemented sandstones having permeabilities of 0.1 to 3 md have just 4 to 40 percent of their pore-throat radii greater than 1.0 μm .

Production Constraints

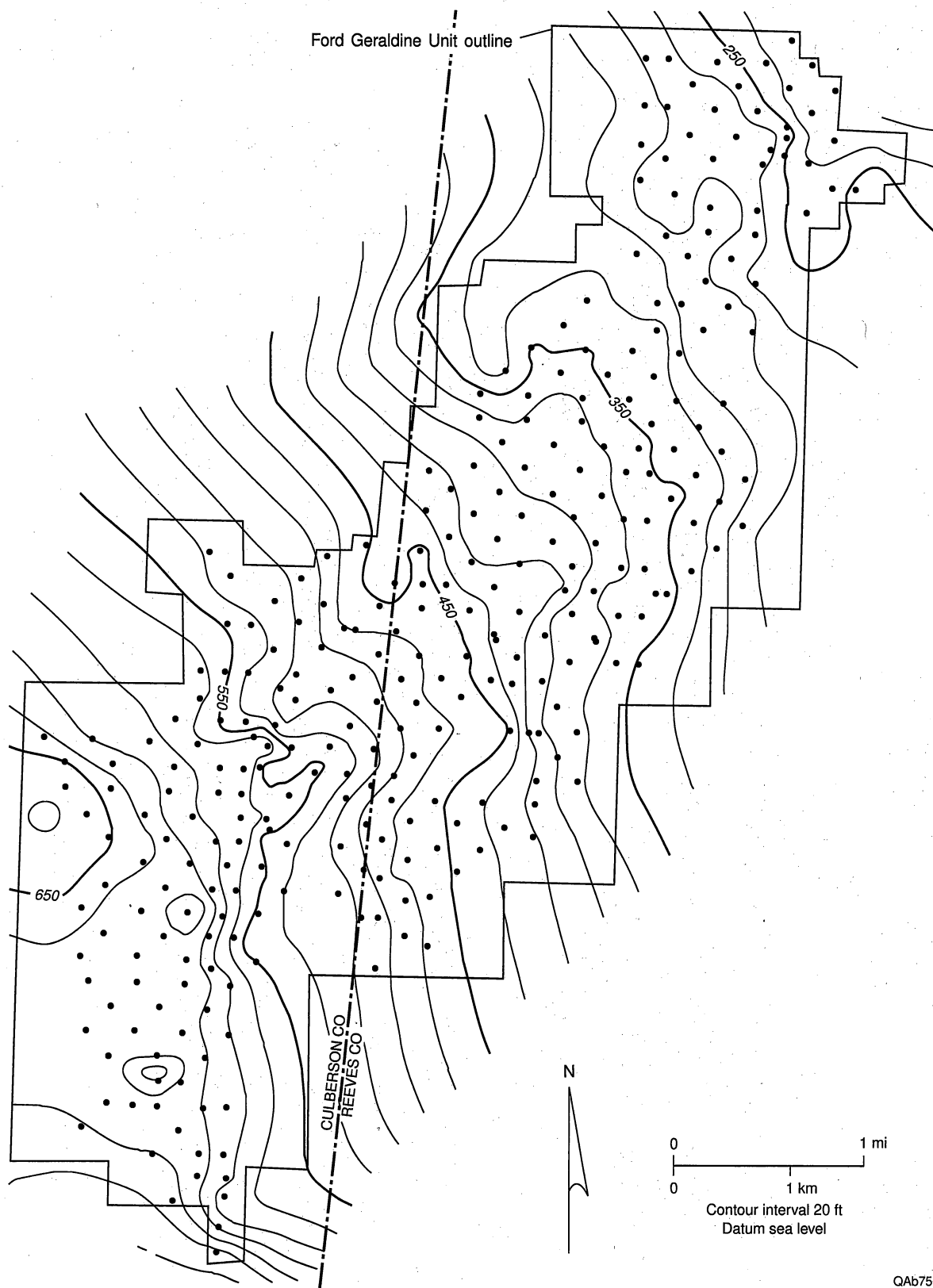
Production from the Ford Geraldine unit generally follows structure, with many, but not all, of the best producing wells occurring along the crest of the compactional anticline (figs. 35, 36). Production from the south part of the field is apparently controlled by a combination of structure and updip porosity pinchout. The best producing wells at the south end of the field are displaced toward the west (up structure) from the trend of thickest Ramsey 1 sandstone (compare figs. 19 and 36). The east-west trend of good production along the northwestern margin of the field follows a channel trend within the Ramsey 1 sandstone where the sandstone bifurcates (fig. 19). The trap is primarily stratigraphic, caused by pinchout of the sandstone into low permeability siltstone to the northwest.

There is a distinct separation between production from the northern and southern parts of the field (fig. 36), with a broad area of low total production in between. This separation is not caused simply by sandstone pinchout against a large erosional remnant as was suggested by Ruggiero (1985), because the Ramsey 2 sandstone pinches out south of the low-producing area. The low-producing zone does include an area where Ramsey 1 sandstone thins markedly over an erosional remnant (fig. 19), but it also includes the thick Ramsey 1 sandstone channel that swings around to the east and south of the erosional remnant. The most likely explanation for low oil production in this area is a combination of (1) high water production, (2) poor reservoir quality, (3) thin Ramsey 1 sandstone in part of the area, and (4) low structural position where the



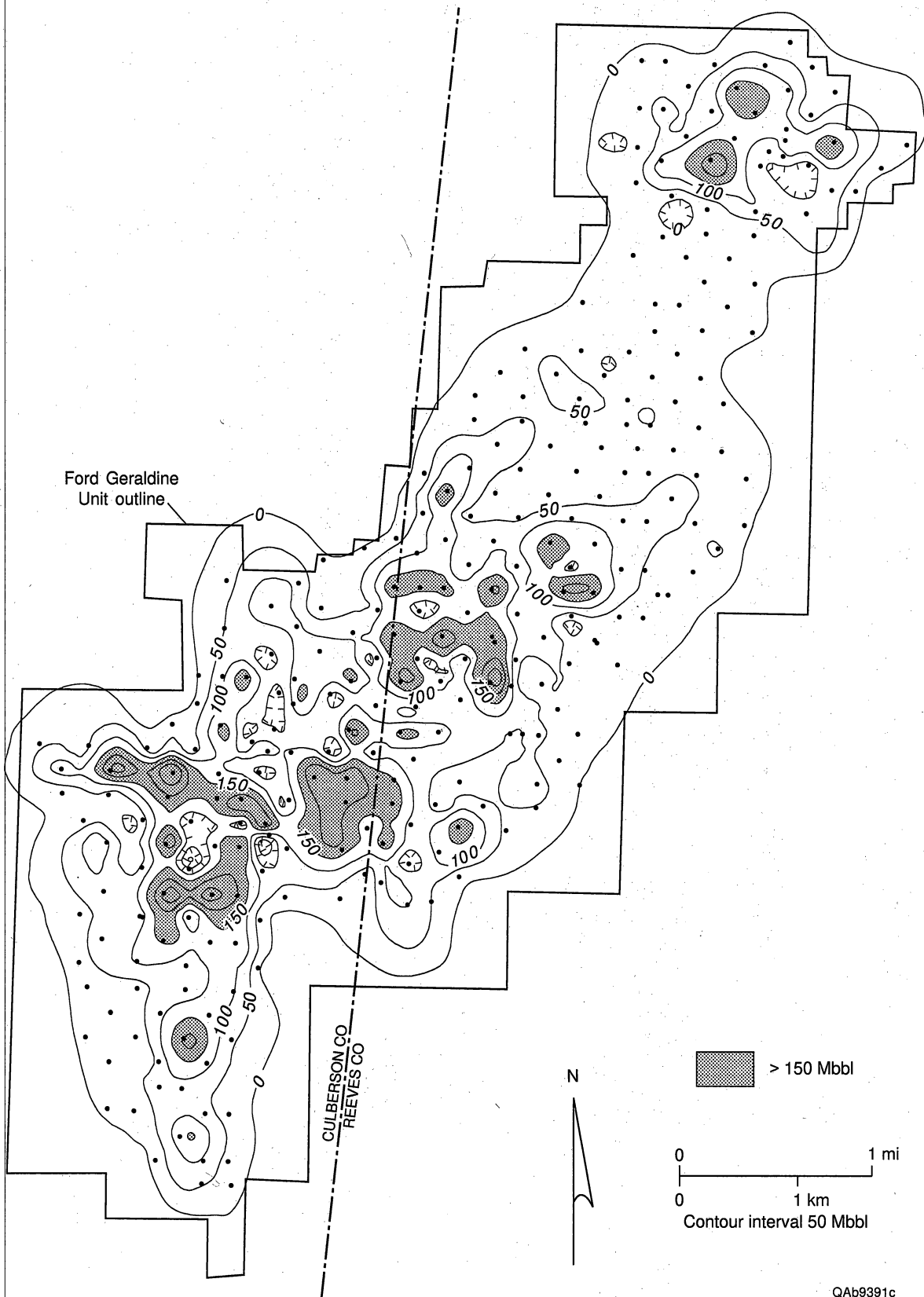
QAb9388c

Figure 34. Capillary pressure curves and calculated radii of pore throats for Ramsey sandstones. Curves are based on analyses of 6 samples having permeability ranging from 1.1 to 116 md. Dashed lines indicate extrapolated data. The analyses were done using the centrifuge method with air and kerosene.



QA67508c

Figure 35. Structure contours on the top of the Lamar limestone dip to the east and northeast. The trap at Geraldine Ford field is formed by pinchout of permeable sandstone into low-permeability siltstone up structural dip. The field has minor structural closure because of differential compaction over the reservoir sandstone body.



QAb9391c

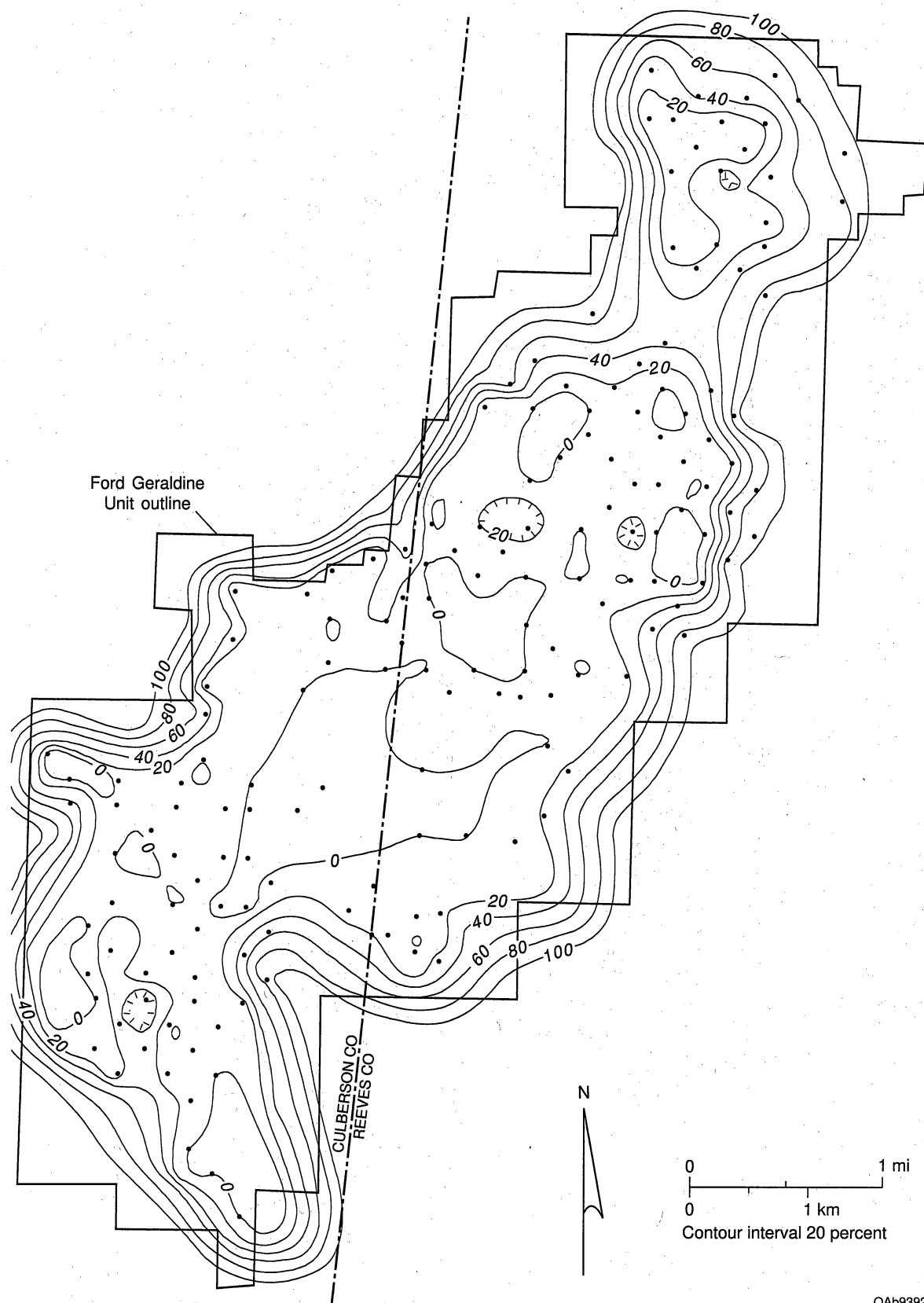
Figure 36. Map of total production from the Ford Geraldine unit through 1995.

Ramsey 1 sandstone is thick. A zone of high water cut during initial production tests (fig. 37) corresponds to the center of the low-producing zone (fig. 36), and the area of high water cut expanded during primary production. A map of water cut in 1969 (fig. 38), before any water injection had been done in the northern part of the field, shows that a wide zone of high (75–100 percent) water cut extended all the way across the field by this time. In addition to high water production, this same area contains some of the poorer quality reservoir in the field, having lower average porosity (fig. 11) and permeability (fig. 18) and high volume of clay (fig. 22). Finally, the Ramsey 1 sandstone thins over an erosional remnant in this area, and where sandstones are thick to east and south of the erosional remnant, they are in a structurally low position (fig. 19).

Total production from Ford Geraldine unit wells shows a statistically significant positive correlation with mobile oil saturation, net pay, and average porosity and significant negative correlation with percent water cut measured during initial potential (IP) tests, volume of clay, and water saturation. The percentage of water produced during IP tests is the single best predictor of eventual total production from a well.

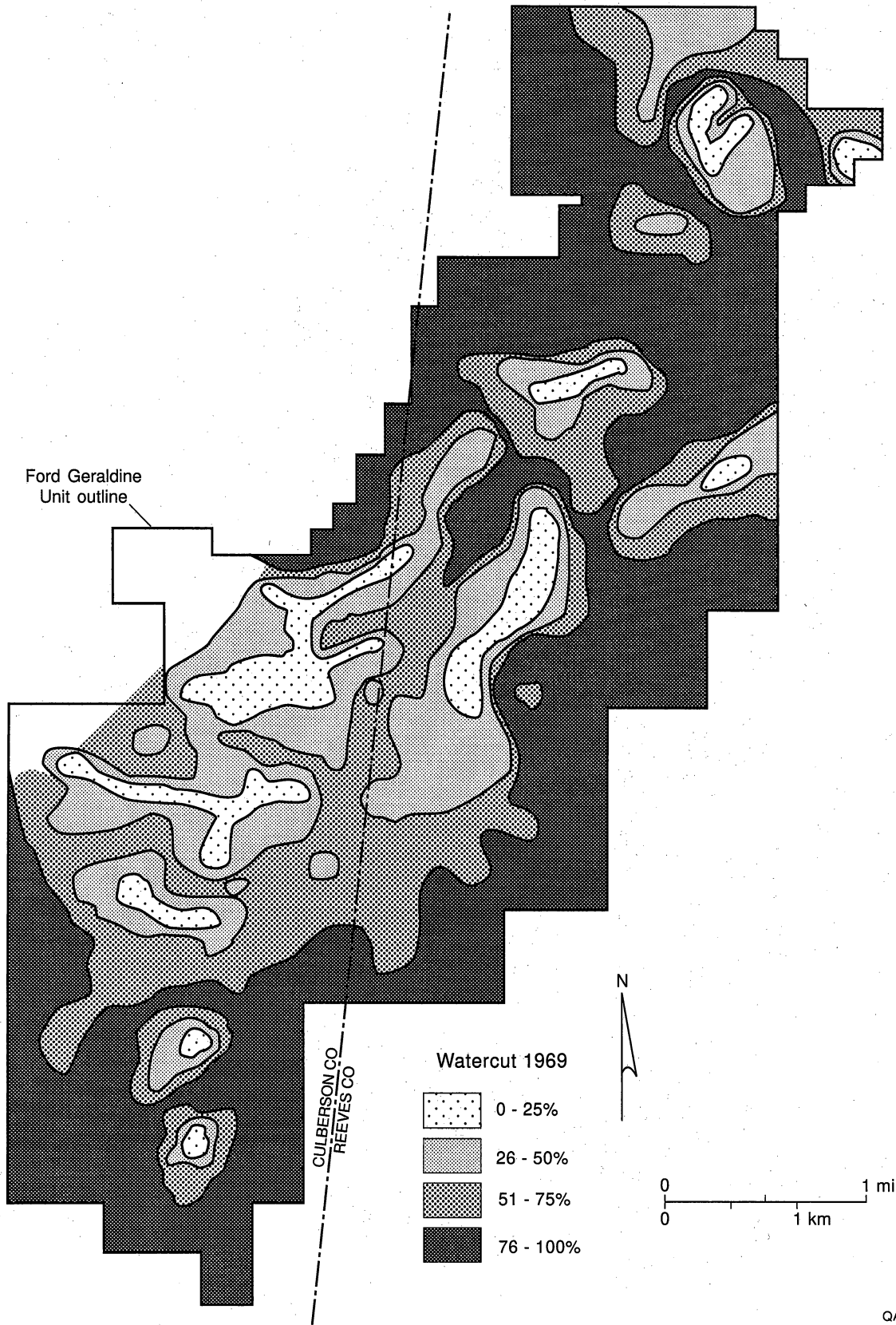
SIMULATIONS OF TERTIARY RECOVERY

To estimate the tertiary recovery potential of the northern end of the Ford Geraldine unit, flow simulations were performed for a CO₂ flood (Malik, 1998). A quarter five spot area was selected for flow simulations, and two cases of permeability distribution were considered. In the first case, stochastic permeabilities generated by conditional simulation (Dutton and others, 1997a, 1997c) were used. The simulation grid in this case was 6 × 5 × 8 (x, y, and z directions, respectively). The second case has layered permeabilities with a 6 × 5 × 6 grid. The block size was 150 ft in the areal (x and y) directions in both cases. In the vertical (z) direction, the block size was 4 ft for the stochastic case and 5.33 ft for the layered case. In the simulation area, both Ramsey 1 and 2 units are present, having an average total thickness of 40 feet. To exclude the



QA69392c

Figure 37. Map of the percentage of water (water cut) produced during initial potential (IP) tests.



QAb9498c

Figure 38. Map of water cut at the end of primary production in 1969 (from Conoco, 1979). The area of good production at the northern end of the field is separated from the rest of the field by an area of high water cut.

intermediate siltstone unit and other smaller siltstone streaks, total net pay was assumed to be 32 ft. The stochastic permeabilities were scaled-up (Malik and Lake, 1997) to reduce the number of blocks in the z direction from 40 to 8. A permeability cut-off of 5 md was used to exclude the nonproducing zones. Maximum permeability was limited to 200 md. The rock compressibility factor used was $7.499 \times 10^{-6}/\text{psi}$, and the water compressibility was $3.15 \times 10^{-6}/\text{psi}$.

Flow simulations were performed using UTCOMP, an isothermal, three-dimensional, compositional simulator for miscible gas flooding (Chang, 1990). The solution scheme is analogous to IMPES (Implicit Pressure, Explicit Saturations). For this work, the Peng-Robinson equation of state (EOS) is used for flash calculations, phase identification, and fluid property calculations (Peng and Robinson, 1976). Three-phase simulations for a CO₂ flood were performed.

Post-waterflood oil saturations in the northern part of the Ford Geraldine unit are estimated at 35 to 39 percent. An average oil saturation of 37 percent was used for these simulations. An exponential relative permeability model for water, oil, and gas flow was fitted to the measured relative permeability data.

In these simulations, five hydrocarbon components were used. Reservoir hydrocarbons were characterized as four pseudocomponents (Khan, 1992), and their properties were calculated from the PVT (pressure, volume, temperature) data. The fifth component is CO₂. Injection pressure is limited to 2,000 psia, and production wells have a flowing bottomhole pressure of 700 psia, in conformity with the prevailing practices in the existing CO₂ flood in other parts of the unit. Fluid characteristics of the reservoir are shown in Table 4.

Simulation Results

Figure 39 is a plot of oil recovery (fraction of remaining oil in place, ROIP) as a function of dimensionless time or pore volumes injected (PVI) for the two cases. This figure shows breakthrough oil recovery of 24 percent for stochastic permeabilities and 10 percent for layered

Table 4. Fluid characteristics of reservoir

Initial reservoir pressure
1,493 psi

Reservoir temperature
83°F

Oil gravity
40°

Oil viscosity
1.4 cp

Oil viscosity at in-situ reservoir condition
0.77 cp at 82° F and 1,380 psi

Initial oil formation volume factor (B_o)
1.287 at bubblepoint

Bubble point pressure
1,383 psi

Initial gas in solution (R_s)
575 solution GOR, scf/bbl

Fluid composition (sample from FGU-157)
CO₂ = 0.01
N₂ = 0.04
H₂S = Nil
Hydrocarbons = 99.95

Gas gravity
1.135

Gas viscosity
0.07 cp

Initial gas formation volume factor (B_g)
0.001522 bbl/scf at bubblepoint pressure

Water density
62.4 lbs/ft³

Water viscosity
0.95 cp

Water salinity
72,200 to 105,000 ppm total dissolved solids

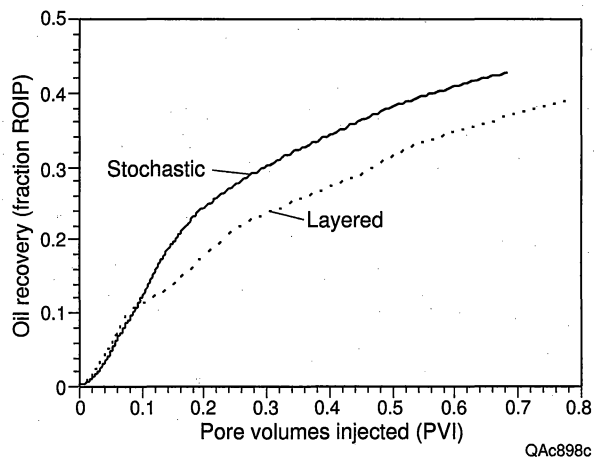


Figure 39. Oil recovery as a fraction of remaining oil in place for stochastic and layered permeability cases (from Malik, 1998).

permeabilities. Unlike a waterflood, these simulations indicate that CO₂ injection results in a gradual increase in recovery even after breakthrough in both cases. Ultimate recovery can exceed 38 percent of ROIP. Oil production rates are shown in Fig. 40. This figure shows a gradual increase in the oil rate until breakthrough. At the time of breakthrough, the oil rate sharply rises to its peak value and gradually declines thereafter. Water-oil ratio (WOR) and gas-oil ratio (GOR) are shown in figures 41 and 42, respectively. WOR gradually decreases with the progress of the flood and remains low even after breakthrough (fig. 41), but GOR increases sharply after breakthrough (fig. 42). Although the oil rates are quite high for some time after breakthrough (Fig. 40), the limiting factor in a CO₂ flood may, however, be the excessive gas production.

Depending on various cut off criteria, estimates of original oil in place (OOIP) in the northern part of the Ford Geraldine unit vary from 12.9 to 18.67 MMSTB (million stock tank barrels). Approximately 2.83 MMSTB of oil has been produced through primary depletion and secondary waterflood in this area. Based on the most conservative estimate of OOIP of 12.9 MMSTB, postwaterflood ROIP in the demonstration area is in excess of 10 MMSTB. The results of the simulations indicate that a minimum of 10% of ROIP (1.0 MMSTB) is recoverable through CO₂ flood. This more conservative estimate is based on the breakthrough recovery of a layered model. The stochastic permeability model shows a breakthrough recovery of more than twice this estimate. If the increased gas production after breakthrough can be handled economically, ultimate CO₂ flood recovery can exceed 30% of ROIP.

A major part of the Ford Geraldine unit is already under CO₂ flood for tertiary recovery. Current data indicate that about 8 percent of OOIP has already been recovered by this CO₂ flood, and ultimate recovery is expected to be 9 percent of OOIP (K. Pittaway, personal communication, 1997). The results of these simulations at breakthrough compare favorably with actual field performance.

In the existing flood, the CO₂ injection is terminated at 0.3 PVI, and acceptable maximum GOR is 30 MSCF/STB. These simulations show that a larger CO₂ slug may be more efficient because of significant incremental recovery. With produced gas recycling, net gas utilization per

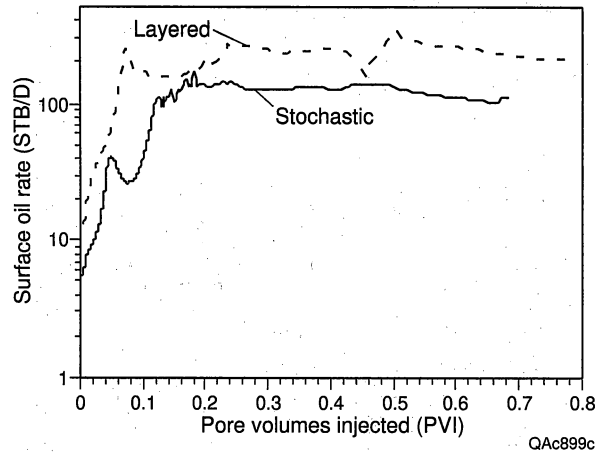


Figure 40. Surface oil rate in stock tanks barrels/day (STB/D) for stochastic and layered permeability cases (from Malik, 1998).

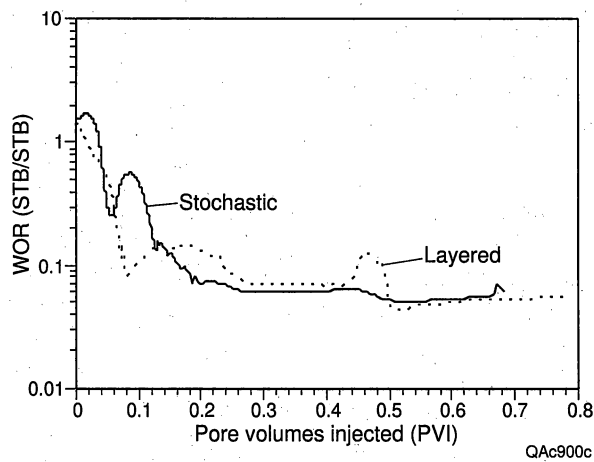


Figure 41. Surface water-oil ratio (WOR) (STB/STB) for stochastic and layered permeability cases (from Malik, 1998).

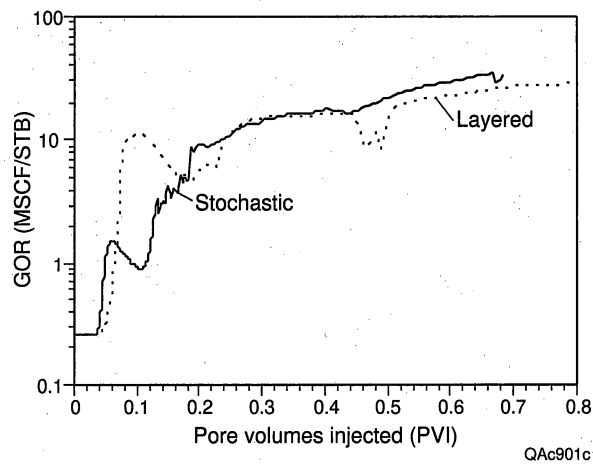


Figure 42. Surface gas-oil ratio (GOR) (MSCF/STB) for stochastic and layered permeability cases (from Malik, 1998).

barrel of produced oil continues to drop (fig. 43). Therefore, a prolonged CO₂ injection after breakthrough may be cost effective.

Sensitivity Study

To improve the reliability of the results, additional simulations were performed to observe the sensitivity of CO₂ flood to the following factors:

1. Increasing the postwaterflood water saturation from 0.63 to 0.70.
2. Implementing a WAG (water alternating gas) flood in place of continuous CO₂ injection.
3. Reducing the vertical to horizontal permeability ratio from 1 to 0.1.
4. Pressuring the reservoir by CO₂ injection.
5. Reducing the injection pressure from 2,000 to 1,500 psia.

Increasing the postwaterflood water saturation from 0.63 to 0.7 has a significant effect on recovery (fig. 44). High initial water saturation results in early breakthrough, and ultimate recovery is reduced by 12 to 15 percent in the stochastic as well as the layered case of permeability distribution. However, these simulations indicate that even under these extreme assumptions, ultimate CO₂ flood recovery can still exceed 30 percent of the remaining oil in place.

The recovery results from WAG simulations are compared to continuous CO₂ injection in the stochastic permeability case with 63 percent water saturation (Fig. 45). The simulation results suggest that the WAG process is slightly more efficient. However, the recovery time increases by about 50 percent, which may offset any gains in real terms. The WAG simulations could not be performed in the layered case because of numerical instabilities.

Figure 46 is a plot of oil recovery for the layered case with 63 percent water saturation and vertical to horizontal permeability ratios of 1 and 0.1. This figure shows that the reduction in vertical permeability causes earlier breakthrough. The recovery curve remains about 5 percent lower in the intermediate region, but ultimate recovery is the same or even higher.

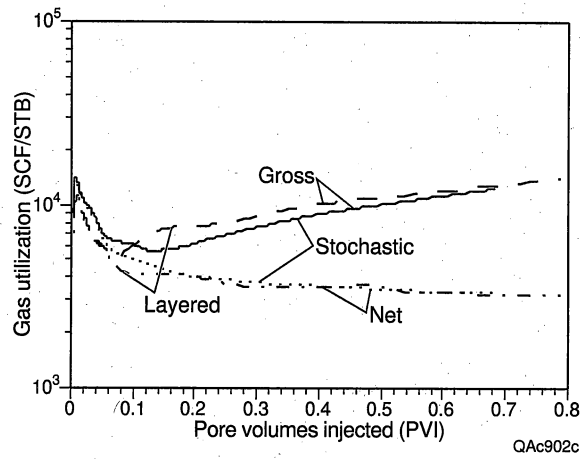


Figure 43. Gross and net gas utilization (SCF/STB) for stochastic and layered permeability cases (from Malik, 1998).

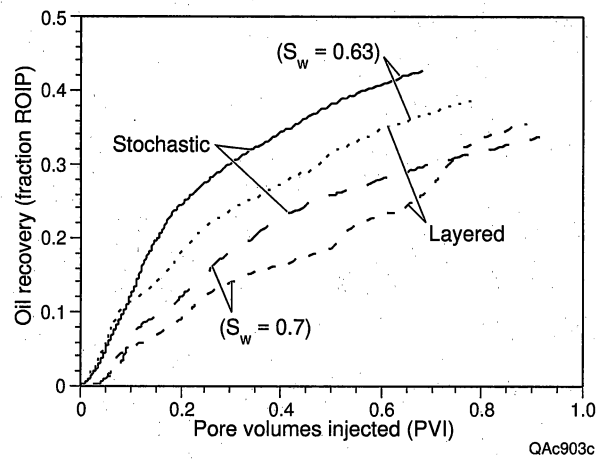


Figure 44. Effect of water saturation (before CO₂ flood) on oil recovery for stochastic and layered permeability cases (from Malik, 1998).

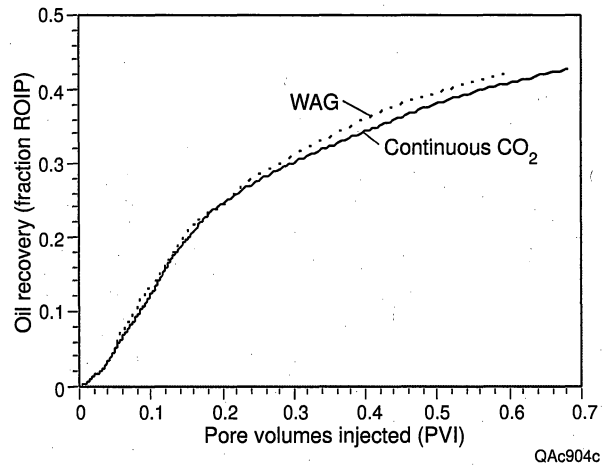


Figure 45. Comparison of oil recovery for WAG and continuous CO₂ injection for stochastic permeability case (from Malik, 1998).

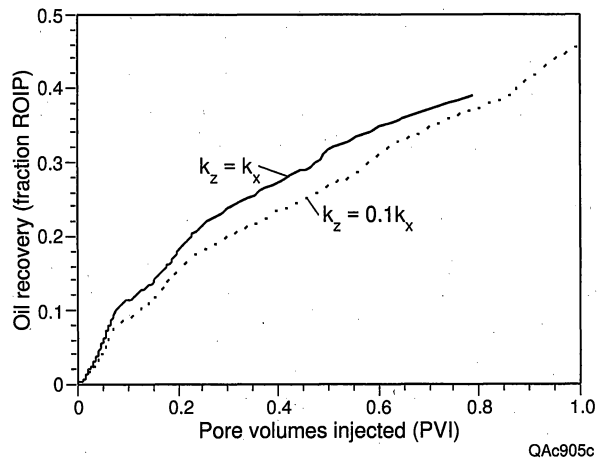


Figure 46. Effect of reduction of vertical permeability on oil recovery for layered permeability case (from Malik, 1998).

The recovery curve for stochastic permeability with 63 percent water saturation (base case) was compared with a case with reduced injection pressure in figure 47. Also shown in this figure is the recovery curve in the case where the field is pressurized by CO₂ injection. It is clear that both cases give poor recovery. Reduction of injection pressure will reduce compression cost for CO₂, but it will also result in earlier breakthrough and about 5 percent drop in oil recovery. Pressuring the reservoir by CO₂ injection appears to be even more detrimental to oil recovery. A significant quantity of gas is required to pressurize the reservoir before any increase in oil recovery is observed. Even with a prolonged flood, oil recovery in this case remains much lower than in the base case.

Economic Analysis

The results of the simulations were used by Conoco, Inc. to perform an economic analysis of a CO₂ flood in the northern part of the Ford Geraldine unit. The economics of the project were found to be positive but did not meet Conoco's profitability criteria (K. R. Pittaway, written communication, 1997). Conoco has therefore elected not to continue into Phase 2 of the project.

CONCLUSIONS

The research effort during the third year of the project concentrated on reservoir characterization and simulation of the Ford Geraldine unit by (1) interpreting sources of reservoir heterogeneity on the basis of the depositional model developed for Delaware sandstones from outcrop characterization, (2) mapping reservoir properties in the Ford Geraldine unit, and (3) simulating a CO₂ flood in the northern part of the unit.

A model to explain depositional heterogeneity in Ramsey sandstone reservoirs was developed on the basis of outcrop characterization. The proposed channel-levee and lobe model for Ramsey sandstone deposition suggests greater macroscopic (interwell-scale) heterogeneity of reservoir sandstones exists at Ford Geraldine unit than previously thought. Progradation,

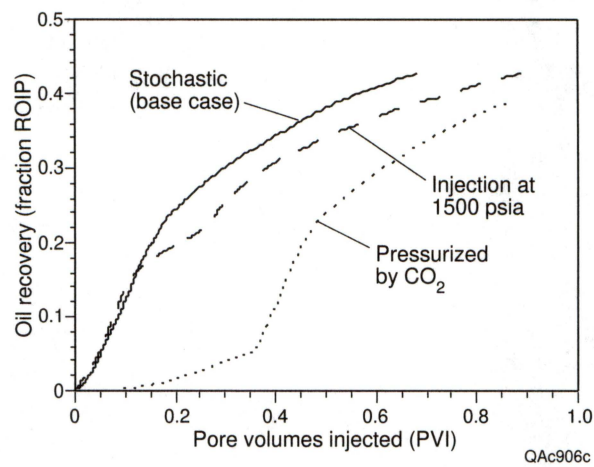


Figure 47. Oil recovery in base with stochastic permeability as affected by (1) reduction in injection pressure from 2,000 to 1,500 psia and (2) pressurizing the reservoir with injection of CO₂ instead of water. From Malik, 1998.

aggradation, and retrogradation of the system resulted in lateral and vertical offset of channel, levee, and lobe facies. Laminated siltstones in the levee and lobe facies provide the greatest amount of depositional heterogeneity because of the grain size and permeability contrast between sandstones and siltstone facies.

Mapping of reservoir properties in the Ford Geraldine unit was improved by supplementing geophysical log data with porosity, permeability, and water saturation data from core analyses. The expanded water-saturation data base was used to improve the maps of mobile oil saturation, net pay, and hydrocarbon pore feet. Many of the reservoir properties are not continuous but instead show areas of better reservoir quality separated by poorer areas, particularly on the margins of the field. These marginal zones of higher porosity and permeability are interpreted as being levee deposits that formed when low-density turbidity currents overtopped the channel margins and deposited sand in the generally lower-reservoir-quality interchannel areas.

Compositional simulations of a CO₂ flood indicate that at least 10 percent of the remaining oil in place can be recovered at breakthrough. Simulation results show that continuing the CO₂ injection beyond breakthrough can result in significant incremental oil recovery. A sensitivity study shows that oil recovery in a CO₂ flood is adversely affected by an increase in postwaterflood water saturation, reduction in injection pressure, and pressurizing the reservoir with CO₂ injection. The recovery is slightly improved by the WAG process, but the flood takes considerably longer.

The economics of the project were found to be positive but did not meet Conoco's profitability criteria. Conoco has therefore elected not to continue into Phase 2 of the project.

ACKNOWLEDGMENTS

This research was funded by the U.S. Department of Energy under contract no. DE-FC22-95BC14936, by Conoco, Inc., and by the State of Texas under State Match Pool Project 4201 and as part of the State of Texas Advanced Resource Recovery project. The Bureau of Economic

Geology acknowledges support of this research by Landmark Graphics Corporation via the Landmark University Grant Program. Susan Hovorka and Edgar Guevara contributed to the early stages of this project. Research was assisted by Carlos Amaya, Radu Boghici, Janaka Paulus, and Mohammad Razi, whose hard work is gratefully acknowledged. Earlier studies of Bell Canyon reservoirs by M. H. Gardner, R. W. Ruggiero, and C. R. Williamson provided the foundation for the present study. Drafting was by the Graphics staff of the Bureau of Economic Geology under the direction of Joel Lardon. Others contributing to the publication of this report were Susan Lloyd, word processing and pasteup and Nina Redmond, proofreading.

REFERENCES

- Allen, J. R. L., 1982, Studies in fluvial sedimentation: Bars, bar-complexes, and sandstone sheets (low-sinuosity braided streams) in the Brownstones (L. Devonian), Welsh Border: *Sedimentary Geology*, v. 33, p. 237-293.
- Asquith, G. B., Dutton, S. P., and Cole, A. G., 1997a, "Delaware effect" and the Ramsey sandstone, Ford Geraldine Unit, Reeves and Culberson Counties, Texas, *in* DeMis, W. D., ed., Permian Basin oil and gas fields: turning ideas into production: West Texas Geological Society, Publication No. 97-102, p. 71-74.
- Asquith, G. B., Dutton, S. P., Cole, A. G., Razi, M., and Guzman, J. I., 1997b, Petrophysics of the Ramsey sandstone, Ford Geraldine Unit, Reeves and Culberson Counties, Texas, *in* DeMis, W. D., ed., Permian Basin oil and gas fields: turning ideas into production: West Texas Geological Society, Publication No. 97-102, p. 61-69.
- Asquith, G. B., Thomerson, M. D., and Arnold, M. D., 1995, The recognition of possible oil and water wettability changes in the Permian Delaware Mountain Group sandstones from petrophysical well logs, *in* R. L. Martin, ed., In Search of New Permian Basin Oil and Gas Fields: West Texas Geological Society Fall Symposium, Publication No. 95-98, p. 39-50.
- Barton, M. D., 1997, Facies architecture of submarine channel-levee and lobe sandstones: Permian Bell Canyon Formation, Delaware Mountains, West Texas: The University of Texas at Austin, Bureau of Economic Geology Field Trip Guidebook, 40 p.
- Berg, R. R., 1979, Reservoir sandstones of the Delaware Mountain Group, southeast New Mexico, *in* Sullivan, N. M., ed., Guadalupian Delaware Mountain Group of west Texas and southeast New Mexico, 1979, Symposium and Field Trip Conference Guidebook: SEPM (Permian Basin Sec.) Pub. 79-18, p. 75-95.

- Bouma, A. H., 1962, *Sedimentology of some flysch deposits: a graphic approach to facies interpretation*: Amsterdam, Elsevier, 168 p.
- Bouma, A. H., 1996, Initial comparison between fine- and coarse-grained submarine fans and the Brushy Canyon Formation sandstones, *in* DeMis, W. D., and Cole, A. G., eds., *The Brushy Canyon play in outcrop and subsurface: concepts and examples: Guidebook, Permian Basin Section, SEPM, Publication No. 96-38*, p. 41-50.
- Bozanich, R. G., 1979, The Bell Canyon and Cherry Canyon Formations, eastern Delaware Basin, Texas: Lithology, environments and mechanisms of deposition, *in* Sullivan, N. M., ed., *Guadalupian Delaware Mountain Group of west Texas and southeast New Mexico, 1979, Symposium and Field Trip Conference Guidebook: SEPM (Permian Basin Sec.) Pub. 79-18*, p. 121-141.
- Chang, Yih-Bor, Development and application of an equation of state compositional simulator, Ph.D. dissertation, The University of Texas at Austin, 1990.
- Conoco, 1979, Ford Geraldine CO2 Project, Internal Report, variously paginated.
- DeMis, W. D., and Cole, A. G., 1996, *The Brushy Canyon play in outcrop and subsurface: concepts and examples: Guidebook, Permian Basin Section, SEPM, Publication No. 96-38*, 188 p.
- Dewan, J. T., 1984, *Essentials of Modern Open-Hole Log Interpretation*: PennWell Publishing Co. Tulsa, Oklahoma, 345 p.
- Dutton, S. P., Asquith, G. B., Barton, M. D., Cole, A. G., Gogas, J., Malik, M. A., Clift, S. J., and Guzman, J. I., 1997a, Application of advanced reservoir characterization, simulation, and production optimization strategies to maximize recovery in slope and basin clastic reservoirs, West Texas (Delaware Basin): The University of Texas at Austin, Bureau of Economic Geology, annual report prepared for the U.S. Department of Energy, DOE/BC/14936-9, 187 p.
- Dutton, S. P., Barton, M. D., Clift, S. J., Guzman, J. I., and Cole, A. G., 1997b, Depositional history of Ramsey sandstone channel-levee and lobe deposits, Bell Canyon Formation, Ford Geraldine Unit, West Texas (Delaware Basin): *in* DeMis, W. D., ed., *Permian Basin oil and gas fields: turning ideas into production: West Texas Geological Society, Publication No. 97-102*, p. 53-60.
- Dutton, S. P., Hovorka, S. D., and Cole, A. G., 1996, Application of advanced reservoir characterization, simulation, and production optimization strategies to maximize recovery in slope and basin clastic reservoirs, West Texas (Delaware Basin): The University of Texas at Austin, Bureau of Economic Geology, annual report prepared for the U.S. Department of Energy, DOE/BC/14936-5, 81 p.
- Dutton, S. P., Malik, M. A., Clift, S. J., Asquith, G. B., Barton, M. D., Cole, A. G., Gogas, J., and Guzman, J. I., 1997c, Geologic and engineering characterization of Geraldine Ford Field, Reeves and Culberson Counties, Texas: The University of Texas at Austin, Bureau of Economic Geology, draft topical report prepared for the U.S. Department of Energy, 115 p.
- Fischer, A. G., and Sarnthein, M., 1988, Airborne silts and dune-derived sands in the Permian of the Delaware Basin: *Journal of Sedimentary Petrology*, v. 58, p. 637-643.
- Friend, P. F., 1983, Towards the field classification of alluvial architecture or sequences, *in* Collinson, J. D., and Lewin, J., eds., *Modern and ancient fluvial systems: International Association of Sedimentologists Special Publication, No. 6*, p. 345-354.

- Gardner, M. H., 1992, Sequence stratigraphy of eolian-derived turbidites: patterns of deep water sedimentation along an arid carbonate platform, Permian (Guadalupian) Delaware Mountain Group, West Texas, *in* Mruk, D. H., and Curran, B. C., eds., Permian Basin exploration and production strategies: applications of sequence stratigraphic and reservoir characterization concepts: West Texas Geological Society Publication 92-91, p. 7-12.
- Gardner, M. H., 1997a, Characterization of deep-water siliciclastic reservoirs in the upper Bell Canyon and Cherry Canyon Formations of the northern Delaware Basin, Culberson and Reeves Counties, Texas, *in* Major, R. P., ed., Oil and gas on Texas State Lands: an assessment of the resource and characterization of type reservoirs: The University of Texas, Bureau of Economic Geology Report of Investigations No. 241, p. 137-146.
- Gardner, M. H., 1997b, Sequence stratigraphy and hydrocarbon habitat of the Permian (Guadalupian) Delaware Mountain Group, Delaware Basin, West Texas, *in* Major, R. P., ed., Oil and gas on Texas State Lands: an assessment of the resource and characterization of type reservoirs: The University of Texas, Bureau of Economic Geology Report of Investigations No. 241, p. 147-157.
- Green, K. M., Frailey, S. M., and Asquith, G. B., 1996, Laboratory analysis of the clays within the Brushy Canyon Formation and their reservoir and petrophysical implications: Red Tank Field, Lea County, New Mexico, *in* W. D. DeMis and A. G. Cole, eds., The Brushy Canyon Play in Outcrop and Subsurface: Concepts and Examples: Permian Basin Section SEPM, Publication No. 96-38, p. 165-171.
- Harms, J. C., 1968, Permian deep-water sedimentation by nonturbid currents, Guadalupe Mountains, Texas: Geological Society of America Spec. Paper 121, 127 p.
- Harms, J. C., 1974, Brushy Canyon Formation, Texas: A deep-water density current deposit: Geological Society of America Bulletin, v. 85, p. 1763-1784.
- Harms, J. C., and Brady, M. J., 1996, Deposition of the Brushy Canyon Formation: 30 years of conflicting hypotheses, *in* DeMis, W. D., and Cole, A. G., eds., The Brushy Canyon play in outcrop and subsurface: concepts and examples: Guidebook, Permian Basin Section, SEPM, Publication No. 96-38, p. 51-59.
- Harms, J. C., and Williamson, C. R., 1988, Deep-water density current deposits of Delaware Mountain Group (Permian), Delaware Basin, Texas and New Mexico: American Association of Petroleum Geologists Bulletin, v. 72, p. 299-317.
- Hills, J. M., 1984, Sedimentation, tectonism, and hydrocarbon generation in Delaware Basin, west Texas and southeastern New Mexico: American Association of Petroleum Geologists Bulletin, v. 68, p. 250-267.
- Holtz, M. H., and Major, R. P., 1994, Geological and engineering assessment of remaining oil in a mature carbonate reservoir: an example from the Permian Basin, West Texas, SPE Paper No. 27687: Society of Petroleum Engineers Permian Basin Oil and Gas Recovery Conference Proceedings, p. 565-576.
- Jacka, A. D., 1979, Deposition and entrapment of hydrocarbons in Bell Canyon and Cherry Canyon deep-sea fans of the Delaware Basin, *in* Sullivan, N. M., ed., Guadalupian Delaware Mountain Group of West Texas and Southeast New Mexico: Society of Economic Paleontologists and Mineralogists (Permian Basin Section) Publication 79-18, p. 104-120.

- Jacka, A. D., Beck, R. H., St. Germain, L. C., and Harrison, S. C., 1968, Permian deep-sea fans of the Delaware Mountain Group (Guadalupian), Delaware Basin, *in* Guadalupian facies, Apache Mountain area, west Texas: Society of Economic Paleontologists and Mineralogists (Permian Basin Section) Publication 68-11, p. 49-90.
- Kerans, C., and Fitchen, W. M., 1995, Sequence hierarchy and facies architecture of a carbonate-ramp system: San Andres Formation of the Algerita Escarpment and western Guadalupe Mountains, West Texas and New Mexico: The University of Texas at Austin, Bureau of Economic Geology Report of Investigations No. 235, 86 p.
- Kerans, C., Fitchen, W. M., Gardner, M. H., Sonnenfeld, M. D., Tinker, S. W., and Wardlaw, B. R., 1992, Styles of sequence development within uppermost Leonardian through Guadalupian strata of the Guadalupe Mountains, Texas and New Mexico, *in* Mruk, D. H., and Curran, B. C., eds., Permian Basin exploration and production strategies: applications of sequence stratigraphic and reservoir characterization concepts: West Texas Geological Society Publication 92-91, p. 1-6.
- Khan, S. A., "An expert system to aid in compositional simulation of miscible gas flooding," Ph.D. dissertation, The University of Texas at Austin, 1992.
- Kneller, B., 1996, When is a turbidity current not a turbidity current? A question of mobility? (abs.): 1996 AAPG Annual Convention, Official Program, v. 5, San Diego, p. A76.
- Linn, A. M., 1985, Depositional environment and hydrodynamic flow in Guadalupian Cherry Canyon Sandstone, West Ford and West Geraldine fields, Delaware Basin, Texas: Texas A&M University, M. S. thesis, 152 p.
- Lowe, D. R., 1982, Sediment gravity flows: II. Depositional models with special reference to the deposits of high-density turbidity currents: *Journal of Sedimentary Research*, v. 52, p. 279-297.
- Malik, M. A., 1998, Compositional simulations of a CO₂ flood in Ford Geraldine Unit, Texas: Society of Petroleum Engineers, Proceedings, SPE Permian Basin Oil and Gas Recovery Conference, Paper SPE 39794, p. 375-383.
- Malik, M. A., and Lake, L. W., 1997, A practical approach to scaling-up permeability and relative permeabilities in heterogeneous permeable media: Society of Petroleum Engineers, Proceedings, 1997 SPE Western Regional Meeting, Paper 38310, p. 485-500.
- Meissner, F. F., 1972, Cyclic sedimentation in Middle Permian strata of the Permian Basin, west Texas and New Mexico, *in* Cyclic sedimentation in the Permian Basin, 2nd ed.: West Texas Geological Society, p. 203-232.
- Miall, A. D., 1985, Architectural-element analysis: a new method of facies analysis applied to fluvial deposits: *Earth Science Reviews*, v. 22, p. 261-308.
- Mutti, E., and Normark, W. R., 1987, Comparing examples of modern and ancient turbidite systems: problems and concepts, *in* Leggett, J. K., and Zuffa, G. G., eds., *Marine Clastic Sedimentology: Concepts and Case Studies*: London, Graham and Trotman, p. 1-38.
- Payne, M. W., 1976, Basinal sandstone facies, Delaware Basin, west Texas and southeast New Mexico: *American Association of Petroleum Geologists Bulletin*, v. 60, p. 517-527.

- Peng, D. Y., and Robinson, D. B., 1976, A new two-constant equation of state: *Ind. Eng. Chem. Fund.*, v. 15, p. 59-64.
- Pittaway, K. R., and Rosato, R. J., 1991, The Ford Geraldine unit CO₂ flood—update 1990: *Society of Petroleum Engineers Reservoir Engineering*, v. 6, no. 4, p. 410-414.
- Ruggiero, R. W., 1985, Depositional history and performance of a Bell Canyon sandstone reservoir, Ford-Geraldine field, west Texas: The University of Texas at Austin, M. A. thesis, 242 p.
- Ruggiero, R. W., 1993, Depositional history and performance of a Permian Bell Canyon sandstone reservoir, Ford-Geraldine field, West Texas, in Rhodes, E. G., and Moslow, T. F., eds., *Marine Clastic Reservoirs*: New York, Springer-Verlag, p. 201-229.
- Ruppel, S. C., Kerans, C., Major, R. P., and Holtz, M. H., 1995, Controls on reservoir heterogeneity in Permian shallow-water-platform carbonate reservoirs, Permian Basin: Implications for improved recovery: The University of Texas, Bureau of Economic Geology Geological Circular 95-2, 30 p.
- Thomerson, M.D., 1992, Petrophysical Analysis of the Brushy Canyon Formation, Hat Mesa Delaware Field, Lea County, New Mexico: unpublished M.S. Thesis, Texas Tech University, Lubbock, Texas, 124 p.
- Walling, S. D., 1992, Authigenic clay minerals in sandstones of the Delaware Mountain Group: Bell Canyon and Cherry Canyon Formations, Waha Field, West Texas: Texas A & M University, MS thesis, 63 p.
- Williamson, C. R., 1977, Deep-sea channels of the Bell Canyon Formation (Guadalupian), Delaware Basin, Texas-New Mexico, in Hileman, M. E. and Mazzullo, S. J., eds., *Upper Guadalupian facies, Permian reef complex, Guadalupe Mountains New Mexico and west Texas*: Society of Economic Paleontologists and Mineralogists (Permian Basin Section) Publication 77-16, p. 409-431.
- Williamson, C. R., 1978, Depositional processes, diagenesis and reservoir properties of Permian deep-sea sandstones. Bell Canyon Formation, Texas-New Mexico, The University of Texas at Austin, Ph. D. Dissertation, 262 p.
- Williamson, C. R., 1979, Deep sea sedimentation and stratigraphic traps, Bell Canyon Formation (Permian), Delaware basin, in Sullivan, N. M., ed., *Guadalupian Delaware Mountain Group of west Texas and southeast New Mexico, 1979, Symposium and Field Trip Conference Guidebook*: SEPM (Permian Basin Sec.) Pub. 79-18, p. 39-74.
- Zelt, F. B., and Rossen, C., 1995, Geometry and continuity of deep-water sandstones and siltstones, Brushy Canyon Formation (Permian) Delaware Mountains, Texas, in Pickering, K. T., Hiscott, R. N., Kenyon, N. H., Ricci Lucchi, F., and Smith, R. D. A., eds., *Atlas of Deep Water Environments, Architectural Style in Turbidite Systems*: London, Chapman & Hall, p. 167-183.